Effects of chitooligosaccharide and glucosamine conjugation on stability and functionality of bovine trypsin

Jóhann Grétar Kröyer Gizurarson

Faculty of Physical Sciences
University of Iceland
2014

Effects of chitooligosaccharides and glucosamine conjugation on stability and functionality of bovine trypsin

Jóhann Grétar Kröyer Gizurarson

90 ECTS thesis submitted in partial fulfillment of a
Magister Scientiarum degree in biochemistry

Advisor
Dr. Hörður Filippusson

Faculty Representative
Dr. Baldur Símonarson

Faculty of Physical Sciences
School of Engineering and Natural Sciences
University of Iceland
Reykjavik, May 2014

Effects of chitooligosaccharides and glucosamine conjugation on stability and functionality of bovine trypsin
90 ECTS thesis submitted in partial fulfillment of a *Magister Scientiarum* degree in XX

Faculty of Physical Sciences
School of Engineering and Natural Sciences
University of Iceland
Hjarðarhagi 2-6
107, Reykjavik
Iceland

Telephone: 525 4000

Bibliographic information:
Jóhann Grétar Kröyer Gizurarson, 2014, *Effects of chitooligosaccharides and glucosamine cross-linking/conjugation on stability and functionality of bovine trypsin*, Master's thesis, Faculty of Physical Sciences, University of Iceland, pp. 83.

Printing: Pixel ehf.
Reykjavik, Iceland, May 2014

Abstract

Over the past four decades, enzymes have become valuable catalysts for industrial and biotechnological purposes. Like other proteins, mesophilic enzymes are only marginally stable at ambient conditions. However, they are usually catalytically more efficient than commonly used thermophilic enzymes, thereby justifying their application. Utilization of mesophilic enzymes is only practical if they are stabilized against otherwise inactivating and unfolding conditions. It is well documented that glycoproteins are usually more stable than unglycosylated proteins.

In this study, three trypsin species were synthesized. D-glucosamine and 1:5/ 1:10 trypsin-to-chitooligosaccharide (or partially acetylated poly-1,4-β-D-glucosamine) was conjugated and cross-linked to bovine trypsin, respectively, via binary carbodiimide/succinimide ester conjugation. The degree of conjugation and sizes of the cross-linked enzymes was determined. D-glucosamine was found to conjugate, on average, to 12 residues on trypsin and the two ratios of cross-linked enzyme were found to form huge and polydisperse complexes with hydrodynamical radii from, on average, from 218 to 330 nm for 1:5 and 1:10 cross-linked trypsin, respectively. The trypsin species gave significantly higher $T_{50\%}$ values, resistance against thermal inactivation and autolysis increased, thermal and storage stability improved, however, stability against urea inactivation was not changed, compared with native trypsin. The proteolytic activity against azocasein improved for the cross-linked trypsins but was slightly reduced for D-glucosamine conjugated trypsin, compared with native trypsin. The species were found to become basophilic upon conjugation and cross-linking. D-glucosamine conjugated trypsin was found to be slightly structurally altered, which displayed 1.2 times higher catalytic efficiency (k_{cat}/K_m) than native trypsin against the substrate L-BAPNA.

Úrdráttur

Síðustu fjóra áratugi hafa ensím orðið verðmætir lífhvatar í iðnaði og líftækni. Eins og flest prótín, eru miðlungshitakær ensím aðeins jaðarstöðug við lífeðlisfræðilegar aðstæður. Hinsvegar eru þau virknilega séð betri lífhvatar en almennt notuð hitakær ensím, sem að hluta til réttlætir mögulega notkun þeirra í iðnaði og líftækni. Notkun miðlungshitakærra ensíma er eingöngu hagnýt ef hægt er að stöðga þau gagnvart annars afvirkjandi og afmyndandi kringumstæðum. Þekkt er að sykruð prótín eru alla jafna stöðugri en samsvarandi prótín sem eru það ekki.
Í þessari rannsókn voru þrjár gerðir af nautatrypsíni myndaðar. D-glúkósamín og 1:5/1:10 trypsín-kítófásykru (eða að hluta afasýtýleruð fjöl-1,4-β-D-glúkósamín) hlutfall, tengt, annarsvegar, og krosstengt, hinsvegar, á nautatrypsín með tvívirku tengingamiðluðu karbódíímíð/súkksínímíð esterhvarfi. Gráða teningar og stærð krosstengdu ensímanna var skoðuð. Fundið var út að D-glúkósamín tengdist að meðaltali 12 leifum á trypsíni og að bæði hlutföll krosstengdu ensímanna mynduðu stóra og fjöldreifða (m.t.t. stærðar) flóka með radíusa á bilinu 218 – 330 nm fyrir 1:5 annarsvegar og 1:10 hinsvegar.
Trypsíngerðirnar sýndu hærri $T_{50\%}$ gildi, þol gagnvart hitaafvirkjun og sjálfmeltu jókst, hita- og geymslu stöðugleiki bættist, en stöðugleiki gagnvart þvagefni (úreu) breyttist ekki samanborið við frjálst form trypsíns. Prótínvatnsrofsvirkni gagnvart azókaseini jókst fyrir krosstengdu trypsínin, en minnkaði aðeins fyrir D-glúkósamín tengt trypsin miðað við frjálst form trypsíns. Trypsíngerðirnar urðu basakærari við tengingu og krosstengingu.
Mælingar sýndu að D-glúkósamín tengda trypsínið breyttist lítið eitt með tilliti til 3. stigs byggingar og sýndi 1,2 falda aukningu í sértæknistuðli (k_{cat}/K_m) gagnvart hvarfefninu L-BAPNA.

Table of Contents

List of Figures

List of Tables

Abbreviations

ref.	Reference
Approx.	Approximately
Da	Dalton
$U_{1/2}$	Concentration of urea that cause half protein denaturation
fig.	Figure
Conc.	Concentrated
NMR	Nuclear magnetic resonance
DA	Degree of acetylation
DD	Degree of deactylation (1-DA)
Eq	Equation
a.k.a.	Also known as
T_m	Melting point
$T_{50\%}$	Temperature where 50% of the orginal activity is retained.
CLEC	Cross-linked enzyme crystal
CLEA	Cross-linked enzyme aggregate
PAGE	Polyacrylamide gel electrophoresis
PEG	Polyethylene glycol
m/z ratio	Mass-to-charge ratio
MALDI-TOF	Matrix-assisted laser desorption ionization-time-of-flight
UV	Ultra-violet
ESI TOF	Electrospray ionization time-of-flight
CD spectropolarimetry	Circular dichroism spectropolarimetry
E_L/E_R	Left/rigth component of electric field of light.
NTA	Nanoparticle tracking analysis
EMCCD	Electron-multiplied charged coupled device
TCC	Trypsin cross-linked with chitooligosaccharides
TGG	Trypsin grafted with glucosamine
EDAC	1-Ethyl-3-(dimethylaminopropyl)-carbodiimide
NHSS	N-Hydroxysulfosuccinimide
L-BAPNA	N- benzoyl-L-arginine p-nitroanilide
PMSF	Phenylmethylsulfonyl fluoride
SAC	Sulfanilamide casein
TLCK	N-α-tosyl-L-lysine chlorometyl ketone
M_W	Molecular weight (Da)
wrt.	With respect to
CLE	Cross-linked enzyme

Acknowledgements

First and foremost, I would like to thank my supervisor Dr. Hörður Filippusson for giving me an exciting and challenging research topic. His helpful guidance and patience were of greatest importance.
I thank Dr. Bjarni Ásgeirsson for the mass spectrometry, introducing me to good data-handling software and helpful conversations. I thank Dr. Magnús M. Kristjánsson for helpful conversation including the two-state approach. I thank Dr. Baldur Símonarson for reading over the thesis and giving me helpful tips.
Kristinn, Einar, Björn, Lilja, Unnur and co-workers at Science Institute are thanked for their company throughout my studies.

I like to thank my girlfriend Marta Serwatko for her endless love and support during my studies. My parents and family are thanked for their shown interest in my studies and support that I have received from them me throughout the years.

1 Introduction

For over 40 years there has been an escalating demand for thermostable but catalytically efficient enzymes in various industries [1][2][3][4][5][6]. Proteins, in general, are relatively unstable and lose their functionality and native conformation fast under various physicochemical conditions [4][8]. Making enzymes more stable is thus desired. Glycoproteins are often more stable than their unglycosylated counterparts [9], which is reflected in increased stability toward proteolysis, heat, storage and chemical denaturation [10]. Several approaches have been used to make more stable enzymes such as use of cosolutes, immobilization, site directed mutagenesis and bioconjugation. Bioconjugation has been gaining popularity since it is relatively simple and the acquired stabilizition can be very high [1].
In this study, trypsin was conjugated to amino groups of chitooligosaccharide (forming intermolecular cross-links) and D-glucosamine via its carboxyl groups (and other groups) by carbodiimide and succinimdyl ester, for determination and comparison of stability and altered functional properties. The D-glucosamine conjugation can also be viewed as glycation. Bovine trypsin was chosen as a model enzyme, since it is throughly studied in the past, has a well-defined three dimensional structure, is rather inexpensive and easily assayed.

1.1 Bovine trypsin

1.1.1 General structure and classification

Bovine trypsin is a proteolytic hydrolase which consists of 223 amino acid residues [11][12][13]. Its molecular weight is 23305 Da, it has an isoelectric point of approx. 10 [12], and the enzyme has an extinction coefficient of 37650 M^{-1} cm^{-1} at 280 nm in water [14]. Bovine trypsin belongs to the S1 family of serine endopeptidases (according to MEROPS classification system [15]) .
Trypsin is classified as β-protein due to its high content of β-sheets. The enzyme has 13 pleated β-strands, which form 2 β-barrel motifs, and 3 small α-helices.
The tertiary structure of trypsin is held together by 6 disulfide linkages [11]. As in all other S1 serine proteases, it contains an active site with the catalytic triad of His46, Asp89 and Ser183 [12][16]. The active site is located in a cleft between the β-barrels.
Figure 1.1 represents the structure of bovine trypsin and figure 1.2 gives the amino acid sequence of trypsin(ogen).

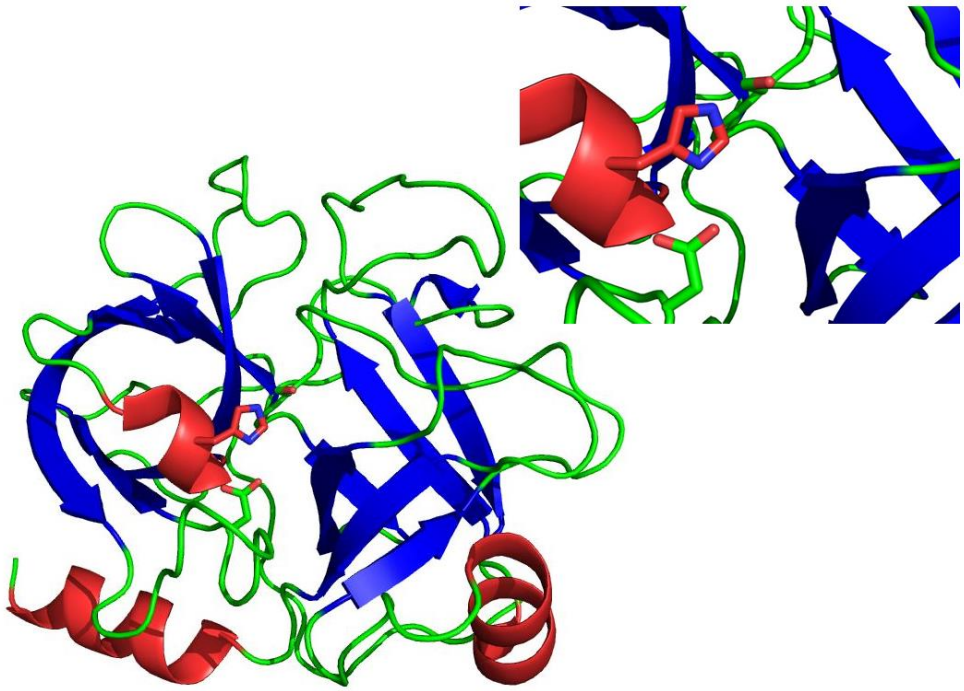

Figure 1.1. *Cationic bovine β-trypsin in a cartoon representation. α helices are colored red, β-sheet blue and loops green. The pleated β-sheets form an antiparalell β-motifs in where the catalytic triad is situated in between (zoomed up in the right corner). Made in Pymol Molecular Graphic system Vs. 1.3 by using trypsin PDB file code: 4i8g.*

```
  3          13          23          33          43          53
VDD DDKIVGGYTC GANTVPYQVS LNSGYHFCGG SLINSQWVVS AAHCYKSGIQ

             63          73          83          93         103
    VRLGEDNINV VEGNEQFISA SKSIVHPSYN SNTLNNDIML IKLKSAASLN

            113         123         133         143         153
    SRVASISLPT SCASAGTQCL ISGWGNTKSS GTSYPDVLKC LKAPILSDSS

            163         173         183         193         203
    CKSAYPGQIT SNMFCAGYLE GGKDSCQGDS GGPVVCSGKL QGIVSWGSGC

            213         223    229
    AQKNKPGVYT KVCNYVSWIK QTIASN
```

Figure 1.2. *The amino acid sequence of active trypsinogen/trypsin. The red colored characters is the hexapeptide of trypsinogen, which when cleaved off yields activated β-trypsin. The characters underlined in blue refer to the catalytic triad of His46, Asp80 and Ser183. The yellow characters refer to the autolytic Lys131-Ser132 bond which upon cleavage leads to the α-trypsin isoform. Further cleavage of the green coloured Lys176-Asp177 leads to ψ-trypsin (a.k.a. pseudotrypsin) isoform. Sequence retrieved from ref. [11].*

1.1.2 Activation of trypsinogen

Bovine trypsin, as well as other mammalian trypsins, is synthesized by acinar cells of the pancreas. It is secreted into the pancreatic duct as inactive trypsinogen [11]. Trypsinogen

is transformed into trypsin by cleavage of the Lys6-Ile7 hexapeptide near to the N-terminus of the zymogen. This activation process is catalyzed by a variety of enzymes in the intestinal fluids such as enterokinase and other activated trypsins [12]. Cleavage of this hexapeptide is essential to enable a structural rearrangement to take place with the newly exposed Ile7 N-terminus, which binds to Asp182 next to the active site Ser183 in the GDSGG motif [12][16]. The hexapeptide at the N-terminus of trypsinogen has a high homology from one organism to the next. The hexapeptide is a highly charged N-terminal peptide with the general sequence X-Asp_4-Lys (Bovine: Val- Asp_4-Lys) which is cleaved to expose the N-terminal isoleucyl residue of the activated trypsin [12].

1.1.3 Calcium ions, stability and optimal conditions

Calcium ions are essential for accelerated activation process of trypsinogen into trypsin [12][17]. At high calcium concentration, calcium ions bind coordinately to the four aspartyl residues of the trypsinogen, without inducing changes in the structure of the zymogen, which increases the affinity of the Lys6-Ile7 bond cleavage [18]. Calcium also stabilizes trypsin against autolysis, increases slightly its proteolytic activity and makes it more heat stable [12][17][19]. Merkel and Sipos showed that in order for the Ca^{2+} to have an effect on heat stability of trypsin at 60 °C, the minimum effective calcium concentration should have to be 2 moles for each mole of trypsin. The heat stability increases with more calcium concentration up to 2000 moles for each mole trypsin. After that, increasing concentration of calcium do not result in further stability [17].
They also demonstrated that calcium induces significant structural changes in the molecule [17]. This altered calcium induced structure possesses greater thermal stability than trypsin without calcium, since calcium reduces interactions between charged residues and causes a shift of the tyrosine and tryptophan chromophores from a polar environment (aqueous) to a nonpolar environment in the interior of the molecule [20], which leads to more compact structure [19]. As stated earlier, calcium ions are essential in order to minimize autolysis of trypsin. It binds to the so-called autolytic loop of Glu58 and Glu68 [21].

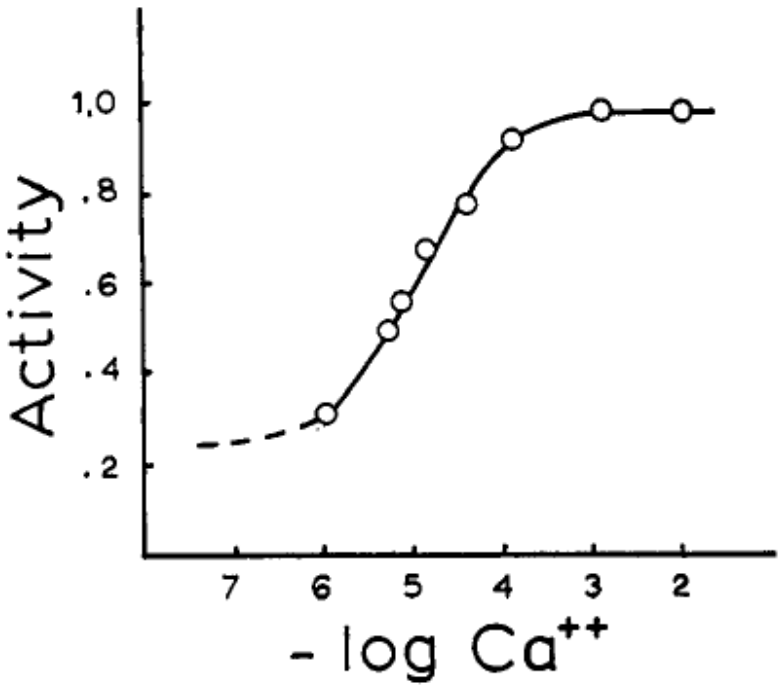

Figure 1.3. *The effect of calcium ion concentration on the activity of trypsin at 60 °C. From ref. [17].*

Trypsin has an optimal pH range of 7-9 [17]. Both trypsinogen and trypsin are reversibly denatured by pH extreme [22] and trypsin loses all enzymatic activity reversibly in 8 M urea. The enzyme still has 50 % activity in 4 M urea at physiological pH and ambient temperature [23], which is close to its $U_{1/2}$ of 4.1 M for PSMF-inhibited (PMSF: phenylmethylsulfonylfluoride) bovine trypsin at pH 8.0 however, at prolonged time the enzyme is irreversibly inactivated under those condition due to autolysis of those trypsin molecules that still retain activity [24].

1.1.4 Enzymatic properties and mechanism of catalysis

One of the most striking feature of trypsin is its specificity towards substrate, as for peptide its catalysis is exclusively directed toward L-lysyl and L-argininyl bonds of peptides and proteins[11][12]. It has the most specific action of any known endopeptidase [12]. Its catalysis is only active toward peptide, amide and ester bonds, with a R-CO-X or R-O-X moiety where R is either lysine or arginine. Synthetic ester substrates such as BAEE (benzoyl-L-arginine ethyl ester) or TAME (p-toluenesulfonyl-L-argininie methyl ester) and synthetic amide substrate such as BEAA (Benzoyl-L-argininamide) and BAPNA (N-benzoyl-L-arginine p-nitroanilide) are frequently used for trypsin activity measurements [12].

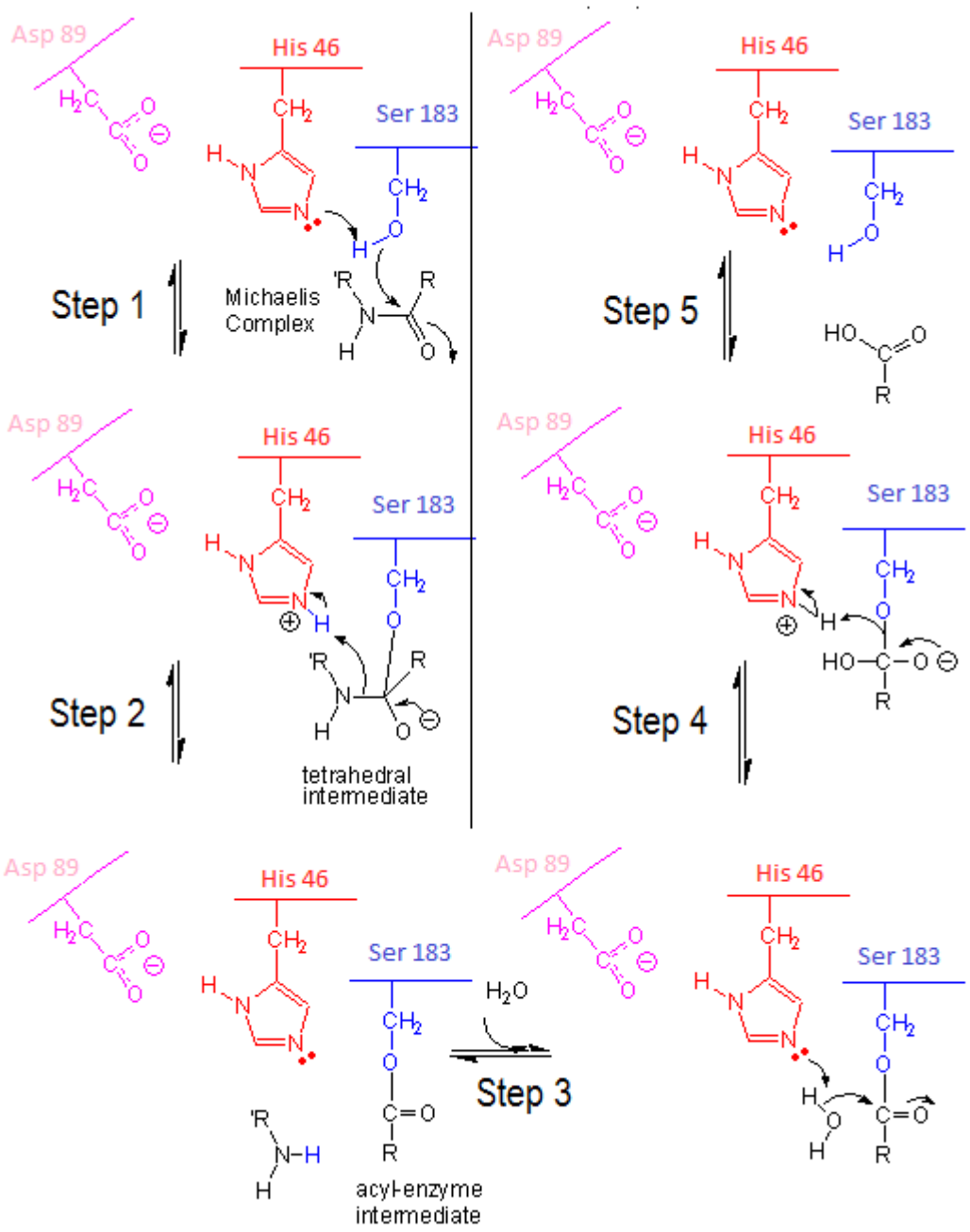

Figure 1.4. *Reaction mechanism scheme of trypsin. Adapted from ref. [25].*

Figure 1.4. represents the reaction mechanism (i.e. catalysis) of trypsin. The catalysis begins when the negatively charged Asp89 of the active site attracts a positive charged arginyl or lysinyl residue of the substrate. When the substrate has been pulled into the active site pocket, a nucleophilic N-atom of His46 takes a proton from the hydroxyl group of Ser183, which in turn makes Ser183 a nucleophile. Subsequently, this deprotonized hydroxylanion of Ser183 conducts a nucleophilic attack on the electrophilic central carbonyl-carbon of the amide (or the central carbonyl-carbon of the ester) (Step 1, figure 1.4). That forms an unstable oxyanion tetrahedral intermediate of the substrate. Meanwhile, the anionic Asp89 stabilizes the positive charge of His57. Next, the electrons of oxyanion forms again a stable π-bond with the central carbon. Simultaneously, the first half of the substrate or the amine leaving groups leaves by stripping a proton from His46. This

procedure changes the oxyanion tetrahedral intermediate into an acyl-enzyme intermediate (Step 2, figure 1.4). In Step 3 of figure 1.4, a water molecule attacks the acyl-enzyme intermediate forming once again a tetrahedral intermediate. Simultaneously, histidine strips a proton from the water molecule. In step 4 of figure 1.4, the unstable oxyanion forms a stable π-bond with the central carbon again, which results in an increased nucleophilic character of the σ-bond between the central carbon of the original substrate and the oxygen atom of Ser183. This σ-bond strips a proton from the His46, which in turn makes this other half of the substrate to leave as a carboxylate (Step 5, figure 1.4) [25].

1.1.5 Isoforms of bovine trypsin

Trypsin has three active isoforms. Of those three isoforms, two are autolytic products of native activated trypsin, but native trypsin is usally refered to as β-trypsin. These isoforms are different with regard to specificity and function. At a suitable conditions, e.g. where there is little or no protection by Ca^{2+} ions, autolysis occur. Cleavage of the Lys131-Ser132 bond leads to α-trypsin and further cleavage of the Lys176-Asp177 leads to ψ-trypsin or pseudotrypsin (fig.2.) [11][12]. More cleavage yields inactive autolytic components. The chains of the autolytic forms (α and ψ) are solely hold together by disulfide linkages. These isoforms can be chromatographically separated [12]. Cleavage of Lys49-Ser50 or Arg105-Val106 yield products that do not deviate much from the properties of β-trypsin, hence these autolytic products are just simply refered as β-trypsin [12]. Table 1.1 shows the different properties of the three isoforms, with respect to their catalytic function towards couple of synthetic substrates.

Table 1.1. *Isoforms of bovine trypsins and their different activity profiles. Abbreviations: BAPNA: N-α-benzoyl-L-arginine p-nitroanilide, BAEE: N-benzoyl-L-arginine ethyl ester, TAME: p-Toluenesulfonyl-L-arginine methyl ester. Adapted from ref. [12]*

Internal bond cleaved	***Isoform***	***Substrate activity***
None	β-Trypsin	All common substrates
Lys49-Ser50	β-Trypsin	All common substrates
Arg105-Val106	β-Trypsin	BAEE
Lys131-Ser132	α-Trypsin	BAPNA/TAME
Lys176-Asp177 and Lys131-Ser132	ψ-Trypsin	BAEE/BAPNA/BAEE

1.2 Chitin and chitosan

Chitin is a biopolymer that consists of repetitively linked 1,4-β-N-acetyl-D-glucosamine units of different lengths (fig 1.5.). Chitin is the second most abundant biopolymer in the biosphere after cellulose [26], with a working estimate for the annual turnover in the range of 10^{10}–10^{11} tonnes [27]. In nature, chitin occurs as two allomorphs, i.e. α and β forms, that can be differentiated by infra-red and solid-state NMR spectroscopy together with X-ray diffraction. These allomorphs occurs as well-ordered crystalline microfibrils, with the polymer chain of alpha form ordered an anti-parallel manner and the β-chitin ordered in a parallel manner (fig 1.6) [27][28].

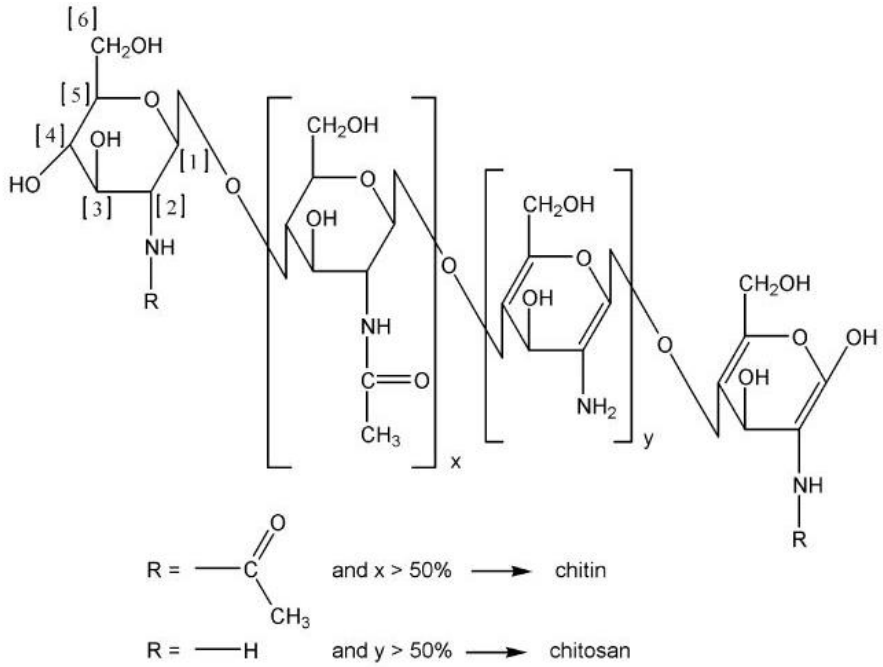

Figure 1.5*. Structures of chitin and chitosan. From ref.[31]*

A third allomorph (γ) has been described, however detailed analysis has showed it to be a variant of the two main forms [28]. The crystalline structure of chitin is well packed and held together by intra-and intermolecular hydrogen bonds, making chitin insoluble in most common solvents, including water [27] . However, chitin can be dissolved in a solvent with high polarity (i.e. dipole moments) such as trichloroacetic acid. α-Chitin is probably thermodynamically more stable than β-chitin, since β-chitin is always recrystallized as α-chitin from a suitable solvent [28, and references therein]. α-Chitin occurs in fungal and yeast cell walls, in krill, in lobster and crab tendons and shells, and in shrimp shells, as well as in insect cuticles. The rarer β-chitin is found in association with proteins in squid pens and in the tubes synthesized by pogonophoran and vestimetiferan worms [27][28, and reference therein].

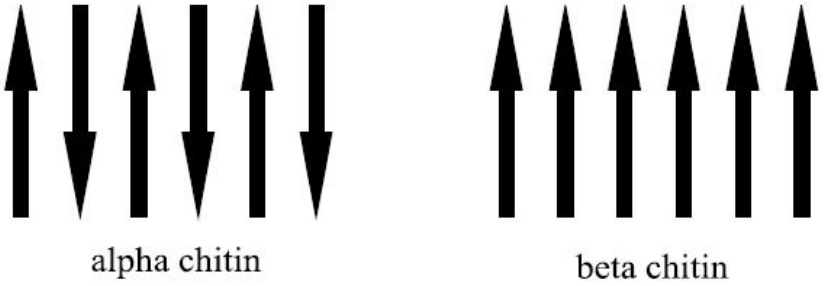

Figure 1.6. *Ordering of the two allomorphs of crystalline chitin. From ref [26].*

Chitin can be readily obtained by simple extraction, e.g. chitin extraction from shrimp shells is usually carried out by using 4 % NaOH for deproteinization and 4 % HCl for demineralization. The major source of industrial chitin comes from wastes of marine food production, mainly crustacean shells, e.g. shrimp, crab or krill shells. In the processing of shrimps for human consumption, between 40 and 50 % of the total mass is waste, whereby 40 % of the waste being chitin [27]. Chitin is mainly used as the raw material to produce chitin-derived products, such as chitosans, oligosaccharides and glucosamine [27].

Chitosan is at least 50 % deacetylated chitin derivative (fig 1.5) [27][28]. Chitosan has thus no fixed stoichiometry, but can be defined as poly-1,4-β-D-glucosamine, with a certain percentage of its amino groups acetylated, known as degree of acetylation (DA). However, chitosan is most commonly reported with respect to degree of deacetylation (DD). The DD is simply 1-DA [29]. When the repeated glucosamine/acetylated glucosamine units of the chitosan polysaccharides are few they are are refered to as chitooligosaccharides. Chitosan can be obtained by partial deacetylation of chitin in the solid state under alkaline conditions (in conc. NaOH) or by enzymatic hydrolysis of chitin deacetylase. Chitosan obtained by a solid-state reaction of chitin, have a heterogenous distribution of the still-occuring acetyl groups along their chain. This is important, since it has been demonstrated from NMR measurements that the distribution of acetyl groups must be random to achieve the higher water solubility, when 50 % of the polymer is still acetylated [28, and references therein].
Chitosan is usually soluble in acidified aqueous media, the extent of its solubility is governed by various factor such as degree of DA, length of the polymer and, as earlier stated, the distribution of the N-acetyl groups. The solubilization in acidified aqueous media occurs by protonation of the amino functional group on the C2 position (fig 1.6) of the D-glucosamine units, turning the polymer into a polyelectrolyte [28]. Hence, the solubility of chitosan is governed by the extent of protonization of the free amino group [30]:

$$R - NH_3^+ + H_2O \leftrightarrow R - NH_2 + H_3O^+ \qquad \textbf{Equation 1.1.}$$

$$K_a = \frac{[R-NH_2][H_3O^+]}{[R-NH_3^+]} \qquad \textbf{Equation 1.2.}$$

For polyelectrolytes, the dissociation constant is not a true constant, but depends on the degree of dissociation at which it is determined.

The variation of pK_a can be calculated using Katchalsky's equation [31]:

$$pK_a = pH + log\left(\frac{1-\alpha}{\alpha}\right) \qquad \textbf{Equation 1.3.}$$

where α is the true degree of dissociation of chitosan [30]. The pK_a value is different with respect to molecular weight and different DD. Wang et al. measured pK_a values of chitosans with different molecular weights in the range from 1370 to 60 kDa and chitosans with different DD in the range from 94.6% to 73.3% . The pK_a decreased from 6.51 to 6.39 for the molecular weight of 1370 and 60 kDa, respectively, but the pK_a increased from 6.17 to 6.51 for the DD of 94.6% and 73.3%, respectively [30]. Generally, chitosan has a pK_a value in the range of 6.2 – 6.5, which makes it soluble in an aqueous solution with pH below 6.5 [26].
Chitosan is the only pseudonatural cationic polymer and thus finds its many applications that follow from its unique character (flocculants for protein recovery, depollution (e.g. heavy metal chelator) etc.). Being soluble in sligthly acidified aqueous solutions, it is has found its use in different applications as such in gels, films or fibers [28]. It has also found its place in medicine, because of its biodegradability, biocompatibility and non-toxicity [27]. Chitosan has also been used in enzyme stabilization studies [59].

1.3 Industrial enzymes

Enzymes are now a considerable sector in the in industry and biotechnology. The global market for industrial enzyme was worth $ 2.3 billion in 2007, with a compound average annual rate of 4% [7]. These industries include biomedicine, textile industry, food and bevarages as well as more recent analytical aids such as in biosensoring [32]. Technical use of enzymes is only practical if they are stabilized against heat, pH extremes and chemical denaturants, e.g. surfactants, high salt concentration etc. for weeks and even months [7][33]. So the challenge is to stabilize them [32] . Finding new ways to stabilize mesophilic enzymes, since they are catalytically more active than thermophilic enzymes, is of practical importance. Justifications of acquiring thermostable mesophilic enzyme include:
1) Enzyme rates and diffusion of substrate are increased at higher temperatures. By increasing temperature from 25 °C to 75 °C the enzymatic rate of a typical enzyme is increased 100-fold.
2) High temperature in enzyme reactors severely decreases possible microbial contamination. Microbial growth can secrete degrading proteases and stopp filters of a reactor system [33].
3) From a productivity standpoint, it is preferred that the substrate is completely dissolved. This can be accomplished by raising the temperature of the reacting system [33].
Most proteases are less stable than other enzymes due to autolysis [34]. Therefore, it is feasible to find solutions to eliminate their autolytic behavior as well as conformationally stabilize them.

1.4 Protein stability

1.4.1 A general overlook over stability of proteins

Folded proteins have well defined three dimensional spatial configuration determined by their amino acid sequence (primary structure) and highly specific secondary structures which are formed to enable proteins to be in their lowest free energy state. The secondary structures to which proteins folds into, are greatly inhibited and only one active combination can be reached [8][35]. This is due to factors such as the permitted rotation of polypeptide backbone, more specifically between N-C_α and C_α-C bond of the primary structure. The rotation angles between these bonds (known as φ and ψ) are sterically restricted in and out of the plane of the polypeptide, forcing the protein to fold only into limited secondary structures: α helices, β sheets and loops. Permitted angles can be seen from a Ramachandran plot of φ and ψ rotational angles [35].

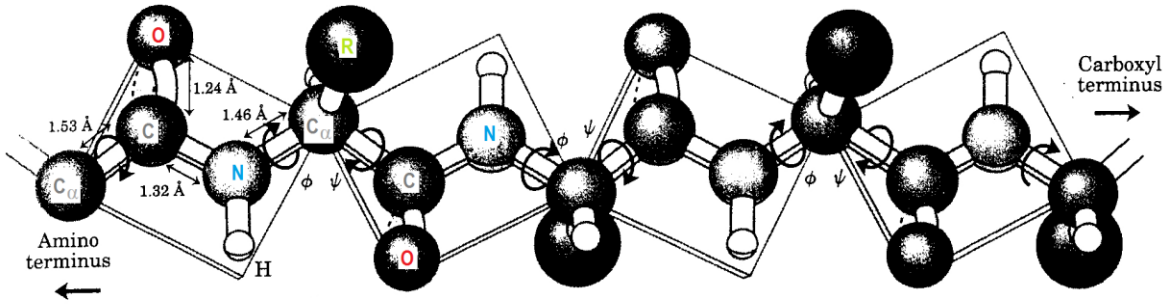

Figure 1.7. *Primary structure of proteins with its corrsponding rotational angles. Adapted from ref. [35].*

Disulfide linkages is the the only covalent interaction that contributes significantly to the conformational stability of proteins [36]. Apart from covalent disulphide linkages (which are absent from some proteins), the free energy of a folded protein is dependent upon four major contributions of noncolvalent interactions: hydrophobic effect, hydrogen bonds, electrostatic interactions and conformational entropy due to restricted motion of the peptide backbone (table 1.2) [8].

Table 1.2. *Noncovalent interactions of proteins and their mode of stabilizing or destabilizing. From ref. [8]*

Noncovalent interaction	**Type of contribution**
Hydrophobic effect (due to van der Walls interactions)	Stabilizing
Hydrogen bonds	Stabilizing
Electrostatic interactions	Stabilizing or destabilizing
Conformational entropy	Destabilizing

Strictly speaking, the hydrophobic effect cannot be viewed as an interaction, but rather a consequence of an unfavorable interaction between polar solvent and apolar solutes. It stems from the entropic effect arising from rearrangement of water molecules into cagelike

semi-crystalline clathrate polyhedron structures around apolar solutes, which is energetically unfavourable, thus driving apolar solutes together [8][37]

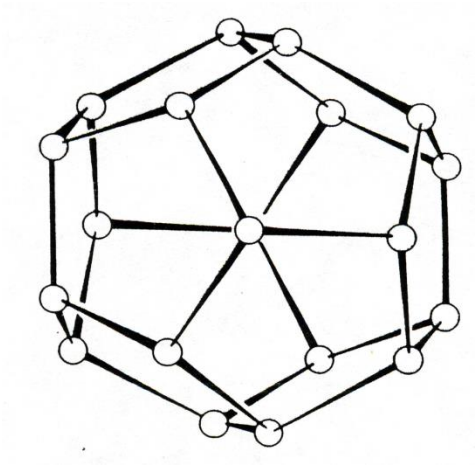

Figure 1.8*. A typical water clathrate that forms around nonpolar residues of proteins. From ref. [37].*

Apolar solutes are therefore packed into the interior of proteins where they interact via van der Waals interactions [8][37].
Hydrogen bonds between the N-H and C=O groups of the peptide backbone act as the „glue“ of secondary structures [37]. They also bind polar side chains of amino acid residues together [38]. The role of hydrogen bonds in a folded protein has traditionally been underestimated, due to their dynamic behavior. However, mutational studies have shown that intramolecular hydrogen bonds do contribute significantly to the overall stability of folded proteins [8, and references therein].
While hydrogen bonds and the hydrophobic effect are essentially nonspecific, electrostatic interactions are largely specific, and therefore play an important role in determining the folding of a protein as well as in protein flexibility and function [8]. Electrostatic interactions are generally between positively charged amino/guanindino groups and negatively charged carboxyl groups [37]. On average, only 1/3 of charged groups form an ion pair and 3/4 of these ion pairs are included in secondary structures [39]. Computational and experimental evidence shows that salt bridges can be stabilizing or destabilizing [8] . Extra salt bridges are commonly seen in thermostable proteins when compared with their mesophilic counterparts [8]. Conformational entropy of the polypeptide is the single most destabilizing contributor to the folded state of proteins, since the intrinsic entropy of the polypeptide chain is greatly reduced in the folded state. The stabilizing effect of the noncovalent interactions enlisted above serves as the enthalpic contributors and the destabilizing conformational entropy serve as the entropic term to the total free energy of a protein according to Gibbs equation:

$$\Delta G = \Delta H - T\Delta S \qquad \textbf{Equation 1.4.}$$

where ΔG is the free energy, ΔH is the enthalpy, T is the temperature and ΔS is the entropy of a protein in a closed system with a constant pressure [8].
According to eq 1.1. one can see that the total enthalpic contribution of noncovalent (and covalent) interaction must counterbalance the the conformational entropy if the protein is to be stable in its folded state. In reality, proteins tend to be only marginally stable, even

under physiological conditions [40]. Conformational stability, ΔG_D, of most globular proteins is only in the range of 20-60 $^{kJ}/_{mole}$ [40][41], which can be compared with one mole of hydrogen bonds [40]. This relative instability of these macromolecules suggests that evolutionary optimization of the protein structure is based on functions such as catalysis and high turnover numbers and not on stability [42].
Proteins unfold or lose their highly specific structure when their enthalpic contribution is outweighed by entropic forces. Unfolding can take place through various physical or chemcial forces such as heat, cold, extreme pH, pressure, presence of denaturing reagents etc. The mechanism of unfolding can be complicated and many models have been proposed [8]. However, the simplest model of unfolding (and refolding) is the two-state model, that involves a single cooperative unfolding step (and refolding), and works well for describing the folding of small proteins:

$$F \leftrightarrow U \qquad \textbf{Equation 1.5}$$

where F is the folded state and the U is the unfolded state. However, intermediates are observed to accumulate during folding of other proteins especially more complex ones. The term „molten globule“ is assigned to intermediate states of proteins which display a sign of an intermediate. All of the proteins that had proved to have to an intermediate state between folded and unfolded state, had an intermediate with compact configuration, native-like secondary structure, however the spatial configuration of the secondary structures (a.k.a. tertiary structures) was interrupted.

$$F \leftrightarrow MG \leftrightarrow U \qquad \textbf{Equation 1.6}$$

where MG is the intermediate „molten globule“ state [8].
Energy landscapes enable one to understand the microscopic behavior of a molecular system. Energy landscape of a system with n degrees of freedom is a energy function:

$$F(x) = (x_1, x_2, x_3, \dots, x_n) \qquad \textbf{Equation 1.7}$$

where the x’s are variables specific for the microstates of the system. For proteins, x’s can for instance be all the dihedral angles of the chain or other microstates relevant to the protein, that specify the conformation of the protein. F(x) is usually defined as the free energy of a given microstate in a macroscopic protein. The stable conformation of the protein can be found by determining the set of values x_1, x_2, x_3,...,x_n , which are parameters dependent upon the conformation of the protein, that gives the minimum value of the free energy function. Generally, random heteropolymer, such as proteins, have a very rugged energy landscape with many local minima. Protein chains thus get trapped in one of many local minima and usually do not have a well defined single stable conformation. In reality, proteins are not random sequences, evolution has optimized them, so they fold quickly into a well defined three-dimensional structures. This optimization of Nature has yielded proteins with funnel shaped energy landscapes.

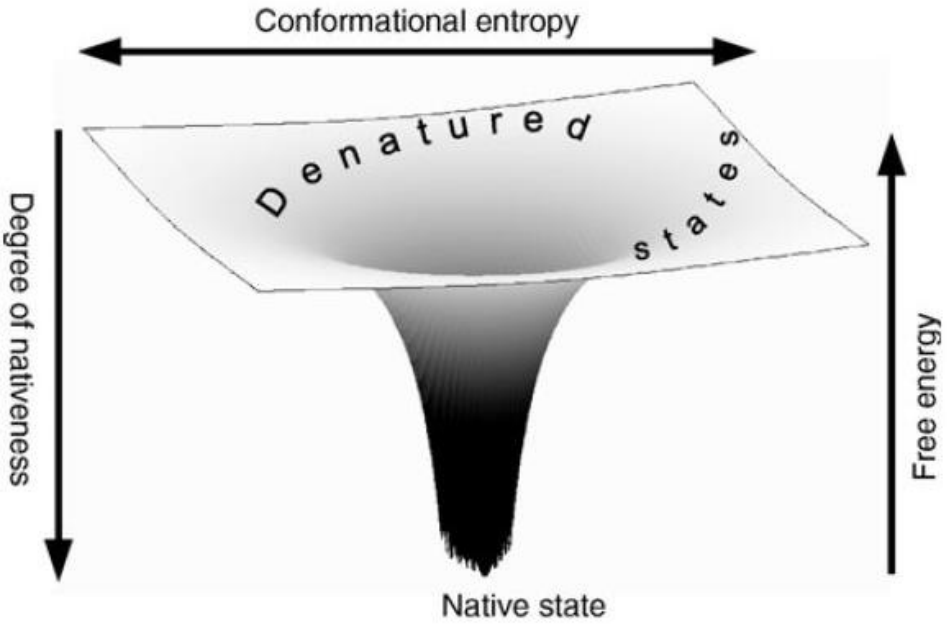

Figure 1.9. *A typcial energy landscape of a protein. Nature optimized proteins to have energy landscapes like a funnel, since the consequence is beneficial to all life form. From ref. [8].*

A funnel shaped energy landscape of proteins (fig 1.9) is not surprising since the free energy and the entropy of the polypeptide are minimized in the native state. In the denatured state the polypeptide can have wide ranges of configuration with similar free energies.
The fact that proteins have funnel shape energy landscapes has two important consequences. First, the native structure should tolerate point mutations here and there, since small pertubations to the energy landscape do not have a great impact to the overall shape and the location of global minima. As a consequence, a mutated protein has therefore essentially the same conformation as the wild type protein, and if two protein sequences are evolutionary highly related, one could be assured that the difference in their conformation is negligible. Secondly, assuming that the energy landscape is a perfect funnel, its shape is completely determined by the topology of the native state, and this completely determines the folding mechanism [8, and references therein].
The energy landscape of proteins is never a perfect funnel, it is always a little rugged. This is because of kinetical traps such as cis-trans isomerization of the peptide bond (trans isomer being the stable one, with the important expection of proline) and formation of correct disulfide linkages of cysteines.
The landscape theory of protein folding also gives a clue to chaperone function. To get a misfolded protein to fold correctly, the chaperone just moves the misfolded protein to the top of the funnel where it can restart the downhill search for correctly folded protein [8].

When a protein unfolds, it ends up exposing its hydrophobic interior towards the solvent. Thus unfolding of proteins is typically accompanied by a high positive heat capacity change (ΔC_p) , which can be treated as a constant for a wide temperature range. If a protein follows a two-state approach with respect to its unfolding, and its ΔH_m and ΔC_p values are known at a given condition, a stability curve of that protein can be evaluate over a given temperature range [43], according to the Gibbs-Helmholtz equation [24]:

$$\Delta G = \Delta H_m \left(1 - \frac{T}{T_m}\right) + \Delta C_p \ (T - T_m + \ln(\frac{T}{T_m}) \qquad \textbf{Equation 1.8}$$

A protein stability curve is thus made by treating ΔH_m and ΔC_p as constants and only varying the temperature [43].

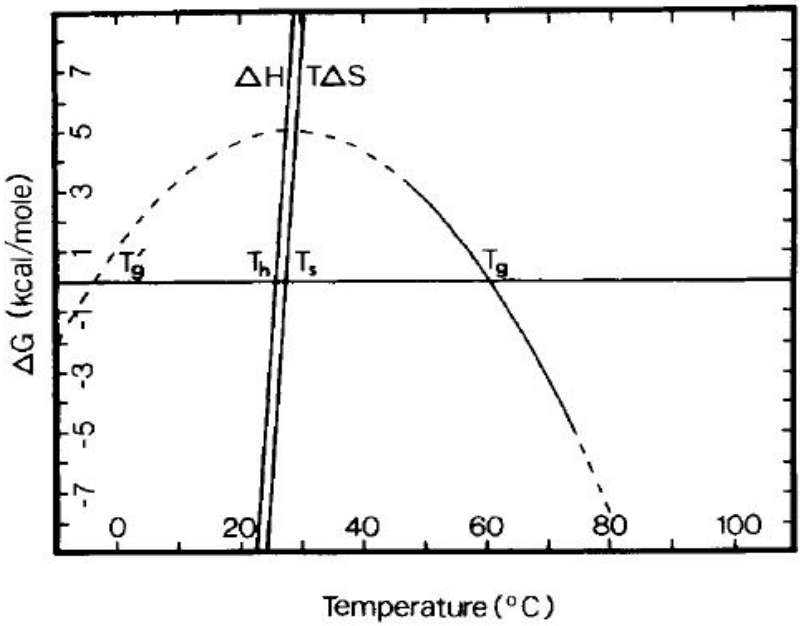

Figure 1.10. *Schematic representation of a typical protein stability curve. From ref. [43].*

As figure 1.10 represents, stability curves of a typical protein is a parabola. The highest point of the curve is T_{max} or the temperature where the protein is the most stable and it is also where ΔG is the highest [24]. One can observe two intersections of the x-axis by the parabola, i.e when $\Delta G = 0$. This represents the temperatures where half of the protein molecules have unfolded (shown as T_g' and $T_g(=T_m)$). As the temperature gets lower in case of T_g' or higher in case T_g, unfolding gets to be more spontaneous process (ΔG gets more negative). This underlines the fact that protein can be unfolded by either cold or heat.

1.4.2 Lessons from hemophilic proteins

Thermophilic proteins share similar three-dimensional conformation with their mesophilic counterparts [7]. Although the structure is similar, there are some notable differences between mesophilic and thermophilic proteins. Thermophilic proteins tend to have an increased number of salt bridges, hydrogen bonds and/or alkyl groups in the interior of the protein [37].
In thermophilic proteins arginine replaces lysine but these amino acids are mostly found on the surface of proteins. The reason of this replacement is because with lysine there is a more unfavourable interaction with the solvent, since lysine has one more methylene group than arginine, as well as the fact that arginine has a 1.5 unit higher pK_a value of the guanidinum group than the ε-amino group of lysine. The consequence of the higher pK_a value is that arginine has a higher capacity to withold an ion pair interaction with increased temperature, because pK_a increase with increased temperature [37]. Other alterations that

are commonly observed in thermophilic proteins include higher proline content, lower asparagine/glutamine ratio, decreased disulfide linkage content, absence of cysteine residues, less content of hydrophobic amino acids and enhanced packing of the hydrophobic interior [7][37].
When proteins adapted to higher temperature (increased intrinsic intrinsic T_m [44]), in terms of evolution, they have had to make a „decision“: either be catalytically more active or thermostable. Evolutionary pressure led thermophilic enzymes to adapt to higher temperature by reducing their overall flexibility and thus lowering their catalytic turnover number (k_{cat}) [37].

1.5 Enzyme inactivation

1.5.1 General overview of enzyme inactivation

Enzyme inactivation tends to be a complex process, but can be simplified with the Lumry-Eyring approach. According to that approach, enzyme inactivation is a two-step process, which consists of reversible unfolding step followed by kinetically irreversible step. The latter step is due to aggreagation, covalent changes and/or autolysis, in case of proteases [7][33]:

$$N \overset{k_1}{\Leftrightarrow} D \overset{k_2}{\Rightarrow} I$$ **Equation 1.9**

The first crucial step of enzyme inactivation of enzyme is full or partial unfolding, as described in previous subchapter (*1.4*). When unfolding occurs, the enzyme loses its highly ordered structure and which causes key catalytic residues to disassemble, rendering the enzyme inactive [33][40]. This process is usually reversible (first step in eq 1.9. with a rate constant k_1), however it is the subsequent steps that lead to total inactivation (second step in eq 1.9., with a rate constant k_2).
Autolysis is one of the main causes of irreversible inactivation of proteases and protein molecules can also refold into stable incorrect structures [33].

1.5.2 Mechanism of enzyme inactivation

Enzymes are typcially rendered inactive at conditions that exposes them to extreme pH, high concentration of chaotropic salts or high salt concentration in general, prolonged oxidation and heat. Unfolding by extreme pH can often lead to irreversible aggregation. Oxidation can have detrimental effects on enzymes, especially of the thiol and aromatic-ring containing residues which can lead to irreversible covalent changes [49]. High concentrations of salts and presence of chaotropic salts can exert an unfolding force upon enzymes, however that is usally a reversible process and the enzyme will refold when the salt is removed. Temperature higher than 60 °C typically render the hydrophobic interaction inactive [45], favoring the unfolded state which typically leads to aggregation or covalent changes. Aggregation is a complex two-step multi-molecular reaction and is due to adsorption of unfolded enzyme molecules via hydrophobic interactions, but depends greatly on protein concentration [33][40] . Small globular proteins in a dilute solution (< 1 mg/mL) tend not to aggregate even at high temperatures [37]. At temperatures over 70 °C,

pH dependent covalent reactions limit the reversability of enzymes e.g. deamidation of asparagine and glutamine residues, Maillard reactions (in presence of reducing sugars), hydrolysis of the peptide bond at aspartic acid residues and oxidation of disulphide linkages [33][40].
Which inactivation mechanism the enzyme follows is dependent upon the enzyme and how harsh a physicochemical strain is exerted on the enzyme [33]. Figure 1.11, shows the two commonly known inactivation pathways.

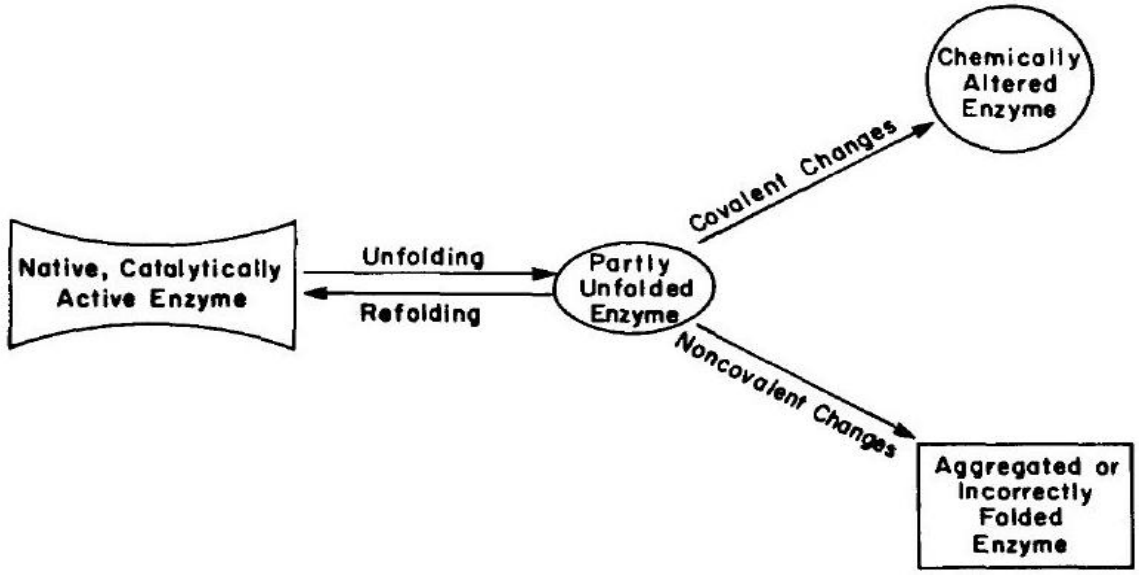

Figure 1.11. *Diagram of enzyme inactivation listing different events. From ref. [33].*

The terms unfolding and denaturation is used interchangably, but inactivation is a related but a different term. Unfolding is a loss of the tertiary and secondary structure of a protein. If the protein is an enzyme, then inactivation takes place when key catalytic residues are not aligned closely enough to engage in a catalytic process [7][33]. This often happens before the mid-transition of unfolding has been reached. Therefore one finds that the $T_{50\%}$ and T_m values for a given enzyme, at same condition, are different.

1.6 Increasing stability of enzymes

As stated earlier, thermophilic enzymes are less flexible and as a consequence have a lower catalytic efficiency than their mesophilic counterparts [7][37]. Based on that fact, many research groups, in the past and in present times, have made effort to stabilize mesophilic enzymes and turn them into thermostable enzymes. Stabilization should ideally meet three criteria. First of all, it should reduce the rate constant of inactivation (k_{in}) of an enzyme. Secondly, it should increase the half-life of an enzyme at given condition. Last but not least, it should be able to tolerate incubation at higher temperatures and conditions, it would otherwise not tolerate [33]. In this chapter, general stabilization methods will be pinpointed: Stabilization by cosolutes, site-directed mutagenesis, immobilization, cross-linked enzyme aggregates /cross-linked enzyme crystal (CLEC/CLEA) and soluble bioconjugation.

1.6.1 Stabilization by cosolutes

Addition of cosolutes is the most popular enzyme stabilization method, particulary for storage stability. Additives are used to most enzyme formulation available on the market [7]. For simplicity reasons, additives will be divided into two classes: Organic additives and salts. Organic additives are usually small molecules or polymers. Sugars, polyols, amino acids, glycerol, polyethylene glycol etc. are all known and widely used stabilizing organic additives. They provide increased stability to enzymes toward desiccation, extreme pH, freezing, high salt concentration and chemical denaturants through a mechanism known as preferential exclusion or preferential hydration [4][7][46][47]. Serge Timasheff [47, and references therein] and coworkers began more than 35 years ago to study the phenomena of preferential hydration of organic additives (a.k.a. preferential exclusion of the additives from the protein surface). Along with his coworkers he observed, without an exception, that of all of the organic cosolutes studied displayed negative binding stoichiometries to proteins, e.g. they observed that when ribonuclease A was suspended in a 1 M sucrose solution, -7.6 mole of sucrose was found to bind to one mole ribonuclease. This negative binding phenomenon is best understood by imagining a protein solution with a cosolute in a dialysis bag. At equilibrium following relation is true:

$$\nu = \frac{[\text{Ligand conc. inside the bag} - \text{Ligand conc. outside the bag}]}{\text{Protein conc.}} \qquad \textbf{Equation 1.10}$$

where binding (ν) is the ratio of moles of cosolute (additive) bound to mole of protein. Negative binding is therefore a depletion or exclusion of additive from the domain of the protein. Hence, binding is in fact a measurement of the relative affinity of the protein for water and the cosolute. Figure 1.12 represents a better picture of this phenomenon.

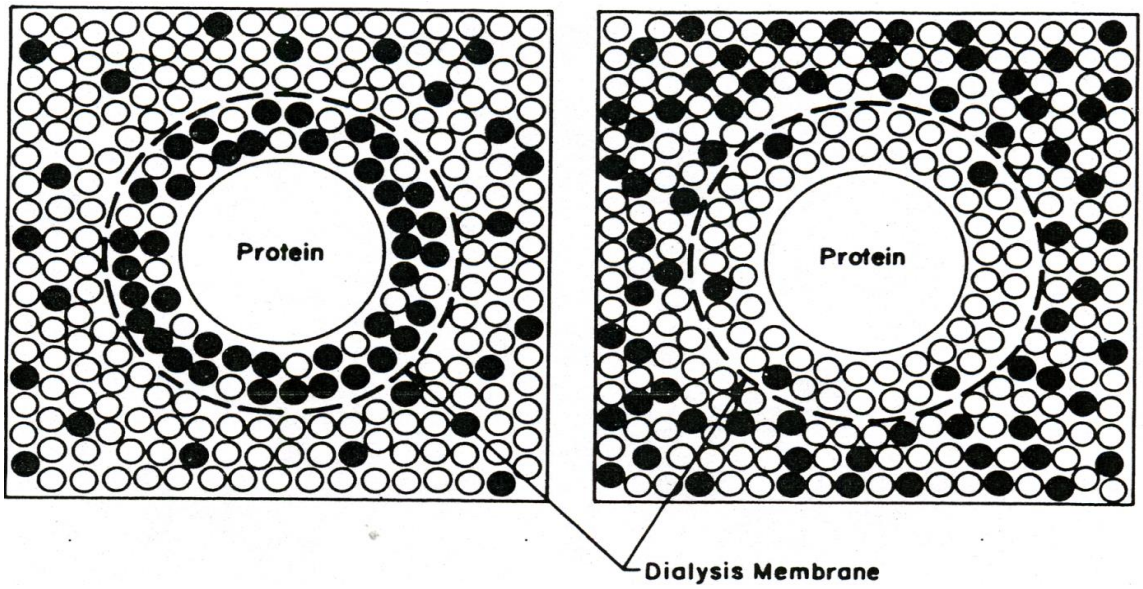

Figure 1.12. *Schematic representation of the preferential exclusion of organic solutes from the protein into the bulk water. On the left: The protein incubated with organic solutes (black-filled circles) in a dialysis bag. The white-filled circles represent water molecules. On the right: The same protein in the dialysis bag after equilibrium has been reached. Most of the solutes have been excluded from the neighboring domain of the protein, and so they are found in the bulk solvent (water) outside the bag. From ref. [47].*

Preferential exclusion of the additives is a consequence of a more favorable interactions of the additives with the bulk water rather than interaction with the enzyme/protein surface. Addition of organic additives in an aqueous protein solution results in a unfavorable positive free energy change in the protein, due to the exclusion of the additive, which is assumed to be higher in the denatured state of the enzyme due to greater surface area, so the equilibrium is supposed to be shifted towards native protein conformation, thus resulting in increased stability [4, and references therein]. It should be noted that additives increase T_m of proteins but they do not affect proteins denaturation free energy, ΔG_D. This means that intrinsic conformational stability does not increase, instead denaturation is made less favorable than without these additives [3] underlining Timasheff's and his coworkers theory of preferential exclusion.
Addition of salts can have a stabilizing or destabilizing effect. Either effect can be deduced from the Hoffmeister lyotropic series [7][40][46]:

$(CH_3)_4N^+ > NH_4^+ > K^+, Na^+ > Li^+ > Mg^{2+} > Ca^{2+} > Ba^{2+} >$ guanidinum$^+$
$F^- \approx SO_4^{2-} > HPO_4^- >$ acetate$^- > Cl^- > NO_3^- > Br^- > ClO_4^- > I^- > SCN^-$

Salts that reduce solubility of nonpolar groups of proteins (salting out) by increasing the surface tension of the protein solution are known as cosmotropic salts and are stabilizing. Furthermore, they also enhance formation of water clusters around the enzyme which leads to a loss in the total free energy of the system, since entropy of the solvent is reduced. The cations and anions on the left of the Hofmeister series are the most stabilizing ions (cosmotrops) .
Salts that preferentially bind to nonpolar amino acids leading to forming of a solvation layer around them, increase the solubility of nonpolar residues (salting in), interrupt salt brigdes and reduce the number of water clusters around the protein are known as chaotrophic salts. Therefore they shift the equilibrium of the protein from folded to unfolded state. The cations and anions on the right of the Hofmeister serie are the most destabilizing ions (chaotrops) [40][46].
The single greatest disadvantage of using additives is that they may interfere with the final use of the enzyme due to incompatibility with the reaction system and may decrease enzymatic rate due to higher viscosity and limited diffusion [7][48].

1.6.2 Stabilization by site-directed mutagenesis

The choice of mutation in an enzyme is based on protein design, sequence similarity, structural modelling or by random mutagenesis [38][49]. Engineering proteins by site-directed mutagenesis focuses on reducing the difference in entropy between the folded and unfolded state (i.e. reducing number of possible conformations of the unfolded state), stabilizing the α-helices and increasing the number of hydrophobic interactions in the interior core. Introducing favorable residue/s can result in dramatically increased stability [38]. Enzyme are commonly made more stable by substituting residues, introducing disulfide linkage/s or cavity filled with site directed mutagenesis [34]. Often, the starting point for site-directed mutagenesis is to replace glycine and introduce proline, since glycine has more conformational freedom than any other amino acid and proline has the least conformation freedom [38]. Introduction of disulfide linkages has been the straightforward answer for reducing entropy between folded and unfolded state. The stability of disulfide linkages is additive, the T_m increases with each linkage added [38]. Asparagine, which is a

thermolabile residue prone to deamidation, has been replaced by threonine or isoleucine which have a similar geometry but is more thermostable [7]. The drawback of site-directed mutagenesis is that there is only a change in a limited number of residues which may or may not stabilize a given enzyme, and mutagenesis is typically limited to the 20 primary proteinogenic amino acids [49].

1.6.3 Stabilization by immobilization

Immobilization has traditionally been the method of choice with regard to enzyme stabilization in industry. Immobilization can be divided into three types: binding onto solid matrices, encapsulation/entrapment into inorganic or organic gel and cross-linking of the protein molecule [50]. Immobilization onto solid matrices is probably the most common immobilization technique to increase stability of enzymes. Sometimes a protein surface is altered with mutatation of surface amino acid residues in order to make immobilization more effective. Immobilized enzyme are more heat stable than native enzymes due to spatial fixation of the enzyme molecule (lesser freedom to aggregate or to autolyze in case of proteases) [51][52]. For industrial uses, they are optimal since the product is easily separated from the enzyme and since they are immobilized they can be be in repetitive use . The drawbacks of immobilization is the excistence of substrate diffusional problems, activity losses due to harsh conditions employed during immobilization, leakage from supports and reduced activity [7][51].

1.6.4 Stabilization by CLEC/CLEA

CLECs is immobilization technique known since in the 1960's [53]. CLEC immobilization of enzymes is unique in the way that the protein matrix is both the catalyst and the support. The CLEC production process consists of two major steps, batch crystallization of enzymes (forming 1 – 100 μm microcrystals) and chemical crosslinking of crystals, in such a manner that the protein activity is maintained and crystal lattice is not disrupted [54]. The crystallization process, is different from one enzyme to another, and there is need for optimization of a given enzyme in order to make functional crystals [53]. However, crystallization can be accomplished by adding saturated Na_2SO_4 (which has a cosmotropic salting-out effect) solution into a fresh acetone-precipitated enzyme solution [53] and subsequently cross-link the crystals with a bifunctional cross-linker, e.g glutardialdehyde [54]. The formed crystals are microporous materials (with a typical solvent content of 30-65 % w/w) with solvent-filled channels, typically in the range of 1.5 – 100 Å, which facilitates the free transport of substrates and products in and out of the crystals. CLECs display exceptional thermal stability and stability in organic solvent, the latter being valuable in fine chemical synthesis. Their stability probably arises from protein-protein interaction and contacts that occur in the crystal and are maintained in the CLEC [54]. CLECs were commercially produced by Altus Biologics in USA (acquired by Althea Technologies in 2010).
The limitiation of CLECs include the laborious and time-consuming process of finding suitable crystallization method, the need for high purity enzyme, inefficiency in using macromolecular substrates, and typical 20-fold loss in catalytic efficiency [54].

CLEAs is another related immobilization technique developed in the early 2000's. Like CLECs, in CLEA the the protein matrix is both the catalyst and the support. This technique

utilizes the well-known aggregation-induced effects of cosmotropic salts (salting out) or water-miscible organic solvent to proteins in solution, commonly known as precipitation. Precipitation thus leads to physical aggregates, held together by non-covalent bonding without perturbation of their tertiary structure. Enzymes used in CLEA are first precipitated into aggregates, typically by NH_4SO_4 or tert-butanol. These aggregates are then cross-linked, commonly by glutardialdehyde, and the amide bond formation between the enzyme and the cross-linked is then reduced irreversibly into a stable Schiff base by reducing them with $NaBH_4$. The CLEAs typically display higher stability in aqeuous and organic media, and sometimes their catalysis can exceed their free-form counterpart. The CLEA technique can be used to precipitate two or more enzymes together in aggregates, and has given rise to so-called ,,combi-CLEA". CLEA Technologies in the Netherlands commercially produce CLEA from different enzymes for e.g. industrial purposes [50].
CLEA seems is more straightforward than CLEC, at least for industrial usage, however inability to catalyze macromolecular substrates is a drawback to the use of CLEA (as well as CLEC).

1.6.5 Stabilization by bioconjugation

Stabilization by bioconjugation has been extensively studied due to the abundance of chemical groups that can be conjugated to enzymes. Conjugation of an enzyme with a molecule/s or a polymer/s that results in chemically modified soluble enzyme products can be divided into two groups [55]:
1) Conjugation where a molecule/s (a low/high molecular weight compound or a polymer) is conjugated to surface functional group/s of an enzyme via single bond, with or without a spacer. This procedure is also known as grafting [7] or a site-specific protein modification if the molecule is directed toward specific protein residue/s [56] .
2) Cross-linking, where a bifunctional agent is conjugated to two functional groups on an enzyme surface forming an *intramolecular cross-link*, or between two functional groups on the surface of two different identical (or nonidentical) enzyme molecules, forming an *intermolecular cross-link*. The latter cross-linking conjugation often leads to highly heterogenous products since it is hard to control selectively the degree of crosslinking, hence it is often refered to be a nonspecific conjugation [55].

Conjugation of small molecule/s or polymer/s on enzymes or cross-linking enzymes with the assistance of bifunctional reagents, is widely used in studies that focus on enzyme stability and/or altered functionality.
The main advantage of bioconjugation is that it allows almost unlimited variety of chemical groups to be introduced on an enzyme. The drawbacks of bioconjugation is e.g. that many bioconjugation reactions yield heterogenous and poorly characterized products [49], and sometimes with low degree of coupling .
In following subchapter (*1.7*) bioconjugation, grafting and cross-linking, will be discussed in greater detail with respect to stabilization.

1.7 Bioconjugation

1.7.1 Grafting enzymes with small and large molecules

As earlier stated, conjugated or grafted enzymes often display different stability and altered functional properties. Stability is increased due to factors such as enhanced rigidity of the structure [57] and if the conjugated molecule contains hydroxyl or amine groups, hydrogen bonds with hydrophilic residues on the surface of the enzyme can contribute to their stability [58]. Enzymes can be made more soluble by conjugation with polymers. Grafting polymers onto proteases often reduces or eliminates their autolytic behavior [3][38]. Conjugation of both oligo – and polymeric carbohydrates remains a popular method of stabilization [38]. Proteins are conjugated via their surface accessible reactive groups. These groups include ε-amino of lysine residues, unreduced thiol groups of cysteine, hydroxyl groups of tyrosine residues and carboxyl groups of aspartic and glutamic acids [39].
Glycoproteins are usually more stable than their carbohydrate-free counterparts [4] [19], so grafting sugars or polysaccharides to non-glycosylated enzymes can increase their thermostability by forming hydrogen bonds between the hydroxyl groups of the carbohydrate and hydrophilic amino acid residues on the surface of the enzyme, [8] and it can also impose increased rigidity on their conformation [7]. Glycoproteins are not only intrinsically stable but are also highly soluble [10].
Darias and Villalonga conjugated chitosan (M_w = 20800 Da) to cellulase by activating the chitosan with sodium periodate. The enzyme lost condsiderable activity after conjugation, however, the $T_{50\%}$ increased from 68.4 °C to 77.3 °C [58].
Non-enzymatic glycation to amino groups of proteins (usually the ε-amino group of the lysine side chain) has been obtained in high yield by first dissolving the protein and a reducing sugar, followed by lyophilization and incubation at 60-85 °C *in vacuo* for few hours [62]. This causes the amino groups of the protein to react with the reducing end of the sugar (e.g. glucose), yielding fructosyl-lysine, Schiff bases and various Amadori rearrangement products. However, it overcomes the most serious diffuculties encountered by in-solution glycation; the production of advanced glycation end-products[61][62][63]. Pham et al. used this procedure to conjugate glucose to trypsin and chymotrypsin, and obtained enzymes that were relatively homogenous (seen from acidic non-denaturing PAGE electrophoretic gels), with on average 12 of total 14 lysine residues being conjugated. The glycated bovine trypsin was more stable toward heat than its native counterpart, e.g. after two hours at 55 °C about 50 % of the activity of the glycated bovine trypsin remained but the activity of the native bovine trypsin had been completely lost. T_m values of porcine trypsin was observed to increase by 4.5 °C after glycation by using CD spectropolarimetry, and the kinetical parameters (k_{cat} and K_m) for glycated bovine trypsin and glycated chymotrypsin were identical to their native counterparts. Thus, *in vacuo* glycation with glucose is an attractive method to confer stability to enzymes [62].

1.7.2 Conjugation by crosslinking with bifunctional reagents

Bifunctional reagents are compounds with two or more reactive groups that selectively form link between two groups of a protein molecule (intramolecular cross-link) or between

two protein molecules (intermolecular cross-link). Bifunctional reagents can be categorized into two groups: Homobifunctional and heterobifuntional reagents. Homobifunctional reagents have the same reactive chemical group on its both end, i.e. glutardialdehyde or chitosan. Heterobifunctional reagents have different reactive chemical group on either end, e.g. sulfosuccinimidyl-4-(N-maleimidomethyl)cyclohexane-1-carboxylate (sulfo-SMCC) [60].
Crosslinking of enzyme stabilizes them by enhancing their rigidity in a way that reduces the unfavorable conformational entropy and thereby makes the enzyme more stable in their native (or near native) conformation [57].
Although cross-linking enzymes with carbohydrates can increase their stability dramatically, there are also cases reported where stability decreased using this approach. Sasvári and Asbóth crosslinked glucoamylase from *A. Niger* with carbohydrates, that reduced its thermostability at the heat range 60-80 °C. They argued that this was probably due to some sort of conformational restrictions [64]. Soluble intermolecularly-crosslinked enzymes with glutardialdehyde often form gelatinious-like aggregates that seem to be hard to control [50].

1.7.3 Bioconjugation of therapeutic proteins

Protein-based therapeutics are now approx. 25 % of all new approved medicine by the American Food and Drug Administration. Bioconjugation has been used to graft therapeutic proteins with polyethylene glycol (PEG) in order to overcome the intrinsic limitation of these therapeutics. PEGylation of therapeutic proteins enhance their stability in storage *in vitro* and their activity *in vivo* by reducing their immunogenicity, delaying renal elimination etc. but without reducing the protein therapeutic properties [5][56]. Several therapeutic PEGylated protein therapeutics have reached the market [56]. Chitosan conjugated protein therapeutics might also find its place in future protein therapeutics due to its biocompatibility and non-toxicity [58].

1.8 Bioconjugation with carbodiimide and NHSS

The carboxyl groups of protein in aqueous solution is a rather inert functional group. In order to make them reactive towards a nucleophile they have to be activated. That is commonly done by using water-soluble carbodiimides[60]. That is a popular method to couple carboxyl and amino group to form a zero-length (i.e. no spacer added) stable amide bond and it has found wide use in bioconjugation. EDAC is the most widely used water-soluble carbodiimide to form a zero-length conjugates [65]. EDAC mediates amide bond formation effectively at pH 4.5-7.5. EDAC, like other water-soluble carbodimides, reacts with a carboxylate of aspartic and/or glutamic acid residue/s to from an active ester adduct (o-acylisourea) followed by a nucleophilic substitution by an amino group on the active ester. If however no nucleophilic amino group is in the vicinity, the active O-acylisourea undergoes rapid hydrolysis regenerating the orginal carboxylate and an N-substituted urea. This hydrolysis has a rate constant measured in seconds [66]. This high instability of the O-acylisorurea intermediate results in lower amide bond formation than one would anticipate [67][68]. Grabarek and Gergely refined this amide bond forming reaction and developed a two-step zero-length procedure to overcome this particular shortcoming of using only EDAC. Their approach is based on the fact that succinmidyl esters form stable adducts. By

using N-hydroxysuccinimide (NHS) they improved a cross-linking reaction between two muscle proteins [68]. N-hydroxysulfosuccinimide (NHSS) can also be employed, and has the advantage over NHS of being more water soluble. EDAC/NHSS coupled reaction are highly efficient and usually increase the yield of a conjugation, over that obtainable solely with EDAC [65].
The EDAC can also react with tyrosyl residues, most likely through the phenolate ionized form of that residue, in a similar manner as for carboxyl groups, but this conjugation can be reversed by incubating the coupled protein in 0.5 M hydroxylamine for a couple of hours [69]. It can furthermore form a stable complex with exposed sulfhydryl groups [70]. EDAC may promote unwanted polymerization of proteins due to the usual abundance of both amine and carboxylates on protein molecules, so it is always advisable to check if protein polymerization is a problem at the condition used for the reaction [65]. Figure 1.13. represents the EDAC/NHSS conjugation of carboxyl and amino groups.

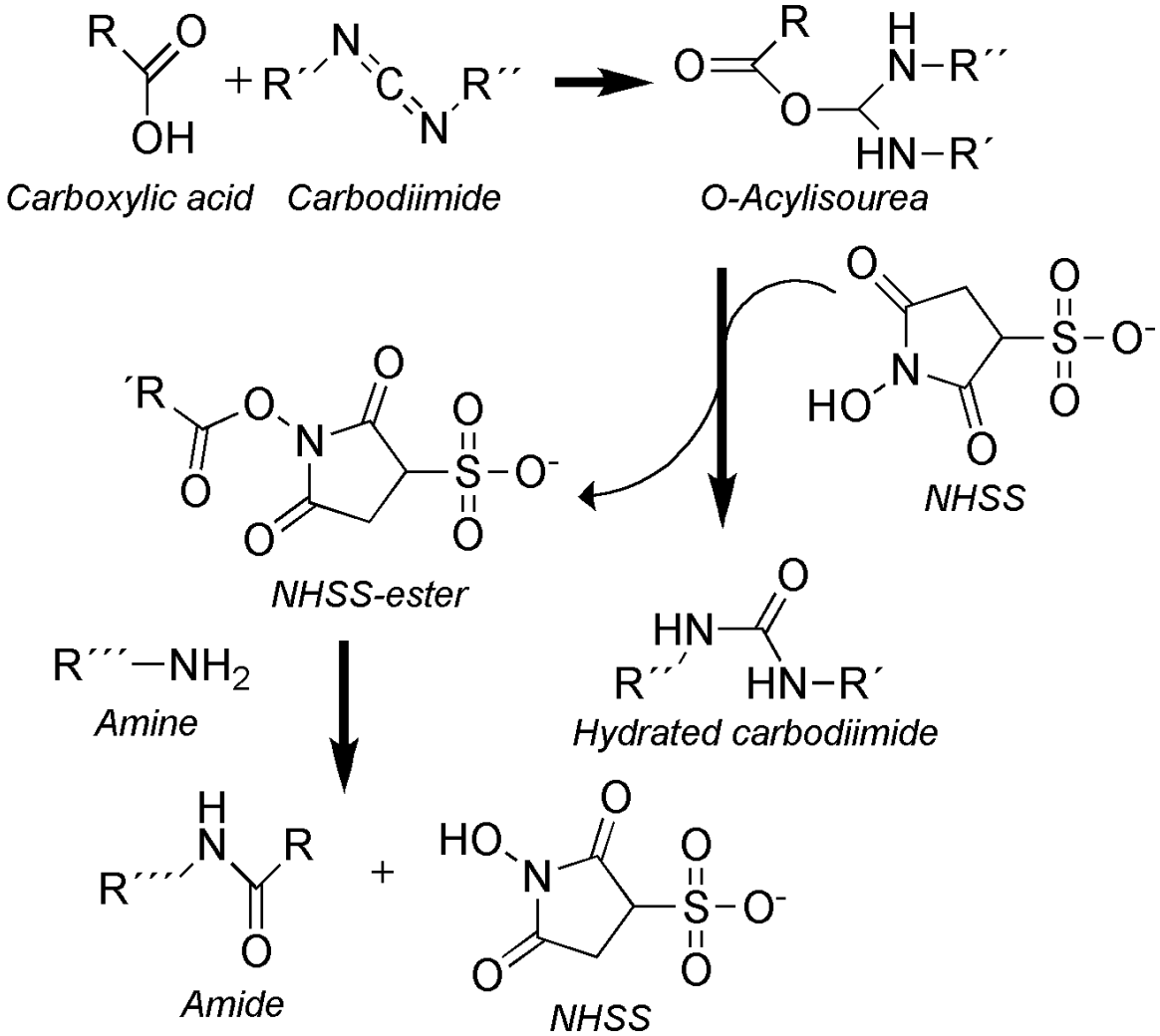

Figure 1.13. *Conjugation reaction of binary EDAC/NHSS conjugant between carboxyl and amino groups.*

1.9 MALDI-TOF mass spectrometry

MALDI-TOF (Matrix-assisted laser desorption ionization-time-of-flight) mass spectrometry is a mass analyzing technique frequently used in molecular biology and biochemistry. The utility of MALDI-TOF for protein and peptide analysis lies in its ability to provide highly accurate molecular weight information on intact biomacromolecules (up to 300 kDa and even higher molecular mass, but that depends on the matrix [71][72][73]), to perform accurate mass determination of peptide mixtures/digests and to resolve complex heterogenous mixtures [73]. The ability to generate such accurate information is very useful for protein identification and characterization. A MALDI-TOF instrument is usually made of three components: a laser ionization source, a TOF tube (0.5 – 2 meters) and a detector [72].
Its should be noted that the name „mass spectrometry“ is a sort of misnomer of this technique as well as other mass spectrometrical techniques. The mass is not what is measured, instead mass spectrometry determines the mass-to-charge (m/z) ratio or a property related to m/z ratio. A mass spectrum is usually a plot of ion abundance versus m/z. Hence, the spectrum is presented in terms of daltons per unit charge [72].
In MALDI-TOF analysis, the analyte (e.g. protein or peptide digest) is first co-crystallized with a large molar excess of a matrix compound, commonly a UV-absorbing weak organic acid [71][72][73], such as 2,5-dihydroxybenzoic acid, sinapinic acid or α-cyano-4-hydroxybenzoic acid [73].

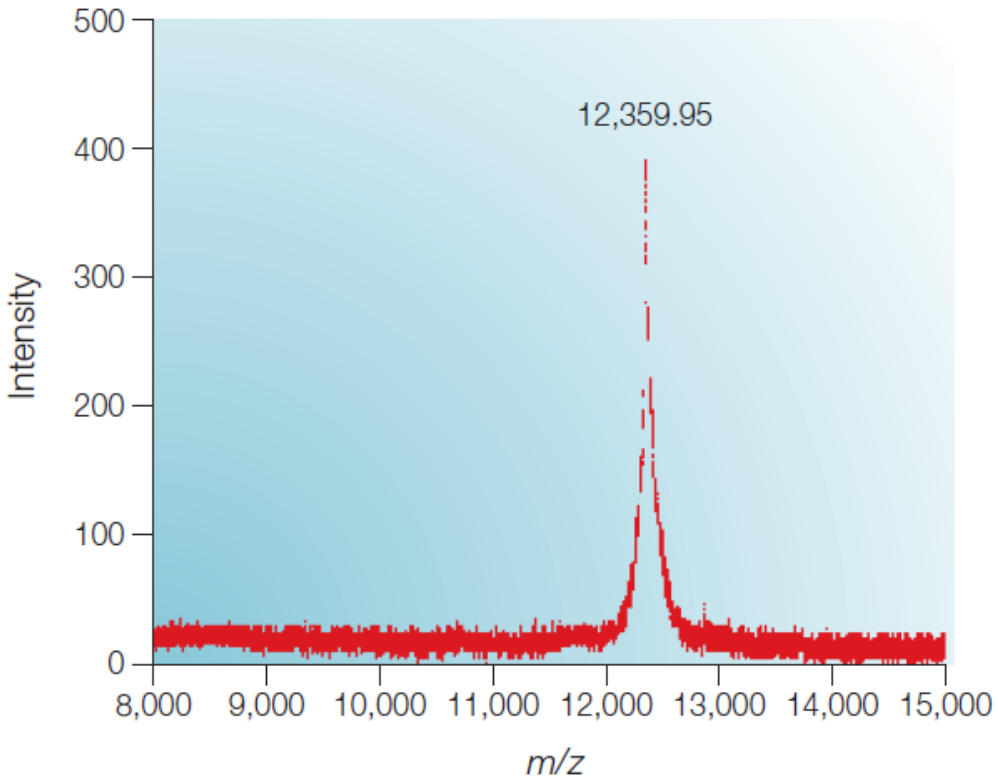

Figure 1.14. *A MALDI-TOF mass spectrum of the small globular protein cytochrome c. MALDI usually produces only singly charged analyte cation, thus producing only a single peak in considerable abundance. (given that there was only one kind of analyte protein in the matrix). From ref. [72].*

The use of matrix preparation method depends on the analyte. Several different methods

are in use such as dried-droplet, thin/thick layer and the „sandwich“ method. The sandwich method has proven to be very successful for intact proteins [73, and reference therin]. After the preparation of the matrix-analyte co-crystallization onto a metallic sample plate, the plate is placed into a MALDI TOF mass spectrometer, where a high voltage is applied to it. A laser then sends in a pulsed radiation, *in vacuo*, of a wavelength which the organic acid matrix strongly absorbs [71][72][73]. This absorption of the matrix causes the matrix to vaporize or desorb, and it carries the analyte with it, even if the analyte is a large molecule like a protein [71]. Therefore the matrix plays a key role by strongly absorbing the incident laser light energy and causing indirect vaporization of the analyte [72][73]. The matrix also serves as a proton donor and receptor, acting to ionize the analyte in both positive and negative ionization modes. It is generally thought that ionization occurs through proton transfer or cationization, so the procedure of transfering charges to the analyte strongly depends on the organic acid used [72][73]. The formation of singly-protonated analytes in MALDI is typical [71], but the mechanism behind it remains to be discovered [72]. After the pulsed laser has been sent in, the vaporized ions are repelled (due to high voltage difference of the repellor and extractor, 1-30 kV) and accelerated from the target plate surface towards the extractor, and subsequently through a crevice into the TOF tube [72]. Figure 1.15 represents the mechanism graphically.

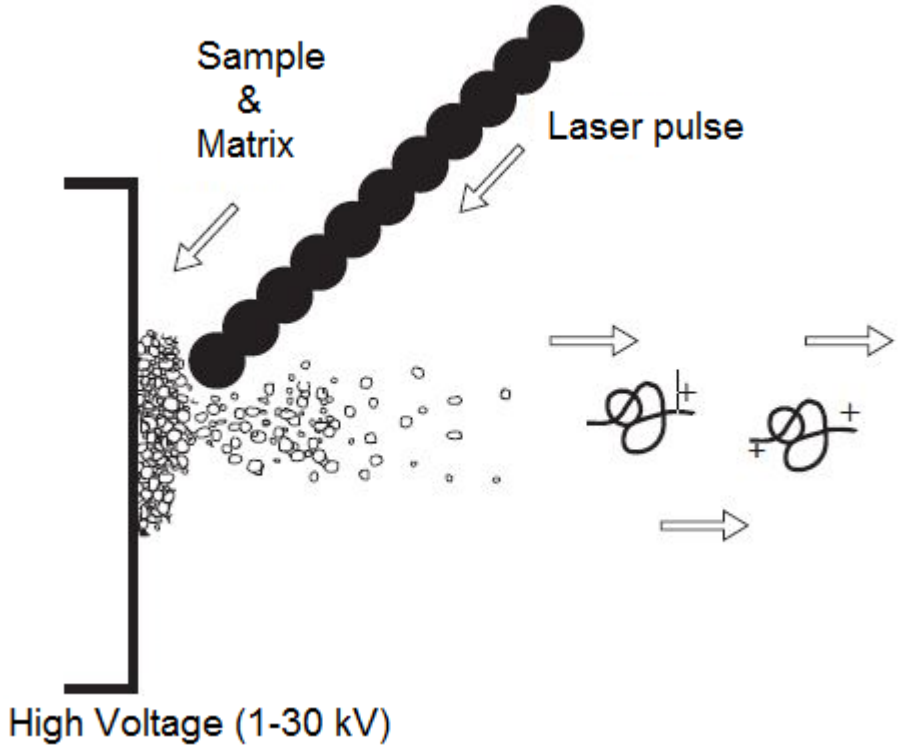

Figure 1.15. *Representation of how the matrix desorbs the intense laser beam. The UV-absorbing organic acid absorbs the incident pulsed-laser light which causes the matrix to desorb from the target plate, carrying the analyte with it. This mixture is then accelerated towards the TOF tube, due to high voltage of the sample plate. The accelerating voltage gives each identical ion almost the same kinetic energy. Adapted from ref. [73].*

In the TOF tube, the ions enter a vaccum field-free drift [71]. All molecules with the same charge [72] leave the acceleration distance with basically the same kinetic energy, yet a

different mass, so the ions reach the detector at different times [71][72][73]. Hence, the arrival time at the detector is dependent upon mass, charge and the kinetic energy (KE) of the ion/s. The kinetic energy is [73]:

$$\mathrm{KE} = \frac{1}{2} \cdot {}^{m}/_{z} \cdot v^2 \qquad \textbf{Equation 1.11.}$$

where v is the velocity of the ion. Since all ions with the same charge are given the same kinetic energy after the pulsed-laser irridation [72][73], their velocities and hence their arrival time at the detector depends solely on their m/z ratio[73]:

$$v = \sqrt{\frac{2 \cdot KE}{{}^{m}/_{z}}} \qquad \textbf{Equation 1.12.}$$

Clearly, according to equation 1.12., the smaller ions reach the detector first and larger ions later. Thus, the m/z ratio is determined from the ions time-of-flight [72]. The above described TOF is usally termed a linear TOF and is most often used when studying macromolecules (> 10000 Da) [72][73]. There are two types of TOF tubes (or one TOF tube with both features): a linear TOF and a TOF reflectron. These two types are illustrated in figure 1.16.

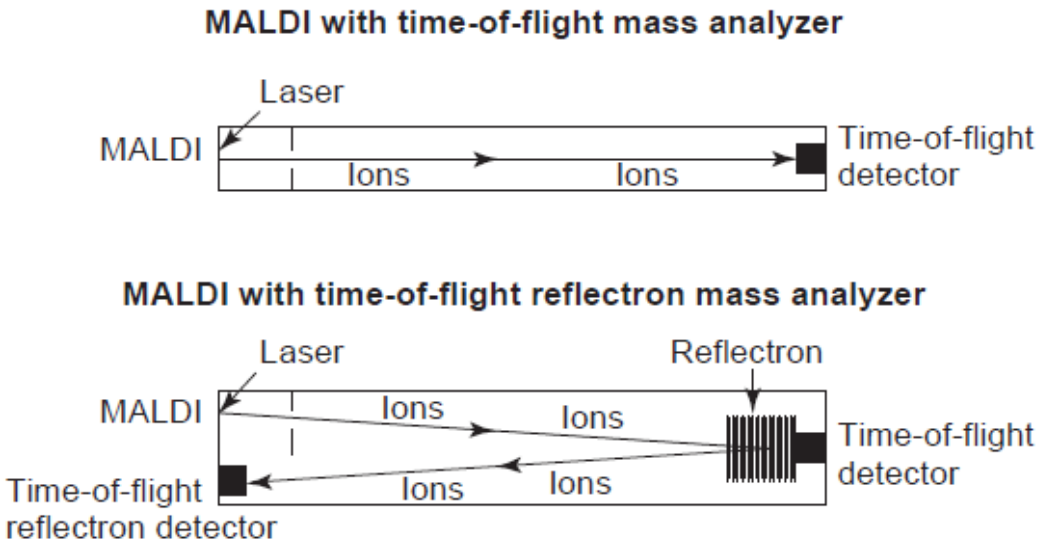

Figure 1.16. *A linear TOF tube (above) and a TOF tube installed with a reflectron (below). From ref. [73].*

The TOF reflectron combines the TOF technology with an electrostatic mirror (i.e. the reflectron) that turns the ions around and sends them down a second flight distance to the detector [72]. This reduces their KE distribution [73], and thus compensates for small differences in the velocities of ions with the same m/z ratio. These differences in velocities between ions with same m/z ratios are due to numerous reasons that are inherent in the experiment [72]. However, this increased resolution comes at the expense of sensitivity for large macromolecules (>10000 Da) [73], so mass spectra of medium to large sized intact proteins are usually collected in a linear TOF analysis. Today, TOF offers mass resolution in the thousands and mass accuracies in the tens of parts per million (on ppm scale) [72].

The advantages of MALDI-TOF include the fact that the irradiating laser is sent in pulses, so ions are formed in discrete events, thus yielding very high levels of sensitivity, which often provides data from sub-femtomole amounts of sampling loading. Formation of singly charged analytes are also MALDI's merits. High throughput can be readily accomplished by using sample plates that are loaded with ~100 different samples and MALDI-TOF has a relatively high tolerance to salts and buffers (<10 mM) compared with other mass spectrometrical techniques such as ESI TOF [72][73].
The main drawback of MALDI-TOF for protein/peptide mass spectrometry include difficulties making a suitable matrix, hence, difficulties obtaining good data since the precence of matrix is required to faciliate ionization, which can be time-consuming [72][73].

1.10 CD spectropolarimetry

CD spectropolarimetry (Circular dichroism spectropolarimetry) is a widely used technique in biochemistry to study protein or nucleic acid conformations, conformational changes due to biological interactions, thermodynamics of folding and unfolding of proteins or nucleic acids, obtain binding constants and kinetics of folding and unfolding of macromolecules [75][76]. This technique utilizes the fact that macromolecules like proteins and nucleic acids have asymmetric chromophores which absorbs the left or right components of circularly polarized light to a different extent.
Circularly polarized light can be produced by passing plane-polarized light through either a quarter-wave plate, Fresnel quartz rhombic crystal or a Pockles cell under certain conditions [74][75]. Figure 1.17 describes left and right circularly polarized light.

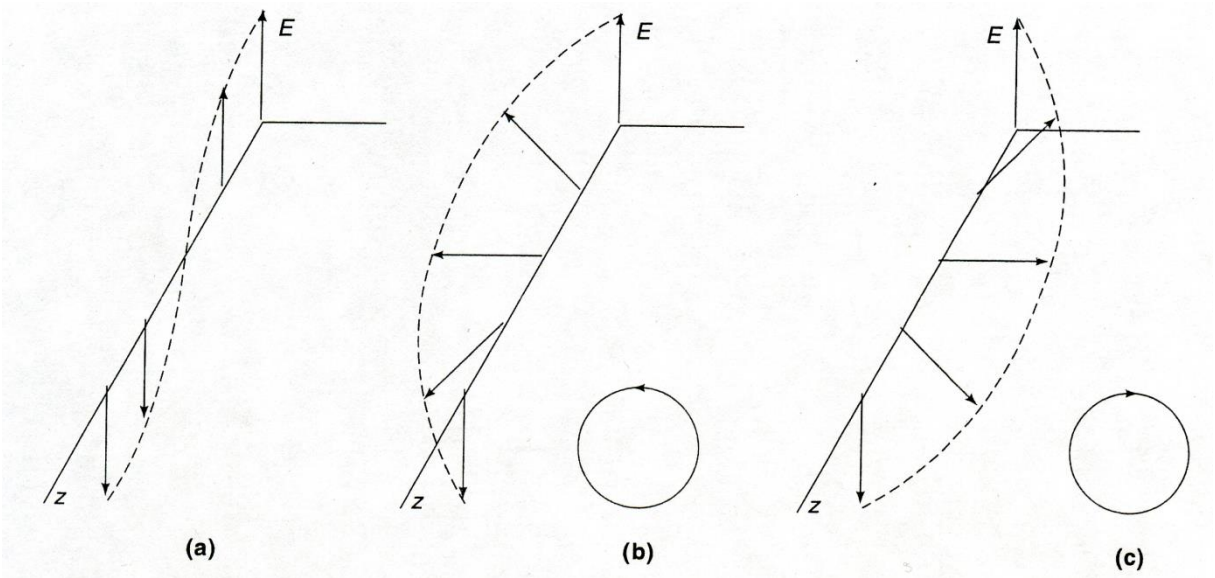

Figure 1.17. *Represents (a) plane polarized light, (b) left circularly polarized light and (c) right circularly polarized light. From ref. [74].*

The circularly polarized light has two vector components of the electric field. These component circulate either left or right: E_L and E_R. In an ordinary medium, the E_L and E_R rotate at the same speed to the xz coordinate (fig 1.17), but in an optically active medium E_L and E_R rotate at different speeds in the plane containing the resultant electrical field (E)

gives rise to the angle α (fig 1.18).

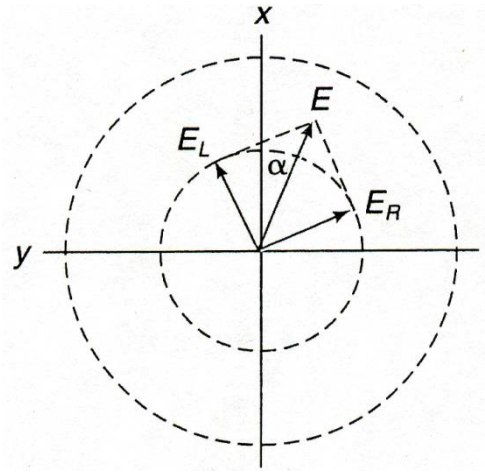

Figure 1.18. *The E_L and E_R circulate to different extent in a medium that displays circular dichroism. From ref. [74].*

This phenomenon is due to the fact that in an optically active medium, the refractive index is different for left or right electrical components of circularly polarized light. Hence, the components will be absorbed unevenly and the medium is said to exhibit circular dichroism. After passing through an optically active media the E_L and E_R components will no longer oscillate along a single line but will rather trace out in an elliptical manner [74], as can be seen in figure 1.19.

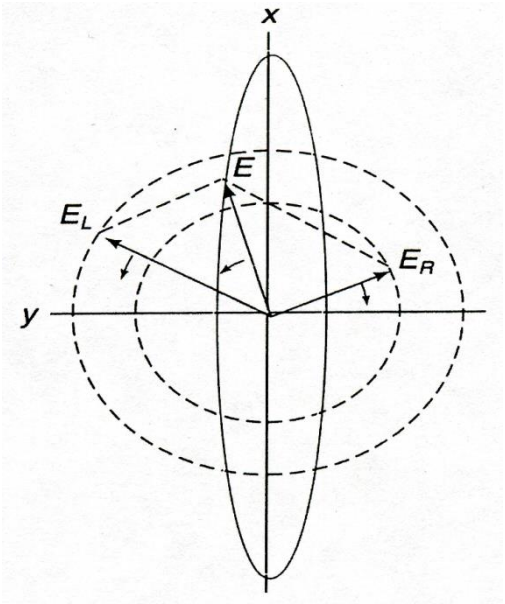

Figure 1.19. *E_L and E_R components of circularly polarized light will not oscillate circularly along a single line after passing through an optically active medium, but rather trace out in an ellipse. From ref. [74].*

The circularly polirized light will thus be elliptically polarized (fig 1.19) when it has passed through the sample. The angle between this induced ellipse is:

$$\alpha = \tan\frac{b}{a}$$ **Equation 1.13**

where α is the angle of the ellipse, b and a are minor and major axes of the resulting ellipse [76].
In reality, CD spectropolarimeters measure the difference in absorbance between E_L and E_R components (defined as A_L and A_R), which circulate in an ellipse after passing the sample and the device transforms the absorbance difference into α (elliptical millidegrees) according to following relation [76]:

$$\alpha_{millidegrees} = 32980 \cdot (A_L - A_R)$$ **Equation 1.14.**

The relationship above for absorbance and the angle, yields the elliptic angle in millidegrees, since the angle on that scale is observed for biomacromolecules.
Most commonly used CD spectropolarimeters use modulation for emission of circularly polarized light. In modulation, incident light is continuously switched between the L and R components under an alternating electrical field induced by a piezoelectrical Pockles cell crystal [75][76]. A CD spectrum is obtained when the dichroism (the elliptical angle) is measured as a function of wavelength of the circularly polarized light.
As stated earlier, optically active chromophores (a.k.a. chiral chromophores) will yield an CD signal.
Proteins under normal conditions are highly ordered structures which form specific secondary structures with an abundance of chiral chromophores [75]. In the far-UV range (180-250 nm), the peptide bond of the protein backbone is the main chromophore of proteins, and its absorbtion of circularly polarized light causes two allowed orbital transitions of outer electrons: $n \rightarrow \pi^*$ and $\pi \rightarrow \pi^*$ transition [75][77]. Since the environment of the peptide bond is different between α-helices and β-sheets, the absorption of the peptide bonds in these two different secondary structures differ. This gives rise to different CD spectral profiles for those two major secondary structures. CD spectra of α-helices are characterized by negative ellipticity signal minima at around 222 nm (due to : $n \rightarrow \pi^*$ transition) and 208 nm (due to $\pi \rightarrow \pi^*$ transition) [77]. Detection of β-sheets is not as straigthforward for the reason that they are less soluble in CD compatible solvents and are generally structurally less defined, can be parallel or antiparallel and of varying lenghts and widths, however, some generalization can made. Usually they give rise to a negative elliptical signal minimum at 216 nm and a positive elliptical signal maximum near 195 nm [77]. In the near-UV range (250-300 nm), the main chromophores are the aromatic amino acid residues and disulfide linkages [77]. CD spectra in the far-UV range gives information about the conformation of the secondary structures (or alteration in their microenvironment) and CD spectra in the near-UV range gives information about the microenvironment of aromatic side chains residues and disulfide linkages [77].

1.11 Nanoparticle tracking analysis (NTA)

Nanoparticle tracking analysis (NTA) is a relatively new technique, that was commercialized in 2004 by NanoSigth Ltd. Since then over 450 scientific papers relying on this technique have been published [78]. A critical review article has been written about this technique in where it was compared with dynamic light scattering (DLS) [79].
NTA utilizes the properties of both light scattering and Brownian motion in order to obtain particle size distributions of samples in liquid suspension. A laser beam, of which can be of different wavelengths, is radiated through a prism glass in the sample chamber (100 µm x 80 µm x 10 µm) of nanoparticle suspension. The angle of the incident beam and the refractive index of the glass surface is designed to be such that when the laser emerges from the interface between the glass and the liquid sample, it refracts to an intense low profile resulting in a compressed beam with a reduced profile and high power density. The particles in suspension in the path of this beam, scatter light in such a manner that they can easily be visualized via conventional microscope fitted with a EMCCD camera or other high-sensitivity camera operating at 30 frames per second. The camera subsequently captures a video file of particles moving under Brownian motion based on their scattering.

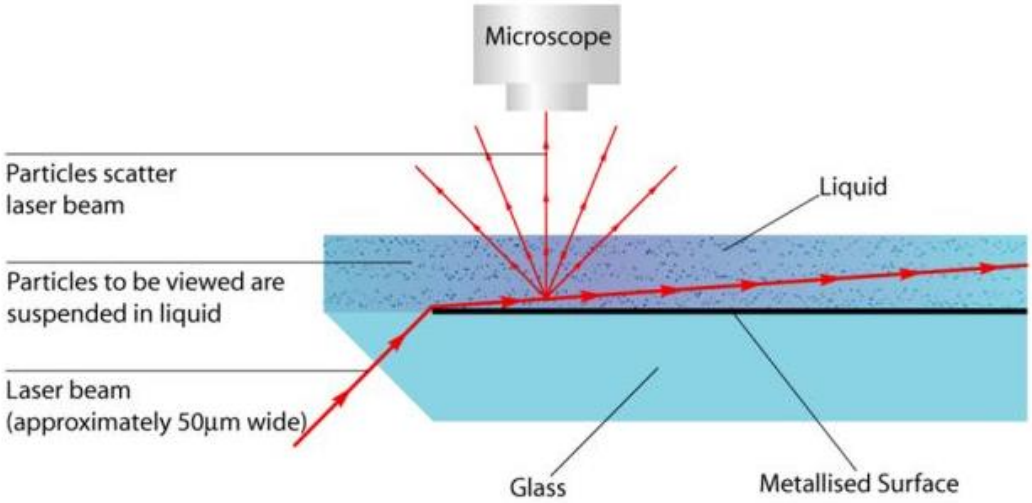

Figure 1.20. *A schematic figure of the experimental procedure of NTA. The microscope is fitted with an external camera. From ref. [78].*

NTA software records a video file of typically 30-60 seconds of the particles viewed and tracks the centre of each followed particle on a frame-by-frame basis, and furthermore allows the software to determine the average distance moved by each particle in the x and y coordinate directions. Brownian motion occurs in three dimensions but NTA observes motion in two dimenstion (x and y coordinates). With this information the diffusion coefficient (D_t) of a single particle can be calculated by knowing the movement of the particle in x,y coordinate direction [78]:

$$D_t = \frac{(\vec{x},\vec{y})^2}{4}$$ **Equation 1.15.**

By knowing the temperature (T) and solvent viscosity (η), the sphere-equivalent

hydrodynamic radius (r_h) of the followed particles can be identified by using Stokes-Einstein equation [78][79]:

$$D_t = \frac{T \cdot k_B}{3 \cdot \pi \cdot \eta \cdot r_h}$$ **Equation 1.16.**

where k_B is the Boltzmann constant. It should be noted that the Stokes-Einstein equation supposes that the particle is spherical.
The amount of ligth scattered by the particle and the efficiency with which that light can be detected acts to limit the smallest size at which nanoparticles can be seen and thus analyzed by NTA. For materials with a low refractive index such as proteins the lower size limit is around 25-35 nm.
NTA is not an ensemble technique for investigating a very large number of particles, but rather each particle is sized individually, irrespective of others so it is important to include enough particles to ensure that the data produced is statistically viable. A concentration range in the region of $10^7 – 10^{10}$ particles per mL provides statistically sound data. Accuracy of NTA is around 2 % under ideal conditions [78]. Its most pronounced strength over the averaging ensemble technique of DLS, is its ability to resolve polydisperse samples and evalute the number of nanoparticles in a given solution [79].

1.12 Aim of the thesis

The aim of this thesis was to study the conjugation of bovine trypsin with D-glucosamine and chitooligosaccharide, with the latter conjugant resulting in an intermolecular cross-linked conjugation of trypsin. This was done in order to create a more stable enzyme than the free form counterpart (native trypsin) without losing the catalytic activity or at least minimizing the effect on catalytic activity, as well as to characterize sizes of the conjugate and the cross-linked species and look for altered functionalities if present.

2 Materials and methods

2.1 Materials

Trypsin (from bovine pancreas, T-8001), N-α-benzoyl-L-arginine-p-nitroanilide (L-BAPNA), N-hydroxysulfosuccinimide (NHSS), 1-ethyl-3-(dimethylaminopropyl)-carbodiimide (EDAC), 2-[N-morpholino]ethanesulphonic acid monohydrate (MES), 5,5′-dithio-bis-2-nitrobenzoic acid (DTNB, Ellman's reagent), guanidium thiocyanate, triethanolamine hydrochloride (TEA), $CaCl_2 \bullet 2H_2O$, tris(hydroxymethyl)aminomethane (Tris/Trizma®), acetic acid, trichloroacetic acid, orthophosphoric acid, 3-(N-morpholino)propanesulfonic acid (MOPS), dodecyl sulfate sodium salt (SDS), Coomassie Brilliant Blue G, methanol, N-α-tosyl-L-lysine chlorometyl ketone hydrochloride (TLCK**)**, phenylmethylsulfonyl fluoride (PMSF) and 37 % HCl were purchased from Sigma-Aldrich, St. Louis, USA. Sodium acetate, NaN_3, Na_2SO_3 and boric acid were purchased from E. Merck, Darmstadt, Germany. D-glucosamine and ethylenediaminetetraacetic acid dipotassium salt (EDTA) were purchased from BDH Chemicals Ltd, Poole, England. Urea and NaOH were purchased from Acros Organics, New Jersey, USA. Dimethyl sulfoxide (DMSO) was purchased from NimbleGen SYSTEMS Inc., Madison, USA. Oxygen (O_2) and nitrogen (N_2) cylinders was purchased from ÍSAGA (part of AGA International), Reykjavík, Iceland. The chitooligosaccharides (Batch No. G020701-K) was kindly supplied by Genís hf., Reykjavik, Iceland. All other reagents were of analytical grade.

PD-10 desalting columns (exclusion limit $M_r > 5000$) were purchased from GE Healthcare, Uppsala, Sweden. Microplates (96 wells) were purchased from Nunc A/S, Roskilde, Denmark. Pre-casted polyacrylamide (4-12 %) NuPAGE electrophoretic gels, LDS sample buffer, and Bench Mark™ protein ladder were purchased from Invitrogen Co., Carlsbad, USA. Cellulose dialysis tubing (retains proteins > 12000 Da) were purchased from Sigma-Aldrich, St. Louis, USA.

All aqueous solutions were made with milli-Q deionized water. Pipettes were calibrated regularly. All proteins preparations were kept refrigerated at 4 °C when not in use and always used within one week with the exception of those used in the storage stability measurement.

2.2 Methods

2.2.1 Conjugation of chitooligosaccaharide and glucosamine to bovine trypsin with binary EDAC and NHSS conjugant.

D-Glucosamine and two different ratios of chitooligosaccharides with an average molecular weight of approx. 1340 Da (on average 4-8 sugar moieties), degree of deacetylation 55 % and salt concentration 20.4 % were used for this study. Since the salt concentration was rather high, the prepared stock solution of the oligochitosaccaharide were compensated for by adding 20.4 % more of them than calculated.

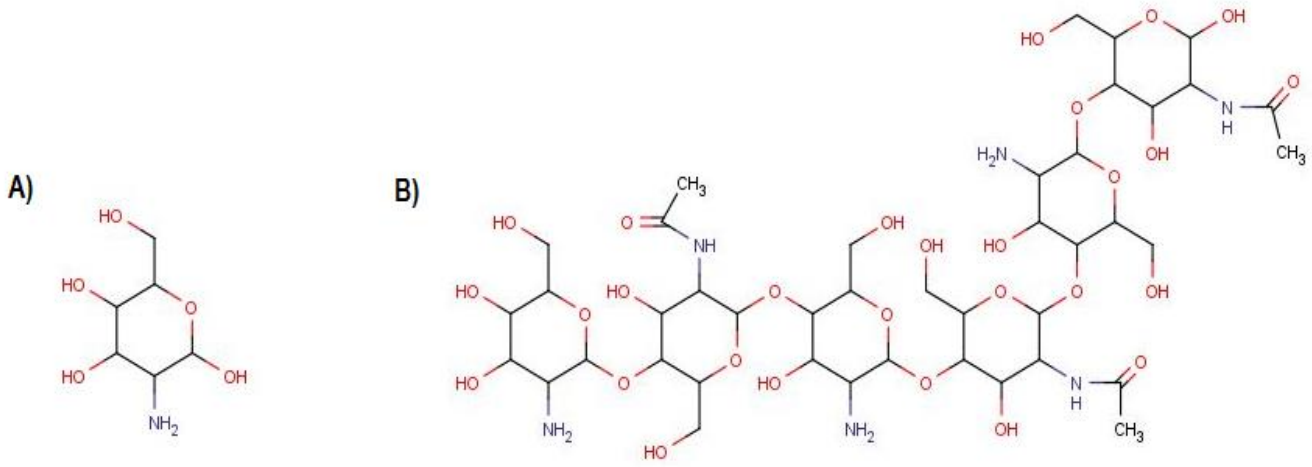

Figure 2.1. *The structure of A) D-glucosamine and B) chitooligosaccharides. The chitooligosaccharides represented in the figure serves as an „average" of those used.*

Stock solutions of 0.58 $^{mg}/_{mL}$ and 1.15 $^{mg}/_{mL}$ (200 mL) of chitooligosaccharide were prepared, but they constituted a 5-fold molar excess and 10-fold molar excess to trypsin, respectively. These formulations will be refered to as TCC 1:5 and TCC 1:10, respectively (**TCC**: Trypsin crosslinked with chitooligosaccharide). These solutions were acidified with 2-3 drops of conc. HCl in order to maximise the solubility of the chitooligosaccaharides. Stock solution of 0.74 $^{mg}/_{mL}$ D-glucosamine (200 mL), which constitute a 40-fold molar excess to trypsin, in deionized water was prepared without acidification since the glucosamine is highly soluble in water. This formulation will be refered to as **TGG** (TGG: Trypsin grafted with glucosamine). Stock solutions were stored at -20 °C.
Trypsin was cross-linked and conjugated by using EDAC along with NHSS using aforementioned D-glucosamine and chitooligosaccharide stock solution. 4 mg of bovine trypsin (yielding a final concentration ~ 0.07 mM) was weighed in a small clean glass cylinder, followed by 22 mg of MES buffer (final concentration of MES was approx. 50 mM). 2 mL aliquots of stock solution (either stock solution of D-glucosamine or different ratios of chitooligosaccharides) was pipetted into the glass cylinder and the solution gently agitated, manually, to facilitate the dissolution of trypsin and the MES buffer. The solution was adjusted to pH 6.5, by adding approx. 0.5 mL (8-10 drops) of 0.2 M NaOH, monitored with a precalibrated pH meter. The glass cylinder was then placed on a balance and 16 mg of EDAC (yielding ~33 mM) and 8 mg of NHSS (yielding ~14 mM) was added to the solution. This reacting mixture was subsequently replaced in a 20 mL plastic cylinder with a cap, and allowed to react for 22-24 hours at a room temperature (22-24 °C) with a gentle

agitation.

The reaction mixture was desalted on a small size exclusion chromatography PD-10 column with a 5000 Da exclusion limit. The column had been preequilibrated with 30 mL of the buffer of choice (5 column volumes) prior to desalting. According to the manual that accompanied the PD-10 columns [80], 2.5 mL of reaction mixture was aliquoted into the column and the effluent from that volume discarded. After all the volume of the reaction mixture had been introduced into the column, 3.5 mL of buffer was added and the subsequent effluent collected, in a small plastic cylinder. The collected effluent consisted of most of the chemically conjugated trypsin.

2.2.2 Protein quantification assay

Protein concentration was quantified by using analysis of disulfide linkages according to Thannhauser et al [81]. This method was chosen instead of other protein quantification methods, such as the frequently used ultraviolet absorbtivity at 280 nm, since chemically modified proteins can deviate from the extinction coefficient of their native counterpart [82].
The disulfide linkage method was originally developed as a sensitive procedure to determine an unknown number of disulphide linkages in peptides and proteins. However, it works equally well as protein quantification method for extracellular proteins with a known number of disulfide linkages. This method can be used to quantify as little as 10^{-8} moles of disulfide linkages with an error of ± 3 – 5 %.
The method relies on that fact that accessible disulfide linkages in unfolded protein are cleaved by an excess of sodium sulfite at above pH 9. That leads to a formation of thiosulfonate and a free sulfhydryl group from the cleaved disulfide linkage according to equation 2.1:

$$R\text{-}SS\text{-}R' \;\; SO_3^{2-} \rightarrow R\text{-}S\text{-}SO_3^{-} + R'\text{-}S^{-} \qquad \textbf{Equation 2.1.}$$

The free sulfhydryl group is then reacted with disodium-2-nitro-5-thiosulfobenzoate (NTSB) salt according to eq. 2.2:

$$R'S + NTSB \rightarrow R'SSO_3^{-} + NTB^{-} \qquad \textbf{Equation 2.2.}$$

For each disulfide linkage broken, one molecule of 2-nitro-5-thiobenzoate (NTB) is produced which has an absorption maximum at around 412 nm. This formation is monitored with a spectrophotometer. NTB has an extinction coeffcient of 13600 $M^{-1}cm^{-1}$ at 412 nm at pH 9.5. Since the disulfide linkages of many globular proteins are resistant to treatment of sodium sulfite, they have to be in a solution with a strong denaturant in order to make their disulfide linkages accessible to cleavage.

Preparation of NTSB solution

Approx. 30 mg of Ellman's reagent (5,5′-dithiobis-2-nitrobenzoic acid or DTNB) was weighed into a small glass flask. The content was then dissolved by adding 3 mL of 1 M Na_2SO_3 aqueous solution, yielding a solution with an intense orange colour. A rubber cap was fitted onto the flask and a thin metal needle, connected to a pure oxygen cylinder, was

fitted through the cap to reach the bottom of the solution. The oxygen was allowed to purge through the solution until the intense orange colour had turned into a pale yellow colour (~8 hours). Subsequently, the pH of the solution was adjusted to pH 9.5 and the solution kept at -20 °C for future use. Figure 2.2 represents the chemical reaction, that turns Ellman's reagent (DTNB) in to NTSB.

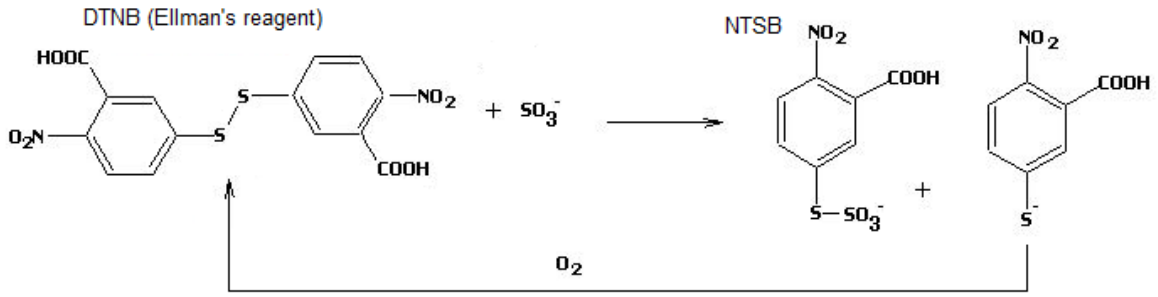

***Figure 2.2**. Preparation of NTSB from Ellman's reagent. Ellman's reagent gives an intense orange colour. When all of it has been oxidized into NTB, the colour turns pale yellow.*

Preparation of the denaturing buffer

NTSB buffer was used to dilute and to denature the protein samples for quantification. It contained 200 mM Tris, 100 mM $NaSO_3$, 10 mM EDTA and 3 M guanidium thiosulfate. The pH was adjusted to 9.5 with NaOH. Buffer was always freshly made.

Quantification procedure

Heλios spectrophotometer equipped with a Peltier heating system was used for the quantification. The wavelength was set to 412 nm and the Peltier system was set to 25 °C at all times. 950 µL of denaturing NTSB buffer, 50 µL of trypsin sample (either native trypsin, TGG, TCC 1:5 and TCC 1:10) and 20 µL of NTSB solution were added into a cuvette, vortexed rigoursly and the cuvette were then placed in the spectrophotometer. Readings were taken after no further increase in absorbance was seen (~ 15 min). Milli-Q water was used as blank. Trypsin is known to contain 6 disulfide linkages.
By using Beer-Lambert law, and modifying it by taking the 6 disulfide linkage, the molecular mass and the 20 fold dilution of trypsin all into account, the concentration of the trypsin species can be found according to eq. 2.3 :

$$C_{Trypsin} = \frac{A \cdot 23305 \frac{g}{mol}}{13600\ M^{-1}cm^{-1} \cdot 6} * 20 \quad \left(\frac{g}{L}\right) \text{ or } \left(\frac{mg}{mL}\right)$$

Equation 2.3.

2.2.3 Residual activity and pH profile measurements

Residual activity measurements

The residual activity measurements for L-BAPNA were carried out as described by the developers of the this synthetic substrate [83], with some modifications [84]. L-BAPNA

stock solution containing 19 mM L-BAPNA in 99.9 % dimethylsulfoxide was regularly mixed. Assay solution were made by diluting L-BAPNA in 112 mM TEA, 11.5 mM $CaCl_2$ buffer pH 7.8 (at ~25 °C). The dilution was 1:23 L-BAPNA to TEA buffer (e.g. making substrate solution suitable for 20 measurements is thus accomplished by mixing 4600 µL of buffer with 200 µL of L-BAPNA solution). After adequate mixture, aliquots of 240 µL from the assay solution were pipetted in an appropriate number of wells on the microplate. Subsequently, either 10 µL of native trypsin, TGG, TCC 1:5 or TCC 1:10 was pipetted into the prefilled wells (with buffer and substrate), just before the measurements began. The final L-BAPNA concentration in the wells was around 0.8 mM and the concentration of native trypsin, TGG, TCC 1:5 and TCC 1:10 in the wells was always 2-10 $^{\mu g}/_{mL}$. All measurements were conducted at room temperature (21-23 °C), by pre-stirring the plate (a feature of the device) and readings were taken regularly for 15 minutes using 405 nm wavelength (total 20 readings). All kinetical plots obtained were observed to be linear.

pH profile measurements

Measurements of pH activity profiles of the trypsin species (i.e. native trypsin, TGG, TCC 1:5 and TCC 1:10) was conducted in a Robinson-Britton universal buffer (40 mM H_3BO_3, 40 mM H_3PO_4 and 40mM CH_3COOH) [85]. Desired pH was achieved by adjusting 50 mL of Robinson-Britton buffer to the desired pH with 0.2 M NaOH. Activity was measured at pH 4.0, 5.0, 5.5, 6.5, 7.0, 7.5, 8.0, 8.5, 9.0, 9.5, 10.0 and 10.5. Relative activity at each pH was set to be the rate at a point (V) divided by the highest rate (V_{max}) at a pH that seemed to be the most optimal. Measurements were conducted by either diluting the samples 10 or 20-fold, in a respective buffer preparation (along with the substrate), before pipetting 10 µL of either native trypsin, TGG, TCC 1:5 and TCC 1:10 into the wells. The activity at each pH is an average of 8 measurements.

2.2.4 Determination of $T_{50\%}$, thermal stability, thermal inactivation, autolysis, storage stability and urea inactivation

Determination of $T_{50\%}$

Determination of $T_{50\%}$ values of native trypsin, TGG, TCC 1:5 and TCC 1:10 was done in accordance to ref. [2]. The trypsin species were heated for 10 minutes at 35, 50, 45, 50, 55, 60, 65, 70, 75 and 80 °C in appropriately corrected (eq. 2.4., below) 112 mM TEA, 11.5 mM $CaCl_2$ buffer, pH 7.8. A stoppered glass tube with the buffer was pre-heated in Julabo13 waterbath. After pre-heating the buffer, an aliquot that resulted in either 10 or 20-fold dilution of the trypsin species, (i.e. addition of either native trypsin, TGG, TCC 1:5 and TCC 1:10) was added, vortexed and inserted back to waterbath and incubated for 10 minutes. After the 10 minute had lapsed, aliquots were transferred from the incubating glass tube to a small plastic tubes placed on ice. The residual activity measurements were then conducted as described in *2.2.3*. Each data point is an average of 8 measurements of the same sample. The $T_{50\%}$ values were inspected and determined visually from residual activity plots and taken at the temperature where 50 % of the activity remained. The visual inspection was conducted because the data did not fit to a sigmoidal model, so it was concluded that the resulted uncertainity is rather high (± 0,5 °C).

The buffer was corrected for temperature by taking into consideration its value for $^{dpKa}/_{dT}$ = -0,021, according to eq. 2.4.:

$$pH_{corrected} = 7{,}80 + (T_{measured} - T_{incubation}) \cdot -0{,}021 \qquad \textbf{Equation 2.4.}$$

where $T_{measured}$ is the temperature pH of the buffer by which the buffer was prepared at, and $T_{incubation}$ is the temperature at which the buffer is incubated.

Thermal stability of the trypsin species

Determination of thermal stability was conducted by incubating native trypsin, TGG, TCC 1:5 and TCC 1:10 at 60 °C in an appropriately corrected 112 mM TEA, 11.5 mM $CaCl_2$ buffer, pH 7.8 for 0 (no incubation), 3, 5, 8, 12, 17, 23 and 30 minutes. A stoppered glass tube containing 112 mM TEA, 11.5 mM $CaCl_2$ buffer pH 7.8 was preheated in a Julabo13 waterbath. After pre-heating the buffer, an aliquot that resulted in either 10 or 20-fold dilution of the trypsin species was added, vortexed and inserted back to waterbath and incubated for 0 (no incubation), 3, 5, 8, 12, 17, 23 and 30 minutes. At listed times, aliquots were transferred from the incubating glass tube into small plastic tubes on ice. The residual activity was then conducted as described in *2.2.3*. Each data point is an average of 9 measurements of the same sample.

Thermal inactivation of native trypsin and TGG

Determination of thermal inactivation was conducted by heating native trypsin at 50, 52, 54, 56, 58, 60 and 62 °C and TGG at 60, 62, 64, 66, 68, 70 and 72 °C in a appropriately corrected 112 mM TEA, 11.5 mM $CaCl_2$ buffer, pH 7.8. Otherwise, the procedure was exactly the same as described for *Thermal stability of the trypsin species*. Each data point is an average of 7 measurements of the same sample.

Autolysis of the trypsin species

The autolytic assay was conducted in accordance with ref. [2]. This was done by incubating the trypsin species in 30 °C for varying amount of time. Trypsin species were all kept in a 112 mM TEA buffer ***without*** $CaCl_2$, pH 7.8. Calcium ions are known to make trypsin more resistant to autolysis and are thus excluded from the assay. A stoppered glass tube containing 112 mM TEA buffer, pH 7.8, was preheated in Julabo13 waterbath. After pre-heating the buffer, an aliquot that resulted in either 10 or 20-fold dilution of the trypsin species was added, vortexed and inserted back to waterbath and incubated for 0 (no incubation), 15, 35, 45, 60, 90, 120, 150 and 180 minutes. At listed times, aliquots were transferred from the incubating glass tube into small plastic tubes placed on ice. The residual activity was then conducted as described in *2.2.3*. Each data point is an average of 9 measurements of the same sample.

Storage stability of the trypsin species

Native trypsin, TGG, TCC 1:5 and TCC 1:10 were assayed for their storage stability for over 2 months (67 days). The samples were incubated either at 4 °C with or without 20 mM $Ca^{2+}$and at 25 °C with or without 20 mM Ca^{2+} in 47 mM Tris, 3 mM NaN_3 buffer, pH

8.1. Sodium azide (NaN_3) was included in order to stop or minimize any microbial growth. The trypsin species where kept in 1.5 mL Eppendorf plastic tube while stored. Samples were taken on day 1, 8, 16, 24, 29, 38, 56 and 67 for measurements of residual activity by diluting the samples 10-fold in 112 mM TEA, 11.5 mM $CaCl_2$ buffer pH 7.8. Samples were kept on ice while waiting for measurements. Residual activity was measured as described in *2.2.3*. Each data point is an average of 5 measurements of the same sample.

Urea inactivation of the trypsin species

The urea inactivation assay was performed in accordance with ref. [52], with modifications. Around 8 M urea solution was prepared in 100 mM Tris, 11.5 mM $CaCl_2$, pH 8.1. In order to obtain exact urea concentration, the difference in refractive indices between urea buffer solution and the buffer solution without urea was measured using an simple refractometer. The exact urea concentration can be then calculated by following empirical equation [40]:

$$C_{urea} = 117{,}66 \cdot \Delta n + 29{,}753 \cdot \Delta n^2 + 185{,}56 \cdot \Delta n^3 \qquad \textbf{Equation 2.5.}$$

where C_{urea} is the urea concentration in $^{mol}/_{L}$ and Δn is the refractive index of urea buffer solution subtracted by the refractive index of the same buffer solution without urea. Stability of native trypsin against urea was measured by incubating native trypsin in 0 M, 2 M, 4 M, 6 M and 7.55 M urea concentration for one hour in a 37 °C water bath. A stoppered glass tube containing 100 mM Tris, 11.5 mM $CaCl_2$ buffer, pH 8.1 along with little more than previously listed amounts of urea, thus when sample was added it yielded the precise urea concentration, was preheated in a Julabo13 waterbath. After pre-heating the buffer, an aliquot that resulted in 10 to 20-fold dilution of the trypsin species was added, vortexed and inserted back to waterbath for one hour. After one hour had lapsed, aliquots were taken and cooled on ice (not diluted in cold buffer as in ref. [52]). Residual activity measured as described in *2.2.3*, **except** that the substrate solutions also contained the identical urea concentrations as the assayed sample. Each data point is an average of 9 data points from the same sample.

2.2.5 Michaelis-Menten kinetics of native trypsin and TGG

Determination of kinetical parameters was conducted by measuring native trypsin and TGG against 2 mM, 1 mM, 0.5 mM, 0.25 mM, 0.12 mM and 0.05 mM L-BAPNA, by pipetting the amount of L-BAPNA into a plastic cuvette that resulted in these concentrations followed by an appropriate dilution with 50 mM Tris, 10 mM $CaCl_2$ buffer, pH 8.1, up to 950 µL. The cuvette was vortexed vigorously and placed into a Heλios spectrometer adjusted to 25 °C with a Peltier heating system. Subsequently, 50 µL of either native trypsin or TGG sample was added to the cuvette, the solution immediately stirred with a clean plastic stirrer and then the enzymatic rate was monitored for 30 seconds at 410 nm.
Enzymatic rate was changed to $^{U}/_{mg}$ by using the molar extinction coefficient of p-nitroanilide of 8800 $M^{-1}cm^{-1}$ at 410 nm [83] and the following relationship:

$$\left[\frac{U}{mg}\right] = \frac{{}^{\Delta A}/_{min} \cdot 1000}{8800 \cdot mg\ enzyme} \qquad \textbf{Equation 2.6.}$$

After the rate measurements were finished, cuvettes were kept for at least one day and then measured for the exact original L-BAPNA concentration by measuring the absorbance of the liberated p-nitroanilide at 405 nm using the molar extinction coefficient of 9951 $M^{-1}cm^{-1}$ [86].
Least-squares nonlinear fitting using Marquardt- Levenberg algorithm of the experimental data to the Briggs-Haldane modified Michaelis-Menten equation was performed in the data analysis software Kaleidagraph (ver. 3.6). The kinetic parameter V_{max} and K_m were obtained according to:

$$V = \frac{V_{max} \cdot [S]}{K_m + [S]} \qquad \textbf{Equation 2.7.}$$

where V is the rate, V_{max} is the maximum theorietical rate, [S] is the substrate concentration and K_m is the Michaelis constant. k_{cat} was obtained according to:

$$k_{cat} = \frac{V_{max}}{[E_t]} \qquad \textbf{Equation 2.8.}$$

where $[E_t]$ is the total enzyme concentration. Each data point is an average of triplicate.

2.2.6 Azocasein assay for proteolytic activity

Sulfanilamide azocasein (SAC) assay was conducted in order to compare the activity of the trypsin species (i.e. native trypsin, TGG, TCC 1:5 and TCC 1:10) towards a macromolecular substrate according to ref. [87].
About 50 mg of SAC was weighed into a 50 mL plastic tube, followed by addition of 25 mL of 112 mM TEA, 11.5 mM $CaCl_2$ buffer, pH 7.8. The solution was mixed vigourosly on a mixer. This cloudy solution was subsequently filtered using Whatman filter paper No.4. into a new identical plastic tube.
Protein concentration of the SAC solution was measured by diluting SAC samples 20 fold in 0.1 M NaOH solution. This diluted solution was placed in a Helios spectrophotometer and absorbance measured at 440 nm. The spectrophotometer had previously been blanked with 0.1 M NaOH and the same dilution of buffer. The concentration of SAC was obtained by using the extinction coefficient of sulfanilamide in 0.1 M NaOH, $E^{440}_{1\%} = 34$ [88]. Three samples of the SAC solution were measured and the SAC concentration was determined to be approx. 0.2 %.
Proteolytic activity of native trypsin and TGG, TCC 1:5 and TCC 1:10 was conducted as follows: 500 µL of SAC solution and 200 µL of either native trypsin, TGG, TCC 1:5 and TCC 1:10 solution were added into a 1.5 mL Eppendorf plastic tubes. This mixture was then incubated at 25 °C for 30 minutes in Julabo13 digital waterbath. After 30 minutes, the proteolysis of SAC was stopped by addition of 200 µL of 10 % trichloroacetic acid (w/v) precipitant, and the samples were subsequently centrifuged in a microcentrifuge, with approx. 12000 $^{rev}/_{min}$ for 6 minutes. The absorbance of the supernatant was measured in Helios spectrophotometer at 340 nm. The device had been pre-blanked with the same solution without proteins (the blank being the buffer).
One enzymatic unit is defined to be the enzyme amount causing an absorption change of 1 within one hour [87]. Measured values are average of triplicates assigned with the appropriate standard deviation.

2.2.7 Comparsion of secondary structures of native trypsin and TGG by CD spectropolarimetry

The CD spectropolarimetry was conducted using a Jasco J-810 spectropolarimeter.
The samples were prepared as follows: 3.5 mL of TGG (approx. 0.8 $^{mg}/_{mL}$ trypsin concentration) in 10 mM sodium acetate buffer, pH 5.0 was frozen in liquid nitrogen and subsequently placed in a HETOSICC freeze drier *in vacuo* for 1 hour and 20 minutes, in order to concentrate the solution by subliming a considerable amount of the water from the TGG solution. The TGG solution (approx. 2 mL) was then thawed and dialyzed against 500 mL of 50 mM Tris buffer, pH 7.0 with magnetic stirring in a cold room (4 °C) overnight. After dialysis the dialyzed TGG solution was pipetted into a 20 mL plastic cylinder and 50 µL of 0.2 M PMSF (PMSF in isopropanol) was added, and the solution gently shaken for 3 hours for maximum inhibition as described elsewhere [24]. Samples were taken from the solution at intervals, and the reduction in catalytic activity was 87 % using the assay in *2.2.3.*, by 10-fold dilution of the sample, after 3 hours had lapsed. This inhibited PMS-TGG was dialysed against 500 mL of 10 mM sodium acetate buffer, pH 5.0 with magnetic stirring in a cold room (4 °C) overnight. After the dialysis, the PMS-TGG solution was put in a 20 mL plastic cylinder and used for CD measurements. The dialysis buffer was collected and used as the background for CD measurments.
Native trypsin was dissolved in 3 mL 50 mM Tris buffer, pH 7.0, yielding a solution that had an approx. trypsin concentration of 1.2 $^{mg}/_{mL}$. Subsequently, 50 µL of 0.2 M PMSF was added and the solution was gently shaken for 3 hours for maximum inhibition. Samples were taken from the solution at intervals, and the reduction in catalytic activity was 99 % using the assay in *2.2.3.*, by 10-fold dilution of the sample, after 3 hours had lapsed. This inhibited PMS-trypsin was dialyzed against 500 mL of 10 mM sodium acetate buffer, pH 5.0 with magnetic stirring in a cold room (4 °C) overnight. After the dialysis the PMS-trypsin solution was put in a 20 mL plastic cylinder and used in CD measurements. The dialysis buffer was collected and used as the background in CD measurements.
Prior to measurements, the calibration of the CD instrument was checked by measuring 1S-(+)-camphorsulfonic acid (0.06 % w/v) solution at 290.5 nm in a 1-cm quartz cuvette . The ellipticity was +187 mdeg at 25 °C so that no calibration was needed [76]. The CD device was always allowed to heat up for at least 30 min prior to measurments. Around 5 L/min of pure N_2 was purged through the device at all times.
Dialysate buffers and samples were scanned from 250 – 200 nm, using 100 nm/min scanning speed, 1 sec in response time and 2 nm bandwith in a fused quartz cuvette with an optical path of 0.1 cm. Each spectrum collected was an average of 4 spectra. Useful spectra were collected from 250 – 202 nm. From 202 - 200 nm the high voltage applied to the photomultiplier exceeded 700 V, which leads to less reliable data [76]. Raw signal (in millidegrees), after subtracting the dialyaste buffer and the cuvette, was converted to commonly used mean residue ellipticity by using :

$$[\theta]_{MRE} = \frac{100 \cdot [\theta]}{C \cdot n \cdot l}$$ **Equation 2.9.**

Where [θ] is raw signal from the CD device (in millidegrees), C is the concentration in millimolarity, n is the number of amino acids in the protein and l is the length of the cuvette in centimeters [89].

2.2.8 Size determination of the trypsin species

SDS-PAGE of the trypsin species

Discontinious electrophoresis was conducted by using pre-casted NuPAGE® (8x8 cm) Bis-Tris gels. The acrylamide concentration of the stacking gel is 4 %, separating gel is 4-12 %, and bisacrylamide (crosslinker) concentration is 3.8 – 5 %, depending on regions [90]. Aliquots of 60 µL of NuPAGE® sample buffer were added in a 1.5 mL Eppendorf plastic tubes, followed by the addition of 20 µL of trypsin species (i.e. either native, TGG, TCC 1:5 and TCC 1:10) yielding a mixture with a protein concentration of approx. 0.25 $^{mg}/_{mL}$. The sample was then heated in a 70 °C water bath for 10 minutes. After heating, 35 µL of samples and 5 µL of Bench Mark™ protein ladder were loaded into appropriate wells. The protein ladder consists of 15 recombinant proteins with the molecular masses of 220, 160, 120, 100, 90, 80, 70, 60, 50, 40, 30, 25, 20, 15 and 10 kDa [91].
The electrophoresis was conducted in a Xcell Sure Lock™ electrophoretic cell with SDS MOPS running buffer (50 mM MOPS, 50 mM Tris (basic form), 0.1 % SDS, 1 mM EDTA buffer, pH 7.7) filled in both chambers. This system was connected to a DC power supply that had been pretuned to 200 V voltage and 117 mA current. The electrophoresis was discontinued when the colored bands had traveled to the edges of the gel (~1 hour).
The gels where stained in a Coomassie dye solution (0.25 % w/v Coomassie Brilliant Blue G, 30 % v/v methanol, 10 % acetic acid v/v) overnight.
The gels were destained in an aqueous 30 % methanol (v/v) solution for a couple of hours, or until the protein bands were visibly resolved from the background.

NTA of the TCCs

Nanoparticle tracking analysis (NTA) was conducted on a NanoSight LM10 instrument fitted with an EMCCD camera. 300 µL, of either TCC 1:5 and TCC 1:10, were injected to the viewing chamber of the instrument, and the trajectories of the sample molecules were measured for 90 seconds with manual shutter and gain adjustments. Neither samples required dilution. Data were collected in the ,,single shutter and gain mode“ and analyzed using NTA 2.0 Build 127 software.

MALDI-TOF mass spectrometry of native trypsin and TGG

The MALDI TOF mass spectrometry was conducted on Brüker Autoflex III MALDI-TOF mass spectrometer. The samples were prepared as follows: approx. 1 $^{mg}/_{mL}$ of either trypsin or TGG sample in a 50 mM Tris buffer, pH 7.0, were inhibited by N-α-tosyl-L-lysine-chloromethylketone (TLCK), by weighing approx. 20 mg of the inhibitor to the sample solutions, yielding a final concentration of the inhibitor of at least 15 mM. The reduction in catalytic activity was monitored with the assay described in *2.2.3*, by a 10-fold dilution in 112 mM TEA, 11.5 mM $CaCl_2$ buffer, pH 7.8, at certain intervals, until 99 % activity of the trypsin sample and around 85 % activity of the TGG sample was lost, compared with uninhibited enzyme. Increments of TLCK to the TGG sample did not cause further inhibition. Around 2 mL of each sample were dialyzed separately, twice in 250 mL of 1 mM HCl buffer, pH 3.0, in a cold room (4 °C), with a magnetic stirring for 24 hours. Insoluble material where observed to accumulate in the dialysis of the TGG sample, which could be a mixture of TGG molecules, unreacted inhibitor and/or leftovers of the

conjugants. Thus, the TGG sample, along with this precipitation, was transferred to three 1.5 mL Eppendorf tubes and centrifuged in an microcentrifuge. The absorbance at 280 nm of the supernatant indicated high concentration of protein (approx. 0.7 $^{mg}/_{mL}$ using the extinction coefficient of native trypsin) in the sample which suggested that the the bulk of this precipitation was not precipitated TGG molecules. After dialysis, of the native trypsin sample and TGG sample (which had also been centrifugated, with only the supernatant collected), the samples were transferred to two 20 mL plastic cylinders, separately.
The „MALDI“ samples were prepared by the „sandwich“ method [92], as follows: 9 µL of TLCK-inhibited native trypsin and 15 µL of TLCK-inhibited TGG sample was mixed with 1 µL of 1 % trifluoroacetic acid (TFA) (w/v) in water, in a 0.5 mL Eppendorf plastic tube , separately. 0.6 µL of concentrated sinapinic acid (SA) in acetone was added onto each spot on the target plate. After the spot had dried completely, 0.5 µL of the previously prepared sample solution was pipetted onto different dried spots and allowed to dry. Finally, 0.5 µL of concentrated SA along with 0.1 % TFA in 50:50 water:acetonitrile (v/v) was added onto the spots.
The target metal plate was installed into the mass spectrometer and spectra collected. The acceleration voltage difference of the extractor and repeller was at least 20 kV. The spectra were collected in linear mode.

3 Results

3.1 Size determination of the trypsin species

3.1.1 Molecular mass of TGG and its possible conjugation sites

MALDI TOF spectra of trypsin and TGG are shown in figures 3.1 and 3.2.

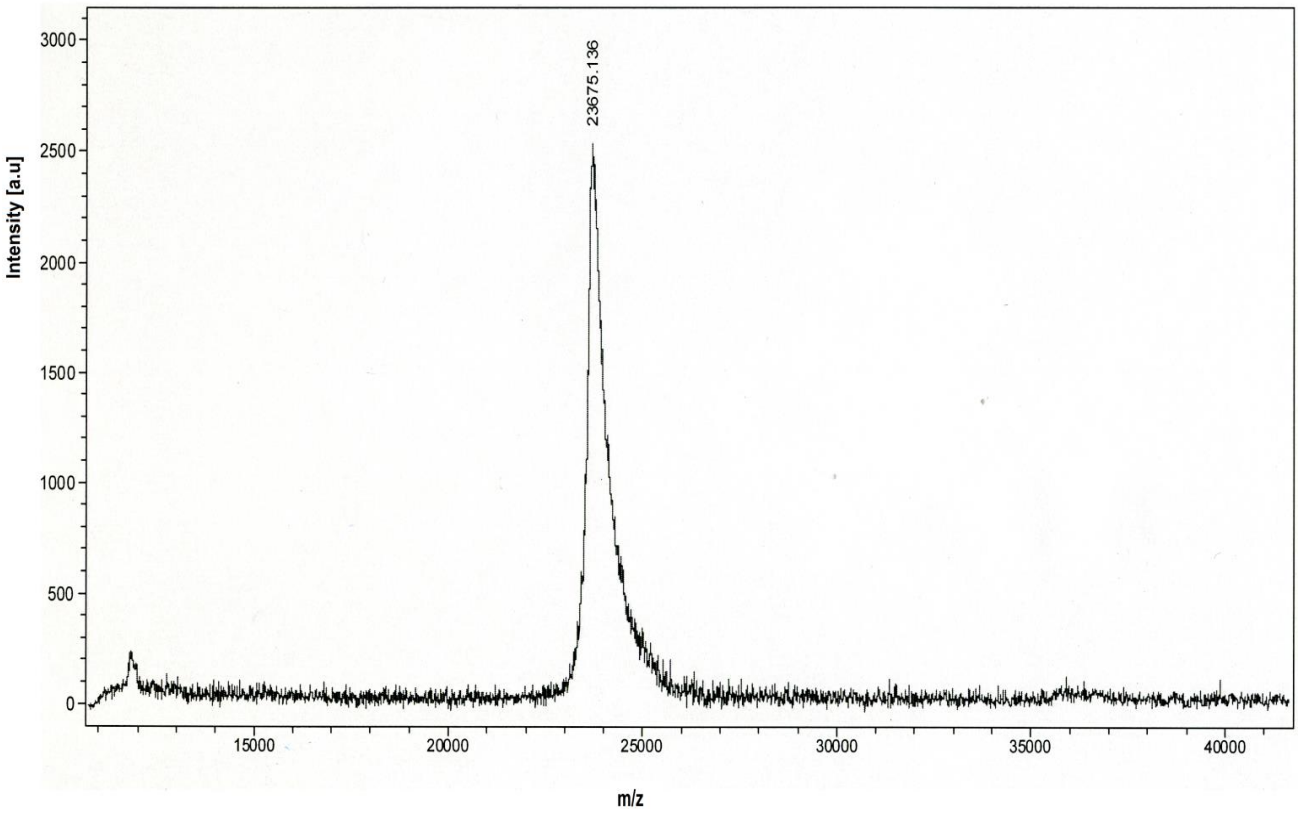

Figure. 3.1. *MALDI TOF mass spectrum of native trypsin. The singly cationized form of TLCK-inhibited bovine trypsin was detected at 23675 m/z.*

The spectrum of native trypsin (fig 3.1.) shows that native trypsin (inhibited with TLCK) has a narrow and high peak at 23675 Da, as anticipated. When the mass of trypsin is substracted from the molecular mass of TLCK (MW = 367,31 $^{g}/_{mole}$), 23305 Da is obtained, which is the exact mass of cationic bovine β-trypsin [11].

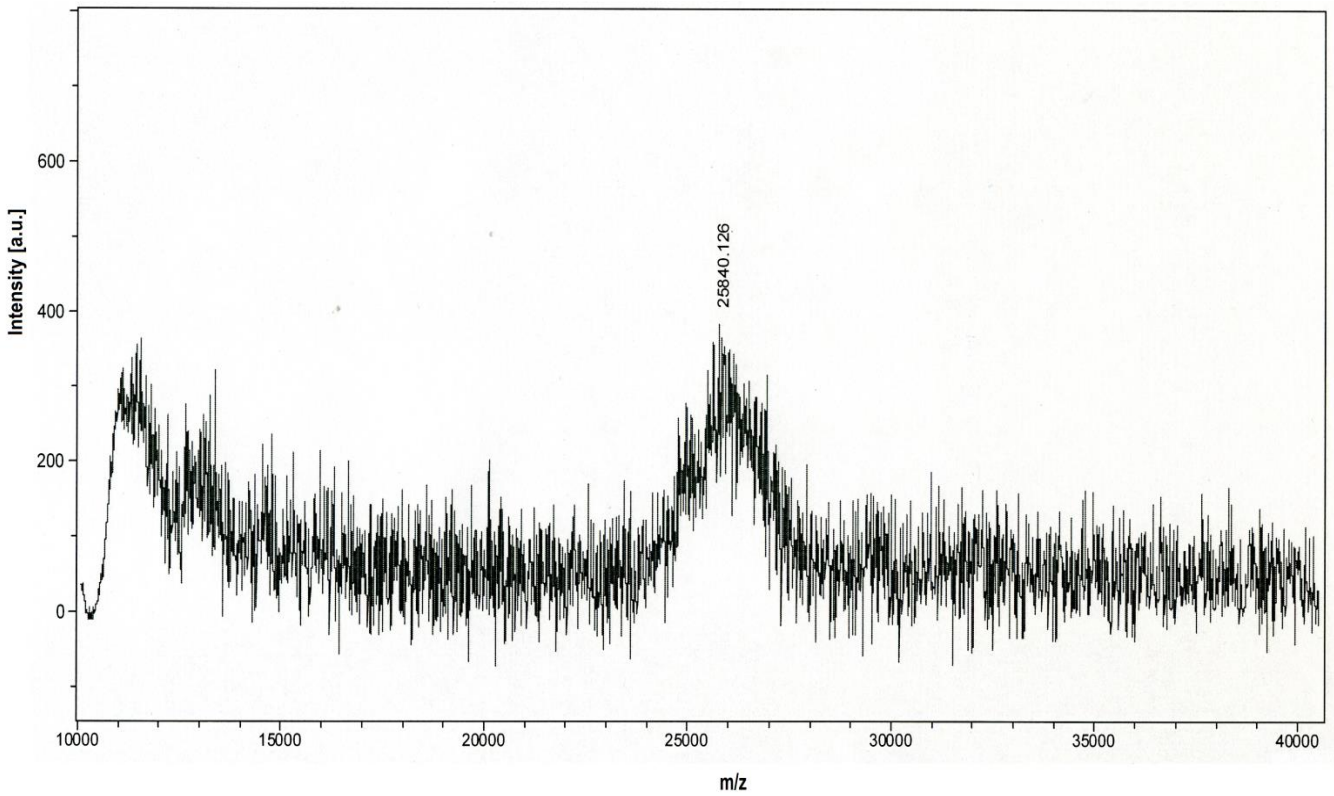

Figure 3.2*. MALDI TOF mass spectrum of TGG. The most abundant singly cationized form of the several glycoforms of TLCK-inhibited TGG was detected at 25840 m/z.*

The mass spectrum of TLCK inhibited TGG (fig 3.2.) is around 1.5 times wider than for native trypsin and the intensity is much lower. This is typical for glycated proteins with several glycoforms [71]. The highest peak of TGG gives a signal at 25840 Da. As mentioned in previous chapter (*2.2.8*) only 85 % af the TGG sample was fully inhibited, so the contribution of TLCK is 85 % of its total mass or 0.85 x 367.31 $^{g}/_{mole}$ = 312.21 $^{g}/_{mol}$, thus 312.31 $^{g}/_{mole}$ of TLCK was adding up to each mole of the TGG sample . Subtraction of the mass contribution of the inhibitor from TGG yields 25528 Da. Hence, the mass difference between native trypsin and TGG is 2223 Da, which indicates that around 12 mole of D-glucosamine (MW 179,16 $^{g}/_{mole}$) reacted, on average, with one mole of trypsin.

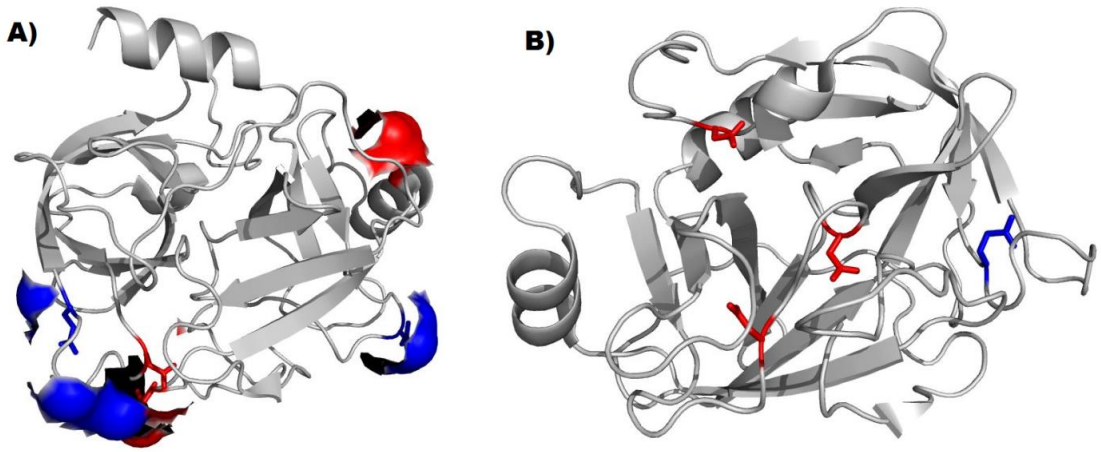

Figure 3.3. *Pymol representations of trypsin with the acidic residues (six residues) forming an significant contact to the solvent A) and B) acidic residues (four residues) forming little or no contact to the solvent. Glutamic acid residues are shown in blue and aspartic acid residues are shown in red. Trypsin PDB code: 4i8g.*

Bovine trypsin has ten acidic amino acid residues. On the basis of molecular visualization of cationic β-trypsin (PDB code: 4i8g) using Pymol [93] and its solvent accessible surface feature, it can been seen that six acidic residues make a significant contact to the solvent and are therefore readily conjugated with D-glucosamine (fig. 3.3). Four acidic residues are buried in the protein structure, but two of them are situated in the middle of a loop. Loop regions are known to be flexible, and therefore it can be rationalized that these residues can be conjugated to D-glucosamine at certain points during the conjugation reaction. Therefore, it is concluded that eigth acidic amino acid residues can take part in conjugation.

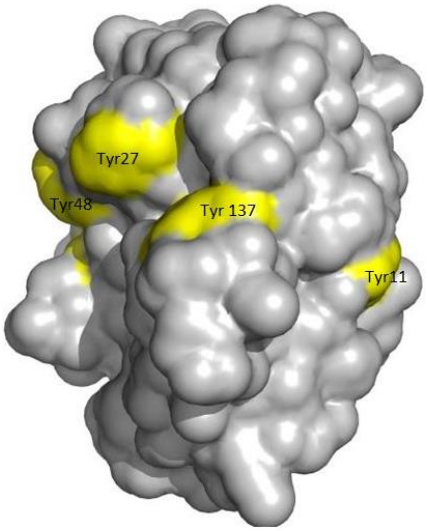

Figure 3.4. *Four tyrosyl residues (Tyr48, Tyr27, Tyr137 and Tyr11) that form a significant contact with the water surroundings.*

It is well known that carbodiimides can conjugate onto tyrosyl residues of proteins and peptides [69]. Four tyrosyl residues in bovine trypsin have a significant surface contact towards the solvent as visualized using Pymol (fig 3.4) using the aforementioned solvent accessible feature, which is in accordance with what has been previously found elsewhere [94].
In summary, it was thus concluded that D-glucosamine is conjugated onto 8 acidic residues and 4 tyrosyl residues, therefore yielding 12 possible conjugation sites, as indicated by the MALDI-TOF mass spectrometrical data of native trypsin and TGG.

3.1.2 Size determination of TCC 1:5 and TCC 1:10 from electrophoretical gels.

The crosslinked protein conjugates TCC 1:5 and TCC 1:10 formed a highly heterogenous mixture with wide ranges of high molecular mass of > 160 kDa as well as a significant fraction of unreacted trypsin (fig 3.5A). This heterogeneity is not surprising since the chitooligosaccharides are „homomultifunctional“ oligomers with different extent of free amino groups. Electrophoresis of native trypsin only reacted with carbodiimide and NHSS **without** either chitooligosaccharides or D-glucosamine, control-trypsin, is shown in figure 3.5B. It seems that a dimerization of trypsin molecules had taken place to a small extent on the control-trypsin. However, no dimerization band was observed for either TGG or TCC 1:5 and TCC 1:10. That indicates that dimerization competes with the conjugation of D-glucosamine and intermolecular cross-linking with the chitooligosaccaharides, of which the latter competitor reaction (i.e. the conjugation with D-glucosamine and intermolecular cross-linking with chitooligosaccharides) is more favorable.

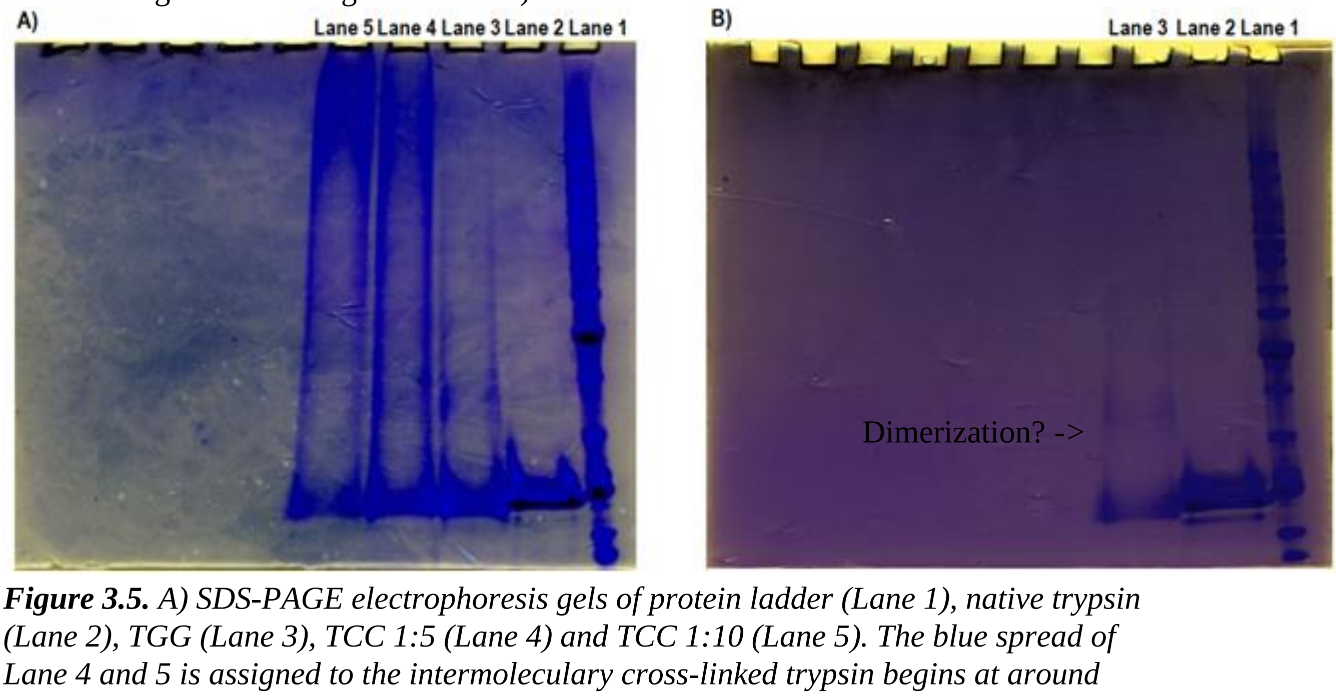

Figure 3.5. *A) SDS-PAGE electrophoresis gels of protein ladder (Lane 1), native trypsin (Lane 2), TGG (Lane 3), TCC 1:5 (Lane 4) and TCC 1:10 (Lane 5). The blue spread of Lane 4 and 5 is assigned to the intermolecular cross-linked trypsin begins at around approx. 160 kDa according to the protein ladder. B) SDS-PAGE electrophoresis gel of protein ladder (Lane 1), native trypsin (Lane 2) and protein reacted with only EDAC/NHSS (Lane3). A possible dimerized trypsin (of small extent) can be visualized for Lane 3, which is at a similar location as the 40 kDa band of the protein ladder.*

3.1.3 Hydrodynamical radii of the TCCs

Measurements of hydrodynamical radii by NTA of TCC 1:5 and TCC 1:10, and comparison of them to trypsinogen, can be seen in table 1.1.

Table 3.1. *Comparison of hydrodynamical radii of trypsin species*

Trypsin species	**Hydrodynamical radius [nm]**
Native trypsinogen	1.96[1]
TCC 1:5	avg. 330
TCC 1:10	avg. 218

Mean values of hydrodynamical radii of TCC 1:5 and TCC 1:10 does not give a good scale on the spread of their sizes. Figure 3.6A and B, shows the relative concentration of TCC 1:5 and TCC 1:10, respectively, as a function of their radii.

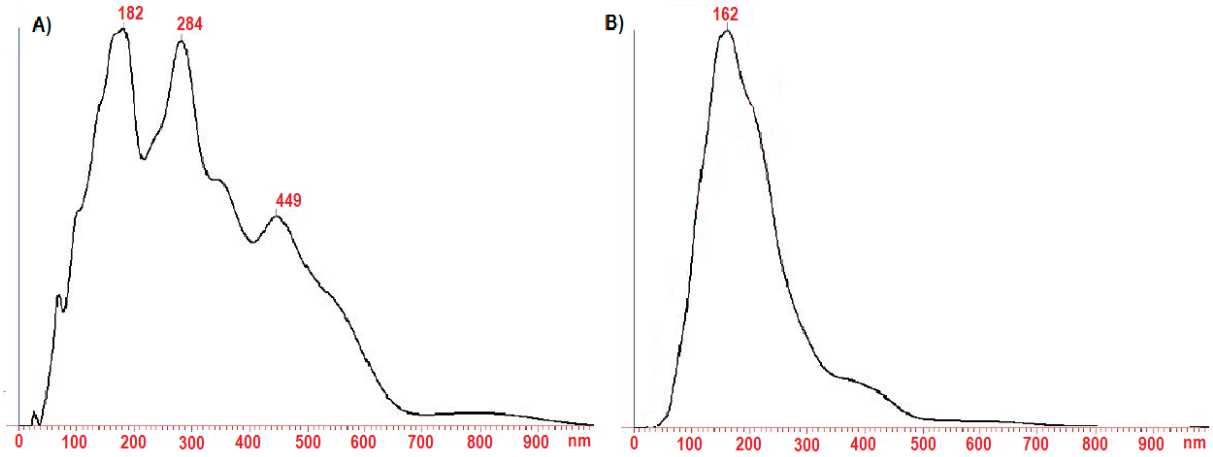

Figure 3.6. *Relative concentration of A) TCC 1:5 and B) TCC 1:10, as function of their hydrodynamical radii.*

As can been seen from figure 3.6A and B, TCC 1:5 forms three population of polydisperse (or heterogenous) complexes with two major peaks at 182 and 284 nm and one minor peak at 449 nm. Only one major peak is observed for TCC 1:10 at 162 nm.

[1] Determined from size-exclusion chromatography measurements according to ref. [95]

3.2 Stability of TGG and the TCCs

3.2.1 Thermal stability of TGG and the TCCs

Thermal stability was determined by incubating the trypsin species at 60 °C over varying time intervals, which is represented in figure 3.7.

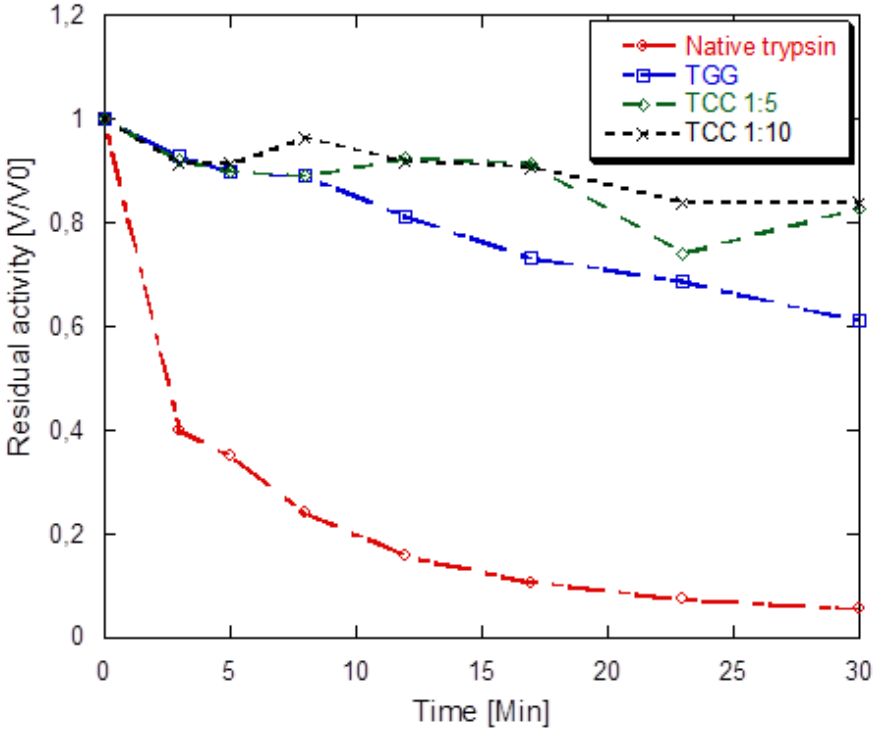

Figure 3.7. *Residual activity of native trypsin, TGG, TCC 1:5 and TCC 1:10 as function of time at 60 °C.*

It can be clearly seen from figure 3.7. that TGG, TCC 1:5 and TCC 1:10 possess considerably higher thermostability than native trypsin.

The $T_{50\%}$ values (i.e. the temperature in which half of the trypsin species are inactive after 10 min incubation) are given in table 3.2.

Table 3.2. *$T_{50\%}$ values of the trypsin species.*

Trypsin species	**$T_{50\%}$ [°C]**
Native trypsin	56,2 ± 0,5[†]
TGG	63,3 ± 0,5[†]
TCC 1:5	64,3 ± 0,5[†]
TCC 1:10	66,7 ± 0,5[†]

[†] Values were determined visually from the plots and therefore assigned with rather high uncertainity.

The $T_{50\%}$ values given in table 3.2. give further clues about the increased thermostability of the trypsin species.

3.2.2 Stability against thermal inactivation of native trypsin and TGG

Thermal inactivation was studied in order to obtain rate constants of inactivation at different temperatures and thus to obtain the inactivation energies for native trypsin and TGG. Due to the heterogeneity and presence of several population of different complexes of TCC 1:5 and TCC 1:10 the measurements of thermal stability of these preparations where omitted.
The inactivation rate constants were obtained according to the first-order inactivation kinetics model:

$$ln\left(\frac{V}{V_0}\right) = k_{in} \cdot t \qquad \textbf{Equation 3.1.}$$

where V is the enzymatic rate at a certain time, V_0 is the initial enzymatic rate before any heating, k_{in} is the first order rate constant of inactivation and t is the time. The slope of a plot with $\ln(V/V_0)$ as a function of t, gives the the first order rate constant by using least-square linear regression.
Half-lifes of inactivation for the native trypsin and TGG species were calculated by using:

$$t_{1/2} = \frac{\ln 2}{k_{in}} \qquad \textbf{Equation 3.2.}$$

Typical biphasic inactivation plot was obtained for the inactivation of native trypsin and TGG, as anticipated, indicating two stable populations of the enzyme [34][96][97]. Figure 3.8 shows a typical biphasic behavior of thermal inactivation of native trypsin. The phase change occurs near 500 seconds. If the inactivation would perfectly follow first order inactivation kinetics then the line of the plot would be perfectly linear [98]. This biphasic behavior may be due to formation of a stable intermediate during inactivation [34][96]. The biphasic inactivation of trypsin and TGG led to two different inactivation rate constants: $k_{in,1}$ and $k_{in,2}$.

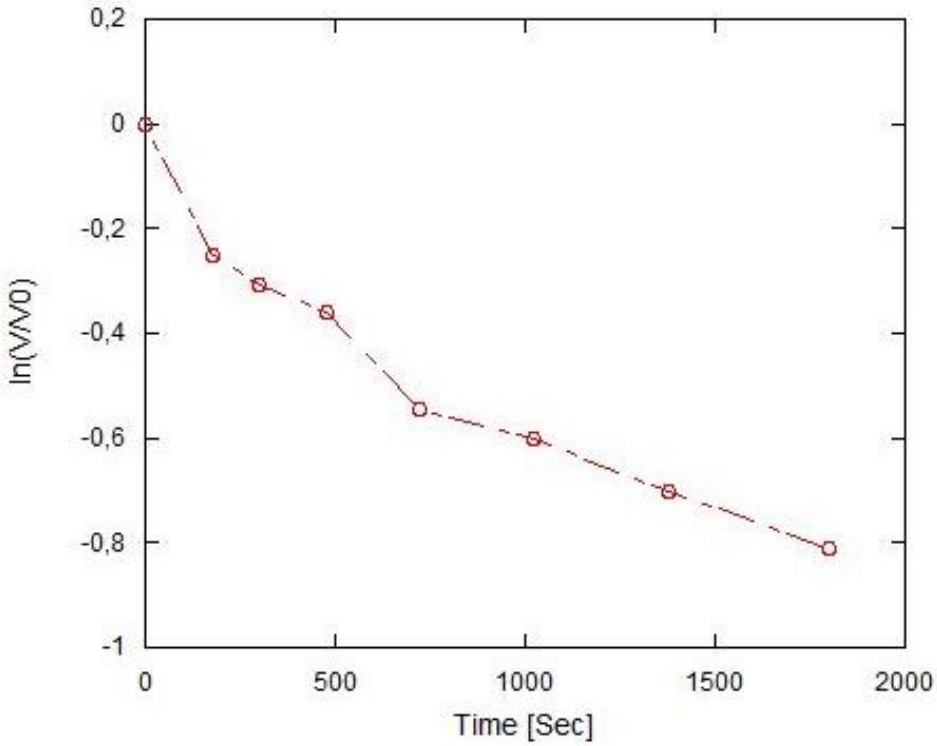

Figure 3.8. *An example of biphasic inactivation. The plot shows the thermal inactivation of native trypsin at 52 °C, plotted with ln(V/V$_0$) as a function of time.*

.

Inactivation energies of native trypsin and TGG were calculated from Arrhenius equation:

$$k_{in} = A \cdot e^{-\frac{E_{in}}{R \cdot T}} \rightarrow \boldsymbol{ln(k_{in}) = A \cdot -\frac{E_{in}}{R} \cdot \frac{1}{T}} \qquad \textbf{Equation 3.3.}$$

where A is a frequency factor (which does not change considerably when working on a narrow temperature range), k_{in} is first-order inactivation rate constant, R is the gas constant, E_{in} is the inactivation energy and T is the temperature (in Kelvin). Inactivation energies of the native trypsin and TGG species were determined by least-square linear regression of the slope of a plot where ln(k_{in}) is a function of 1/T.

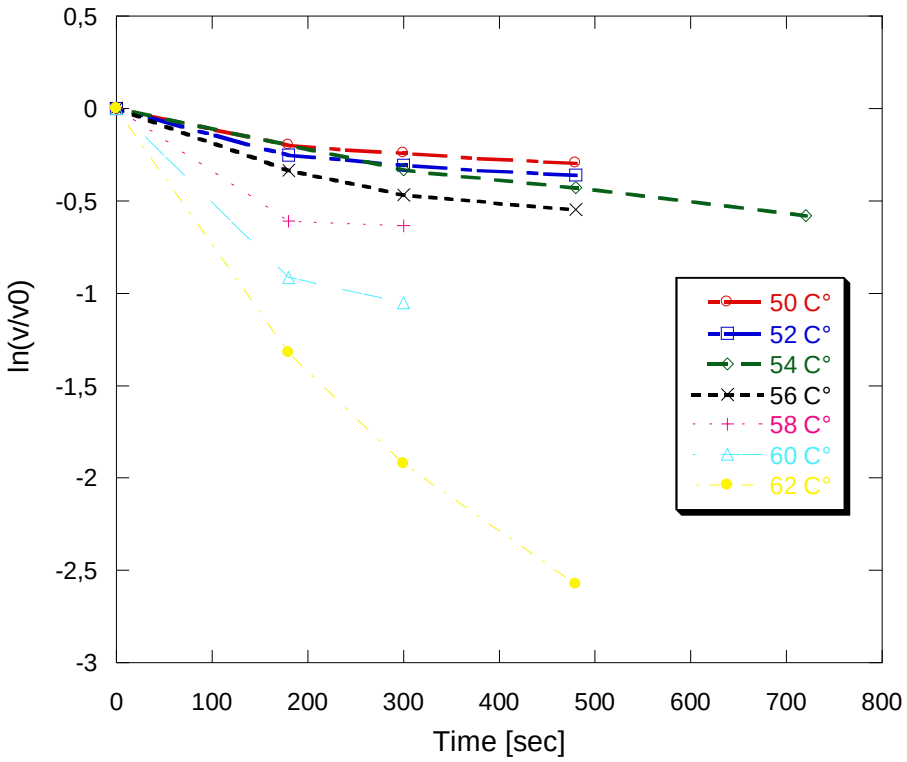

Figure 3.9. *Natural logarithm of residual activity of the first phase as a function of time for native trypsin. Rate constants ($k_{in,1}$) at different temperatures were obtained from the respective curves.*

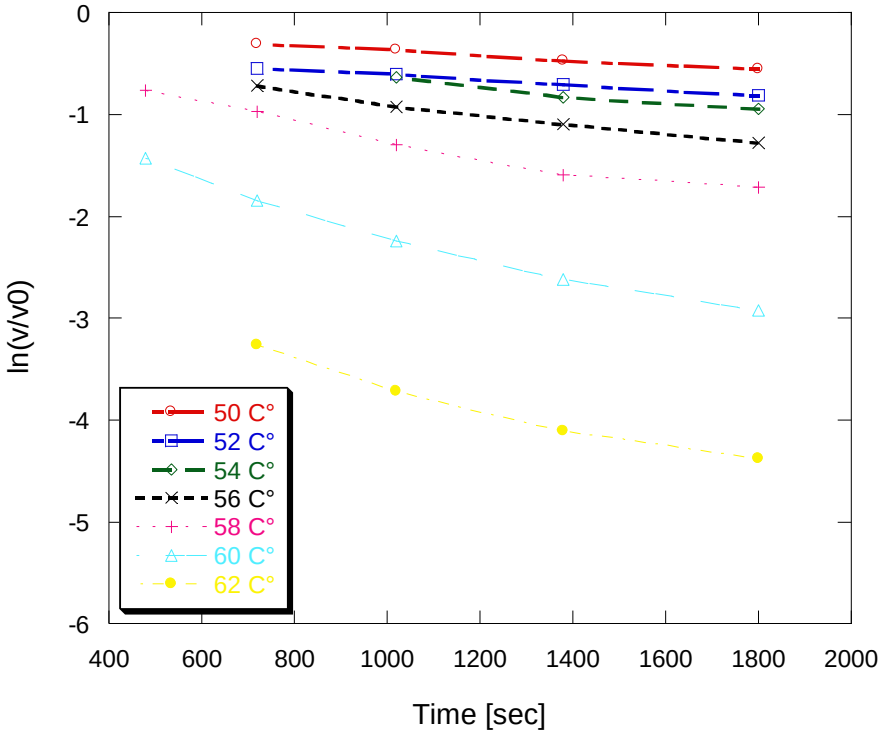

Figure 3.10. *Natural logarithm of residual activity of the second phase as a function of time for native trypsin. Rate constants ($k_{in,2}$) at different temperatures were obtained from the respective curves.*

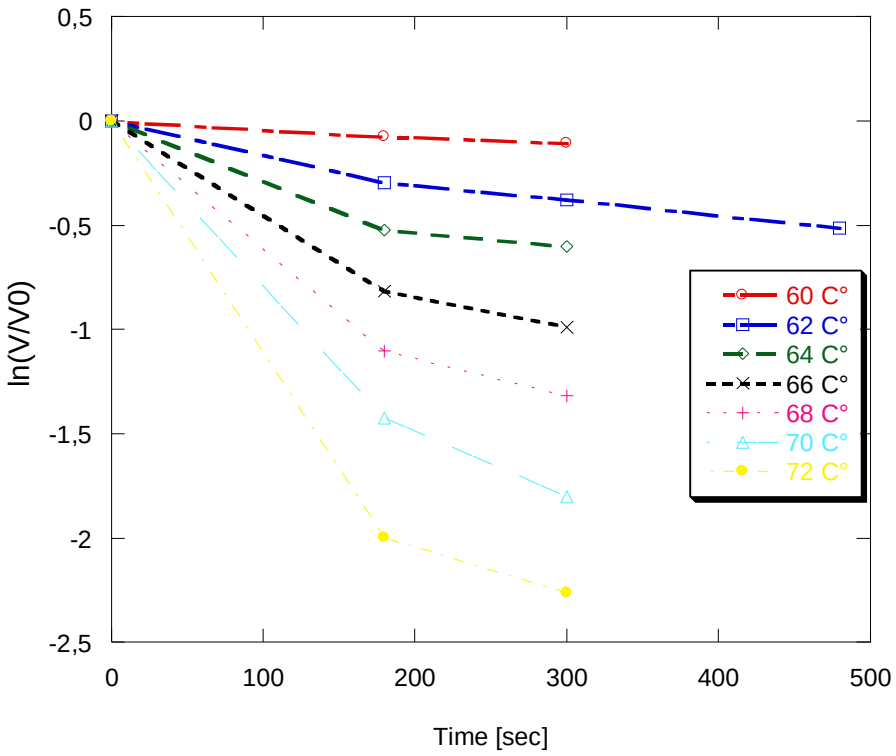

Figure 3.11. *Natural logarithm of residual activity of the first phase as a function of time for TGG. Rate constants ($k_{in,1}$) at different temperatures were obtained from the respective curves.*

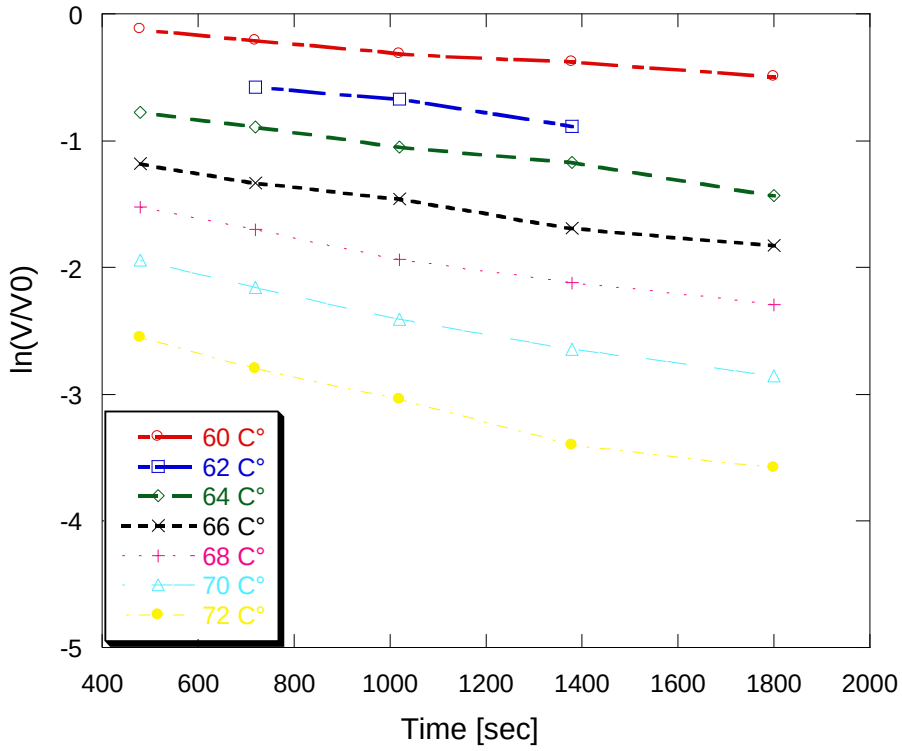

Figure 3.12. *Natural logarithm of residual activity of the second phase as a function of time for TGG. Rate constants ($k_{in,2}$) at different temperatures were obtained from the respective curves.*

R^2 correlation coefficients of the data in figures 3.9-3.12 were always higher than 0.864 and most commonly on the range of 0.900 – 0.980.

The rate constants for $k_{in,1}$ and $k_{in,2}$, obtained by linear least-square regression of figures 3.9-3.12, are given in table 3.3 and 3.4, and their corresponding half-lives are given in table 3.5 and 3.6.

Table 3.3. *The rate constants for the thermal inactivation of native trypsin. Assigned uncertainties are the standard error of the corresponding slope.*

Temperature [°C]	**$k_{in,1}$ [s^{-1}]**	**$k_{in,2}$ [s^{-1}]**
50	$5.98 \times 10^{-4} \pm 1.52 \times 10^{-4}$	$2.36 \times 10^{-4} \pm 1.25 \times 10^{-5}$
52	$7.34 \times 10^{-4} \pm 2.06 \times 10^{-4}$	$2{,}52 \times 10^{-4} \pm 1.02 \times 10^{-5}$
54	$7.98 \times 10^{-4} \pm 0.993 \times 10^{-4}$	$3.91 \times 10^{-4} \pm 8.22 \times 10^{-5}$
56	$11.4 \times 10^{-4} \pm 2.61 \times 10^{-4}$	$5.13 \times 10^{-4} \pm 4.02 \times 10^{-5}$
58	$22.1 \times 10^{-4} \pm 8.74 \times 10^{-4}$	$7.49 \times 10^{-4} \pm 9.30 \times 10^{-5}$
60	$36.2 \times 10^{-4} \pm 10.7 \times 10^{-4}$	$11.2 \times 10^{-4} \pm 10.7 \times 10^{-5}$
62	$53.4 \times 10^{-4} \pm 6.76 \times 10^{-4}$	$10.2 \times 10^{-4} \pm 13.4 \times 10^{-5}$

Table 3.4. *The rate constants for the thermal inactivation of TGG. Assigned uncertainties are the standard error of the corresponding slope.*

Temperature [°C]	**$k_{in,1}$ [s^{-1}]**	**$k_{in,2}$ [s^{-1}]**
60	$0.360 \times 10^{-3} \pm 0.405 \times 10^{-4}$	$2.75 \times 10^{-4} \pm 2.01 \times 10^{-5}$
62	$1.04 \times 10^{-3} \pm 1.76 \times 10^{-4}$	$4.47 \times 10^{-4} \pm 7.34 \times 10^{-5}$
64	$2.07 \times 10^{-3} \pm 6.22 \times 10^{-4}$	$4.82 \times 10^{-4} \pm 2.63 \times 10^{-5}$
66	$3.40 \times 10^{-3} \pm 8.44 \times 10^{-4}$	$4.97 \times 10^{-4} \pm 3.27 \times 10^{-5}$
68	$4.52 \times 10^{-3} \pm 11.8 \times 10^{-4}$	$5.91 \times 10^{-4} \pm 4.83 \times 10^{-5}$
70	$6.16 \times 10^{-3} \pm 13.1 \times 10^{-4}$	$6.93 \times 10^{-4} \pm 4.74 \times 10^{-5}$
72	$7.82 \times 10^{-3} \pm 24.3 \times 10^{-4}$	$7.95 \times 10^{-4} \pm 6.66 \times 10^{-5}$

Table 3.5. *Half-lives of native trypsin at measured inactivation temperatures. Assigned uncertainties are calculated from the standard errors of the slope.*

Temperature [°C]	Half lives - first phase [min]	Half lives - second phase [min]
50	19 ± 4.9	49 ± 2.6
52	16 ± 4.4	46 ± 1.9
54	14 ± 1.8	30 ± 6.2
56	10 ± 2.3	23 ± 1.8
58	5 ± 2.1	15 ± 1.9
60	3 ± 0.9	10 ± 1.0
62	2 ± 0.3	11 ± 1.5

Table 3.6. *Half-lives of TGG at measured inactivation temperatures. Assigned uncertainties are calculated from the standard errors of the slope.*

Temperature [°C]	Half lives - first phase [min]	Half lives - second phase [min]
60	32 ± 3.6	42 ± 3.1
62	11 ± 1.9	26 ± 4.2
64	6 ± 1.7	24 ± 1.3
66	3 ± 0.8	23 ± 1.5
68	3 ± 0.7	20 ± 1.6
70	2 ± 0.4	17 ± 1.1
72	1 ± 0.5	15 ± 1.2

The rate constants, whom where previously obtained , where used to produce figures 3.13-3.16.

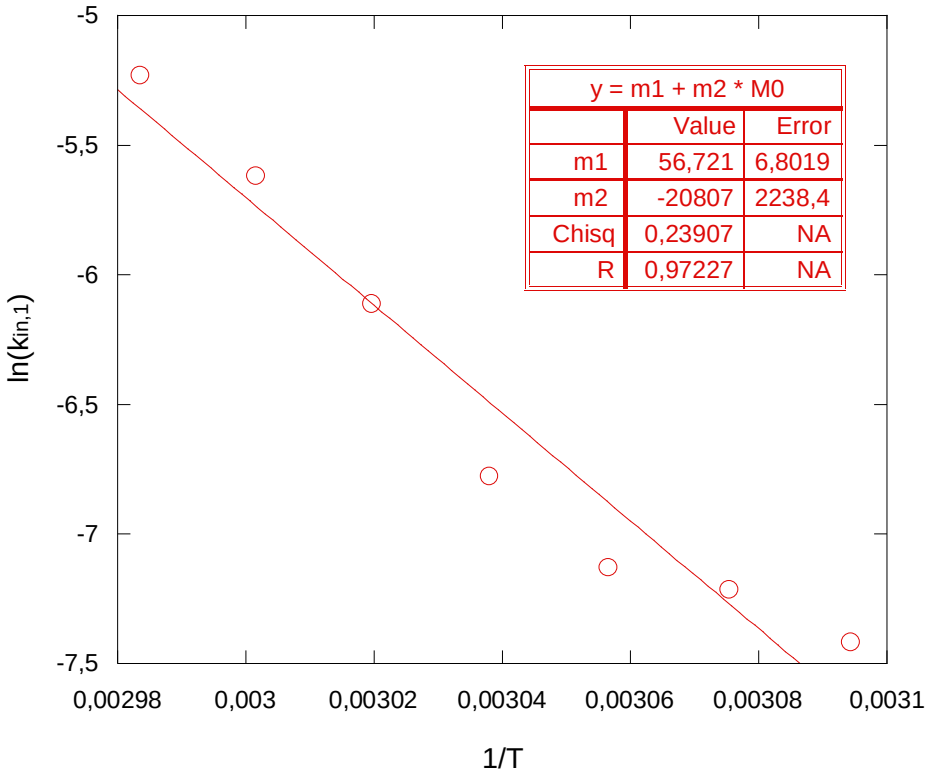

Figure 3.13. *Arrhenius plot of the first phase inactivation of native trypsin. The slope of the fitted line equals* $-E_{in}/R$.

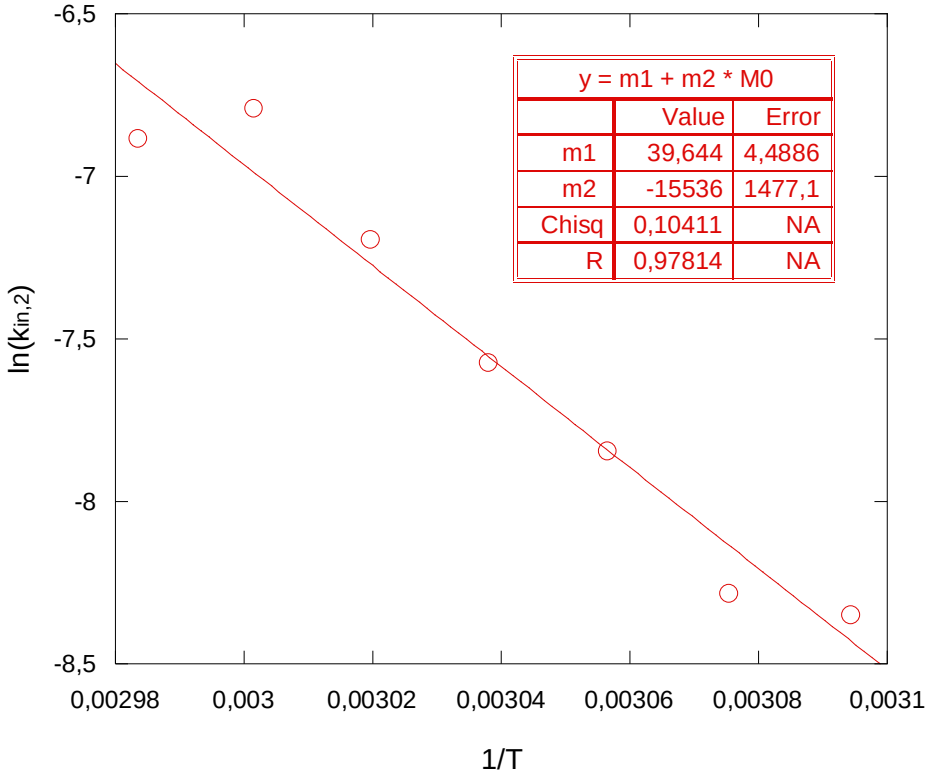

Figure 3.14. *Arrhenius plot of the second phase inactivation of native trypsin. The slope of the fitted line equals* $-E_{in}/R$.

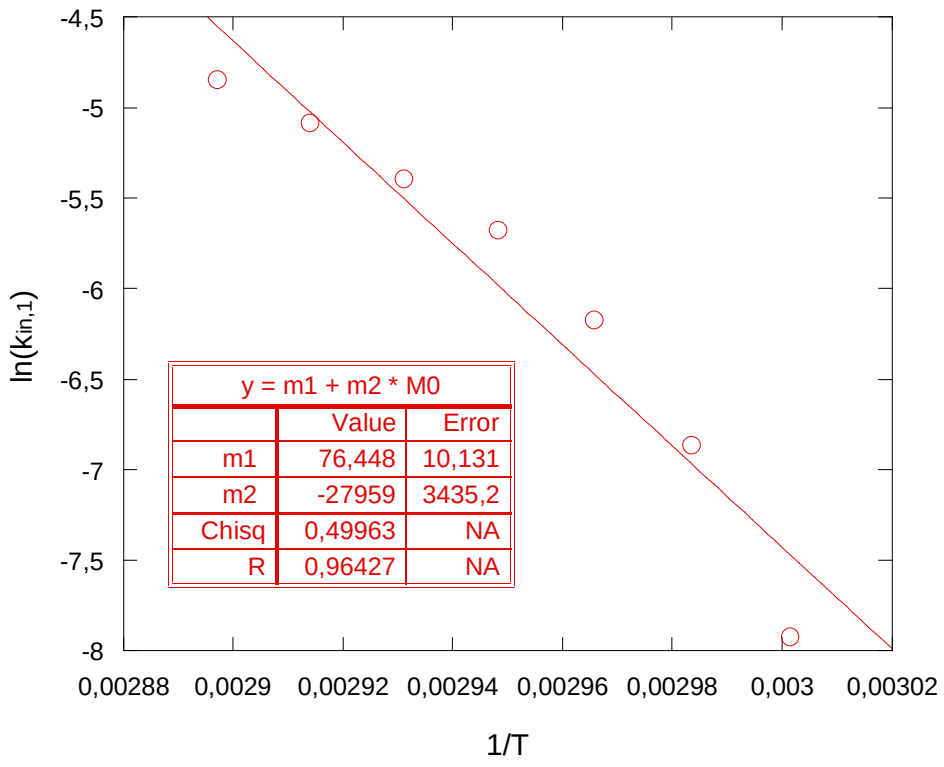

Figure 3.15. *Arrhenius plot of the first phase inactivation of TGG. The slope of the fitted line equals* $-E_{in}/R$.

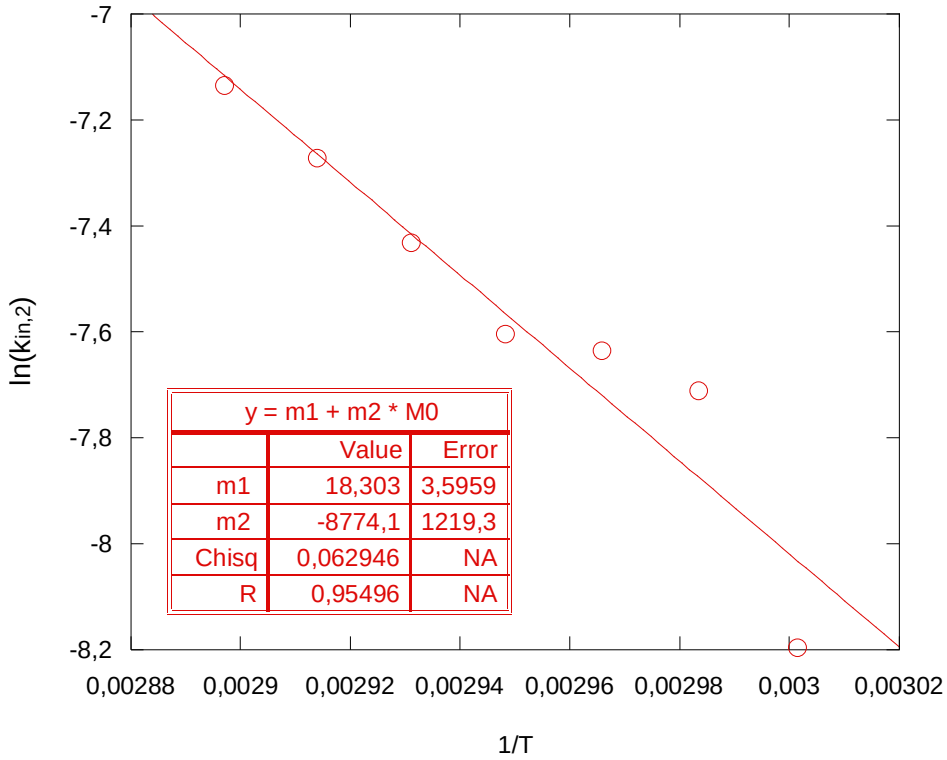

Figure 3.16. *Arrhenius plot of the second phase inactivation of TGG. The slope of the fitted line equals* $-E_{in}/R$.

Inactivation energies, obtained by linear least-square regression of the data of figure 3.13 – 3.16 are given in table 3.7 and 3.8.

Table 3.7. *Inactivation energies of first and second phase of thermal inactivation of native trypsin.*

	Inactivation energy [kJ/mol]	**R^2**
Inactivation of first phase	172.95 ± 18.607	0.945
Inactivation of second phase	129.16 ± 12.280	0.957

Table 3.8. *Inactivation energies of first and second phase of thermal inactivation of TGG, with an increase comparison to native trypsin.*

	Inactivation energy [kJ/mol]	**R^2**	**Increase wrt. native trypsin [%]**
Inactivation of first phase	232.36 ± 28.642	0.929	34,4
Inactivation of second phase	79.922 ± 10.160	0.911	-43,5

3.2.3 Stability against urea of TGG and the TCCs

Figure 3.17, shows the residual activity plot for urea denaturation of the trypsin species. As can be seen from the figure, no significant difference was observed between the species.

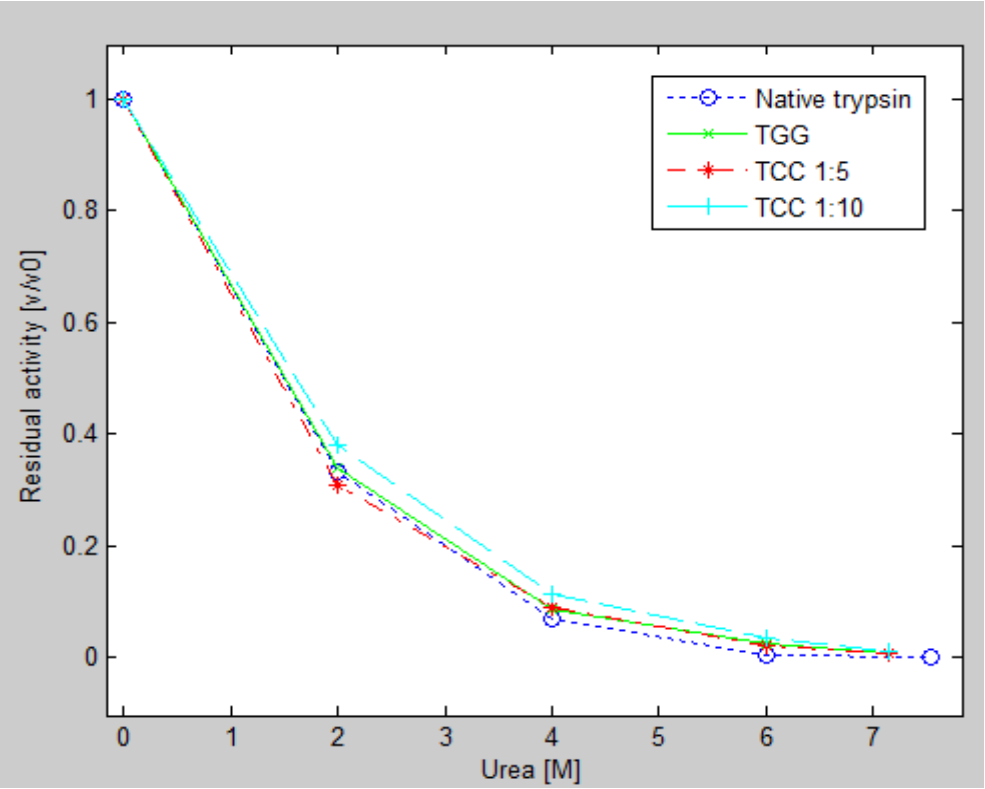

Figure 3.17. *Residual activity of incubated trypsin species as a function of urea concentration.*

3.2.4 Autolysis of TGG and TCCs

Figure 3.18 shows the residual activity plot for autolysis. The incubation buffer did not contain any Ca^{2+} ions since these ions are known to protect trypsin against autolysis. As can be seen from the figure, TGG, TCC 1:5 and TCC 1:10 are dramatically more resistant toward autolysis compared with native trypsin.

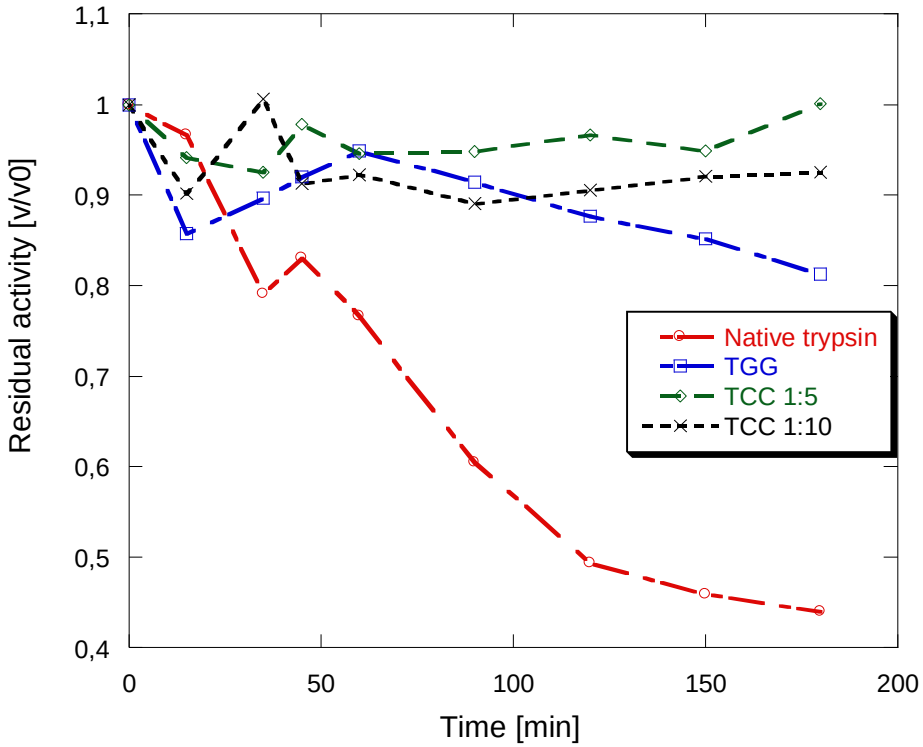

Figure 3.18. *Residual activity of incubated trypsin species as function of time due to autolysis.*

3.2.5 Storage stability of TGG and the TCCs

Storage stability was determined by incubating the trypsin species under different conditions for more than two months. Figures 3.19 – 3.22 represent the results of the storage stability determination.

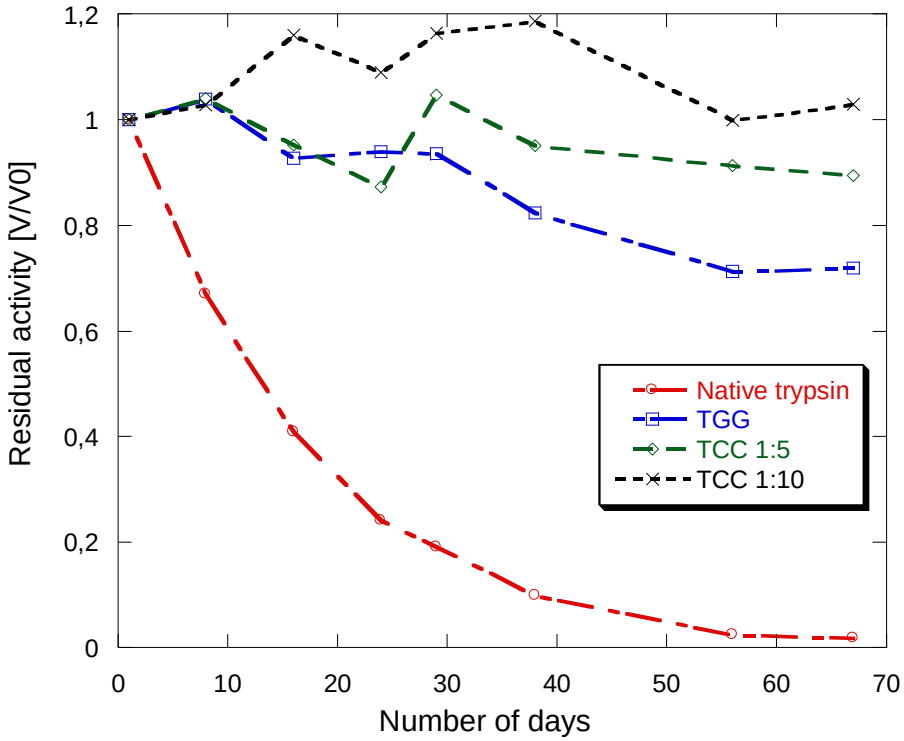

***Figure 3.19**. Residual activity of the trypsin species incubated at 4 °C without Ca^{2+} ions.*

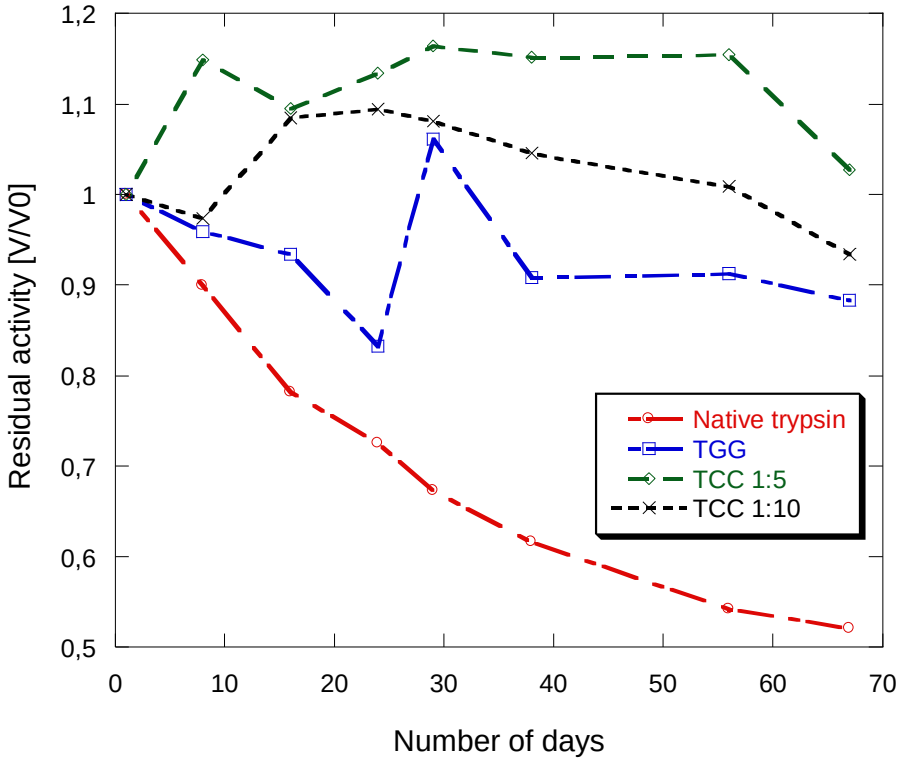

***Figure 3.20.** Residual activity of the trypsin species incubated at 4 °C with Ca^{2+} ions.*

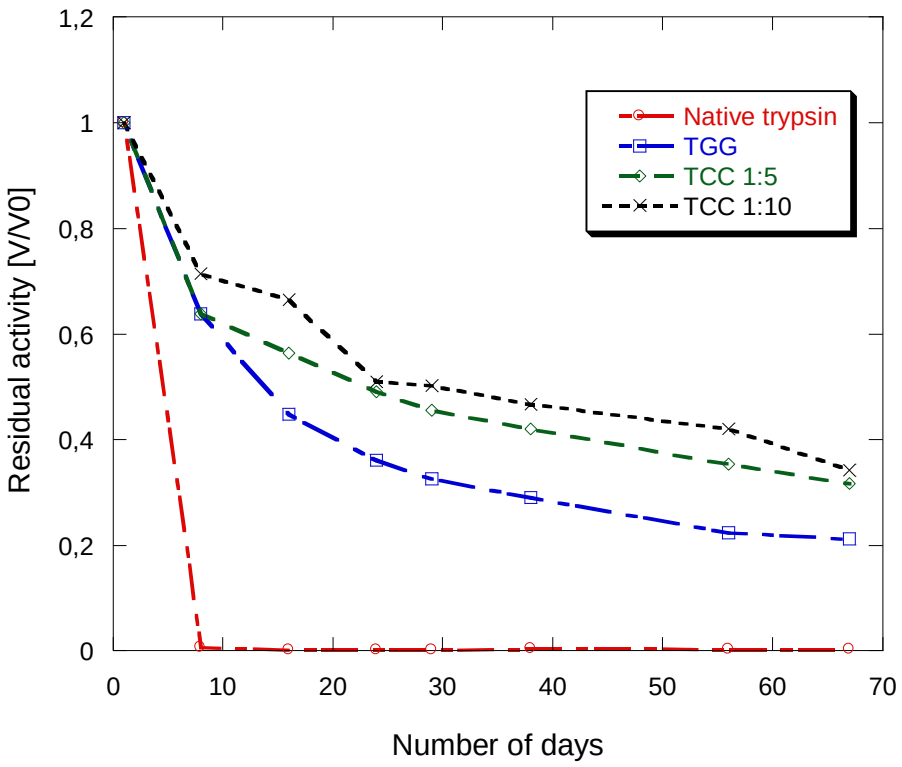

Figure 3.21. *Residual activity of the trypsin species incubated at 25 °C without Ca^{2+} ions.*

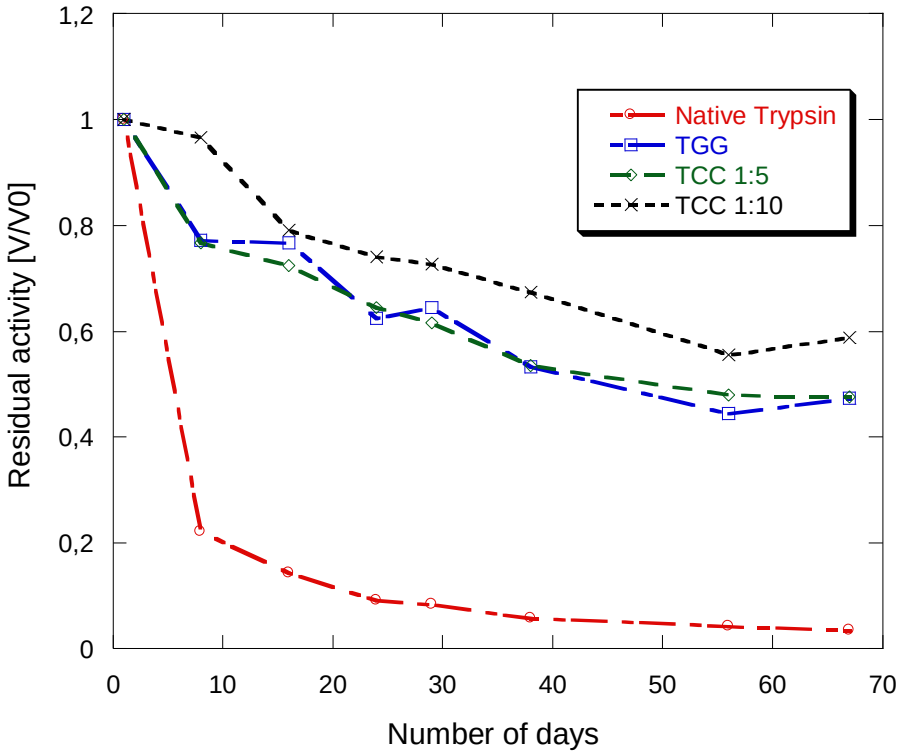

Figure 3.22. *Residual activity of the trypsin species incubated at 25 °C with Ca^{2+} ions.*

Table 3.9 gives the relative stability of the trypsin species with respect to native trypsin.

Table 3.9. *The relative stability of the trypsin species with respect to native trypsin at 4 °C and 25 °C, with and without the presence of Ca^{2+} ions. The values represented is the respective residual activity divided by the residual activity of native trypsin. Each value thus represent how many times the respective species is more stable than native trypsin*

	4 °C		*25 °C*	
	Without Ca^{2+}	**With Ca^{2+}**	**Without Ca^{2+}**	**With Ca^{2+}**
TGG	38	2	70	14
TCC 1:5	47	2	107	14
TCC 1:10	54	2	113	17

3.3 Functional properties of TGG and the TCCs

3.3.1 pH profiles of TGG and the TCCs

Relative activities at different pH can be seen in figure 3.23.

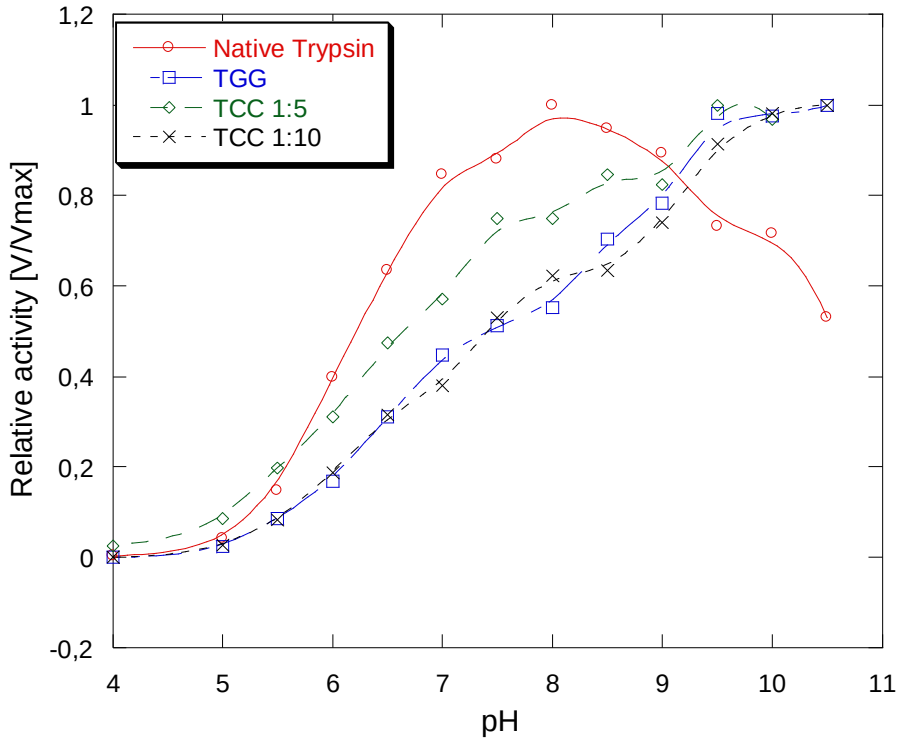

Figure 3.23. *Relative activities of the trypsin species as a function of pH. The scatter points were connected by a smooth curve fit by applying the Stineman function to the data.*

As can be seen from figure 3.23, the TGG, TCC 1:5 and TCC 1:10 species became more basophilic compared with native trypsin.

3.3.2 Proteolytic activities of TGG and the TCCs

The results of proteolysis of the trypsin species on sulfanilamide casein substrate is given in table 3.10.

Table 3.10. *Proteolysis of sulfanilamide casein substrate. Assigned uncertainties are standard deviation of triplicates.*

Trypsin species	Proteolytic rate [U/mg]
Native trypsin	13.6 ± 0.050
TGG	11.6 ± 0.194
TCC 1:5	19.5 ± 0.154
TCC 1:10	16.6 ± 0.042

The proteolytic activity of TCC 1:5 and TCC 1:10 was observed to be slightly higher than for native trypsin and the activity of TGG was observed to be slightly less than for native trypsin.

3.3.3 Michaelis-Menten kinetics of native trypsin and TGG

Non-linear fitting of the data to the Brigg-Haldane modified Michaelis-Menten equation are given in figure 3.24 and 3.25.

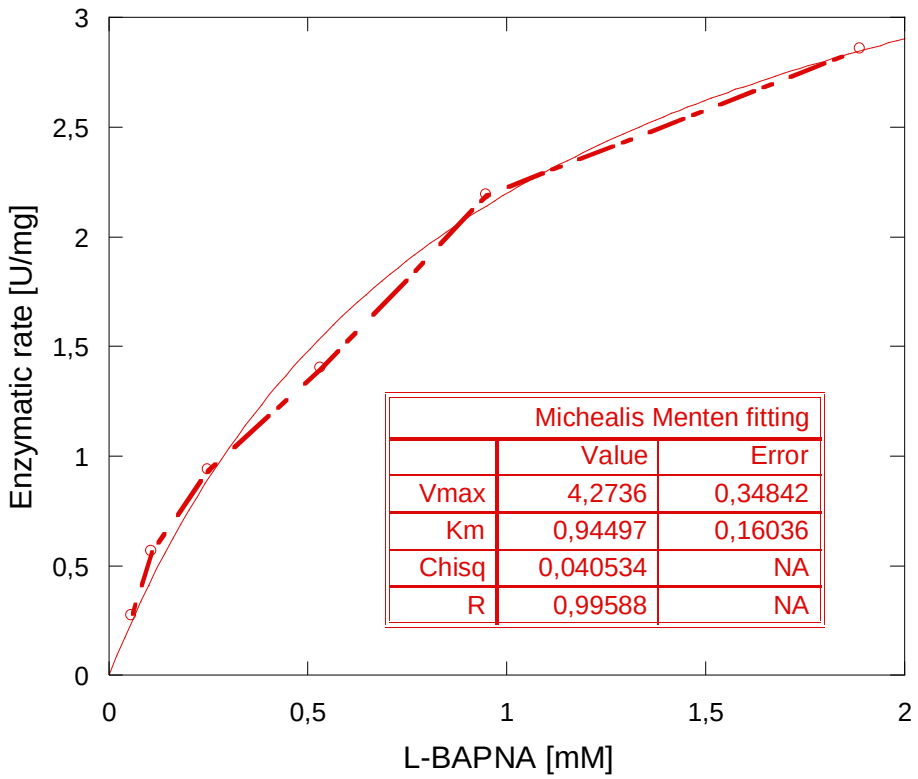

Figure 3.24. *Non-linear fitting of native trypsin data to the Michaelis-Menten model.*

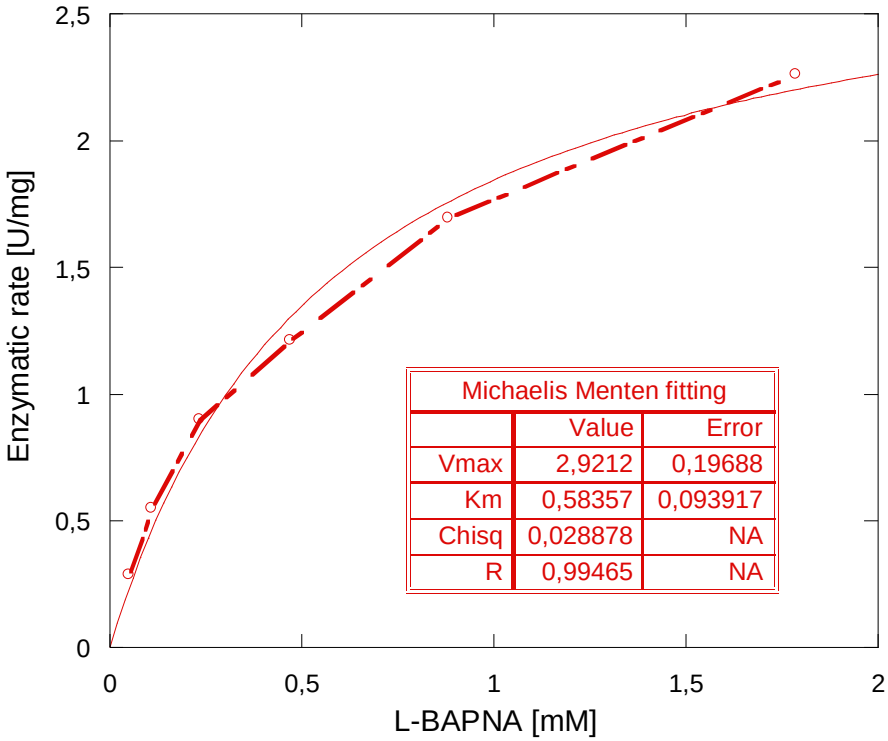

Figure 3.25. *Non-linear fitting of TGG data to the Michaelis-Menten model*

The kinetical parameters obtained from figure 3.24 and 3.25 are given in table 3.11.

Table 3.11. *Kinetical parameters obtained from non-linear fitting of the data to Michaelis-Menten equation. Assigned uncertainties are calculated from the standard errors of the slope.*

	k_{cat} [s^{-1}]	K_m [mM]	k_{cat}/K_m [$mM^{-1}s^{-1}$]
Native trypsin	1.661 ± 0.135	0.945 ± 0.160	1.758 ± 0.309
TGG	1.236 ± 0.083	0.583 ± 0.093	2.120 ± 0.120

It can be seen from the data, given in table 3.11, that the catalytic efficiency constant (k_{cat}/K_m) is increased for TGG compared with native enzyme.

3.3.4 Structural comparsion of native trypsin and TGG

CD spectra of native trypsin and TGG is given by figure 3.26.

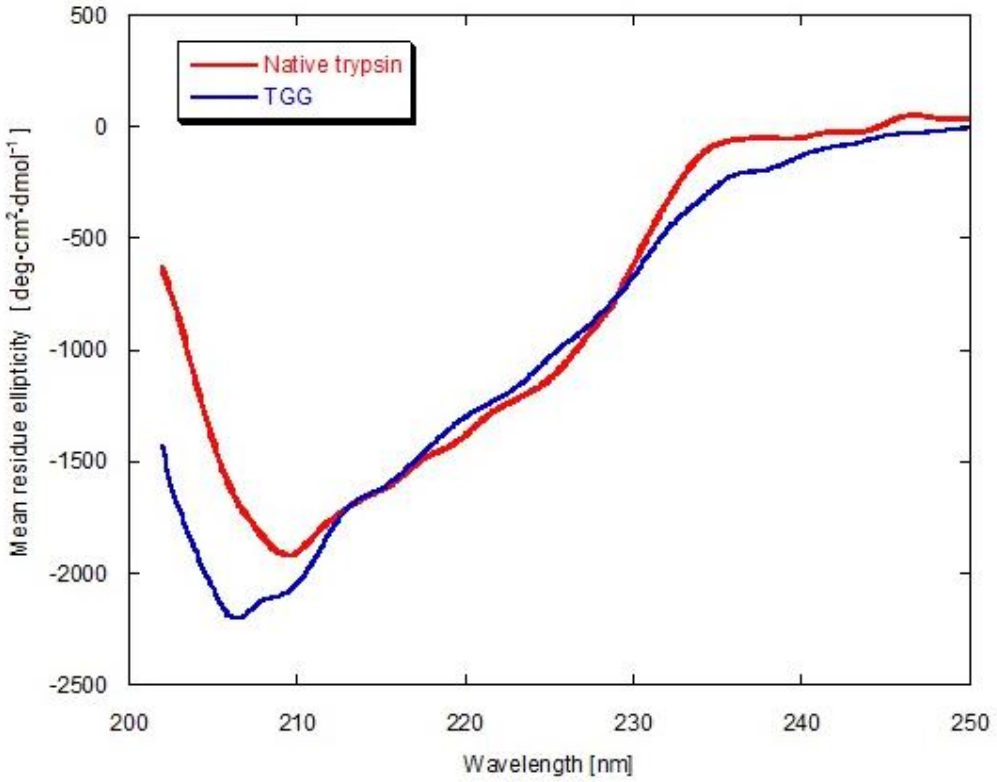

Figure 3.26. *CD spectra of PMSF-inhibited native trypsin and TGG.*
The spectra was collected from 250-202 nm.

As can be seen from figure 3.26. the microenvironment of the secondary structure of TGG has slightly changed compared with native trypsin.

4 Discussion

4.1 Mass and size determination of the trypsin species

The MALDI-TOF mass spectrometrical results of TGG indicate that the EDAC/NHSS conjugation reaction is highly effective in conjugating the D-glucosamine moieties to the trypsin. Conjugation with D-glucosamine (a.k.a. glycosylation) by using solely EDAC has been reported previously [48][67][99]. The degree of glycosylation (i.e. number of mol sugar/protein grafted onto) by only using EDAC has resulted in low and sometimes extremely low degree of glycosylation. This poor glycosylation might be attributed to the fact that the active ester formed by solely carbodiimide hydrolyses quickly [68]. However, the mass spectra shows that by including NHSS along with the carbodiimide, glycosylation yields are very good with respect to the degree of conjugation of the D-glucosamine to the trypsin molecules.

By assuming that the highest peak of the mass spectra represented the average molar weight of the TGG, it was found out that on average 12 D-glucosamine moieties are reacted to each trypsin molecule. The EDAC/NHSS conjugation is primarily directed toward exposed carboxyl groups on the surface of proteins. However, EDAC is known to be reactive toward tyrosyl (and other) residues. On the basis of molecular visualization in Pymol and utilizing the surface-accessible feature of that program it was suggested that 8 carboxyl residues and 4 tyrosyl residues are reacted to D-glucosamine. Furthermore, the mass spectra indicate that the TGG preparation contained several glycoforms. However, it is likely that these glycoforms are rather few since otherwise they could not be resolved from the from the noise.

The cross-linked enzymes (TCC 1:5 and TCC 1:10) formed highly heterogenous products since the chitooligosaccharides are multifunctional oligopolymers, with different extent of free amino groups from one oligomer to the next. Thus, the enzyme conjugation site reacted to each amino group of chitooliogosaccharide will result in many and different combinations of cross-linked enzyme, yielding highly heterogenous cross-linked enzymes with a variety of sizes and molecular mass.

Discontinous electrophoresis was conducted in order to get a visual sight of the extension of the modification procedure. The resulting gels displays (fig 3.5A) a range of different mass distribution (or populations) of the TCCs as well as significant proportion of unreacted trypsin. The size of the cross-linked trypsin are at least 160 kDa, judged from the location of the protein ladder of the gel in figure 3.5A.

These different populations where then resolved by NTA. TCC 1:5 are typical polydisperse samples with ranges of hydrodynamical radii, but TCC:10 are polydisperse to a lesser extent. To our surprise, TCC 1:5 formed bigger complexes than TCC 1:10, with two major and one minor population distributions (figure 3.6A&B). The molecular mass of the TCC 1:5 and TCC 1:10 complexes could not be precisely determined due to heterogeneity, however, the NTA measurements gave a good indication of their enormous size. Their hydrodynamical radii are given in table 3.1. Compared with native trypsinogen, TCC 1:5 and TCC 1:10 have on average 168 times and 111 times greater hydrodynamical radii, respectively. It should be mentioned that the TCCs complexes were always observed to be water-soluble, and there was never any indication of precipitation or presence of gelatinous-forming material, as often are observed for intermolecularly cross-linked proteins [50].

4.2 Stability of the trypsin species

Both TCCs species after 30 minute incubation at 60 °C turned out to be almost 16 times more stable than native trypsin and TGG under same conditions was more than 11 times more stable than native trypsin (fig 3.7). $T_{50\%}$ values given in table 3.2 of trypsin species showed that TCC 1:10 was the most stable species, more than 2 °C and 10 °C higher than TCC 1:5 and native trypsin, respectively.This indicates that size in terms of hydrodynamical radii is not a determining factor for enhanced thermostability of the TCCs. TGG had similar $T_{50\%}$ as TCC 1:5, 7 and 8 °C higher than for native trypsin, respectively.

Stefán Bragi Gunnarsson determined the melting temperature (T_m) of trypsin and intermolecularly cross-linked trypsin with the same chitooligosaccharides as used in this current study. Differential scanning calorimetry of TLCK inhibited native trypsin and intermolecularly cross-linked trypsin showed that T_m had increased 74.1 °C for native trypsin to 78.9 °C for intermolecularly cross-linked trypsin in a 0.2 M sodium acetate buffer, pH 5.0, which is an increase of 4.8 °C [26]. However, the ratio of chitooligiosaccharide to trypsin was much higher in his synthesis, and this value is likely to be different from one batch to another.

The thermal inactivation of native trypsin and TGG displayed typical biphasic inactivation, as expected [34]. The biphasic nature of trypsin inactivation suggests formation of a stable intermediate during inactivation, which gives rise to two different inactivation rates [34]. Thus, during the inactivation process there might be a buildup of stable intermediates which are identical and possess the same catalytical activity as their native trypsin counterpart, differing only in inactivation rate constant.

$$N \overset{k_1}{\Rightarrow} Int \overset{k_2}{\Rightarrow} I$$ **Equation 4.1.**

where N is the native conformation of trypsin/TGG, Int is the possible intermediate and I is the inactive trypsin/TGG. The rate constants of inactivation, k_1 and k_2, refer to the first and second phase, respectively (Tables 3.3. and 3.4.).

The inactivation plots of native trypsin and TGG displayed a similar biphasic behavior in contrast to the more complex inactivation of TCC 1:5 and TCC 1:10 (data not showned).

That fact underlines, again, that TGG is most likely constituted by a relatively few glycoforms of narrow mass range.

Half-lives of inactivation for the both phases of native trypsin and TGG (Tables 3.5. and 3.6.) can be compared at 60 and 62 °C. The half-lives of TGG are more than 10 times and more than 4 times longer, for the first and second phase at 60 °C compared with native trypsin, respectively. At 62 °C the half lives of TGG are more than 5 times and more than 2 times longer, for the first and second phase compared with native trypsin, respectively.

The inactivation energies of the first phase ($E_{in,1}$) for native trypsin and TGG are 173 $^{kJ}/_{mole}$ and 232 $^{kJ}/_{mole}$, and the inactivation energies of the second phase ($E_{in,2}$) for native and TGG are 129 $^{kJ}/_{mole}$ and 80 $^{kJ}/_{mole}$, respectively. Venkatesh and Sundaram measured the inactivation energy of native trypsin for the first phase to be 173 $^{kJ}/_{mole}$ and second phase to be 146 $^{kJ}/_{mole}$ [34], which is similar to the values obtained here.
According to our data, TGG is 34 % more stable toward thermal inactivation than native trypsin. However, the intermediates of native trypsin (second phase) seem to be more 43 % more stable than the intermediates of TGG. Thus, the D-glucosamine moities confer a stabilizing effect to the native conformation of the enzyme, but confer a destabilizing effect to the intermediate form of trypsin, somehow driving the enzyme faster toward inactivation.

Urea inactivation was conducted to see if the trypsin species were protected from its denaturing effects. Urea solutions were freshly prepared since they were kept at alkaline pH (degradation of urea into cyanate is accelerated at alkaline pH, this degradation is a well-known problem since cyanate is known to react to and thus alter certain amino acids [40]). Urea is a polar organic molecule and molecular dynamics simulation has revealed that urea selectively binds to peptide groups of the protein backbone and shifting the equilibrium towards the unfolded state. The denaturing force of urea is exerted primarily on the peptide bond of the protein backbone via hydrogen bonds [100][101], thus if the protein backbone is well shielded from the external solvent due to bulky side chains introduced, e.g. polymers covering the surface, one could deduce that denaturation of the protein is delayed and thus hindered, resulting in little loss of activity over time. However, this is not the case for the trypsin species assayed. The trypsin species all lost their activity fast with increasing urea concentration, and there was no increased stability against the denaturant of the TGG and the TCCs compared with native trypsin (fig 3.17). Our findings are not consistent with the results of Marshall and Rabinowitz [52]. Their obtained data shows that native trypsin had still 78 % activity after identical incubation time at 37 °C. Our buffer condition was similar (i.e. same pH and same Ca^{2+} concentration) to those of Marshall and Rabinowitz, however instead of using borate buffer as Marshall and Rabionwitz did, we used triethanolamine (TEA) and their actvity assay of was carried out using the substrate TAME (tosyl-L-arginine-methylester), but we used L-BAPNA. Furthermore, we included the same urea concentration in the substrate solutions as in the incubation buffer, in order to block any possible refolding of the enzyme, but Marshall and Rabinowitz did not. It was thus concluded, that the covalent conjugation of D-glucosamine and cross-linking with the chitooligosaccharide had no protecting effect on the urea inactivation of trypsin. The main reason why trypsin and other proteases are inactivated at certain denaturant concentration is due to hydrolysis on the behalf of the still-active undenatured proteases on those proteases that have lost their tertiary and secondary structure [34]. It should be noted that Ca^{2+} ions

do not confer any anti-autolytic properties to unfolded trypsin
Autolysis for the trypsin species can be seen in figure 3.18. As can be seen from the that figure, TGG and the TCCs confer dramatical stabilization towards autolysis. TCC 1:10, TCC 1:5, and TGG are all little less or little more than two times more stable against autolysis than native trypsin after three hour incubation at 30 °C. TCC 1:5 had not lost any activity after 3 hour incubation. Thus, TGG and the TCCs are dramatically stabilized against autolysis. It is well-known that carbohydrates attached to proteins confer anti-proteolytic effects. It might be due to steric shielding of the bulky carbohydrates of otherwise optimal residues for proteolysis.

Table 3.9 gives the relative stability at all different storage conditions. The highest storage stability gain is achieved for the TGG and TCCs at 25 °C without the presence of Ca^{2+} ions compared with native trypsin, and the lowest stability gain is achieved for TGG and TCCs at 4 °C with the presence of Ca^{2+} compared with native trypsin. Ca^{2+} ions are known to confer stability on trypsin against autolysis. Therefore, since autolysis is hindered it does not matter if Ca^{2+} is present *in vitro*, and as a consequence, the TGG and TCCs show drastical long-term stability improvements. Activity of the trypsin species is largely retained at 4 °C in the presence of Ca^{2+} after two months compared with native trypsin, with the residual activity of TGG being 72 %, TCC 1:5 89 % and with no loss of residual activity of TCC 1:10. The TCCs display greater stability improvements than TGG after two months incubation, probably due to the fact that TGG is more prone to autolysis than the TCCs. Activtity loss of TGG and TCCs still happens at 25 °C even in the presence of Ca^{2+}, with the residual activity of TGG being 47 %, TCC 1:5 48 % and TCC 1:10 59 % which indicates, at that temperature, they are directed into another degradative pathway than autolysis. Presence of e.g. oxygen in the sample at 25 °C might have had detrimental effects on the trypsin species, since it is known to react with aromatic residues. Including an antioxidant such as ascorbic acid into the buffer formulation could have been practical.

TGG and the TCCs displayed higher stability in all assays conducted, except in urea inactivation. TGG might be stabilized by forming favorable hydrogen bonds between the the D-glucosamine units and hydrophilic residues on the surface of trypsin, and D-glucosamine migth also impose rigidity on the enzyme structure. The TCCs are probably stabilized by reduced, destabilizing, conformational entropy, making the cross-linked trypsins more stable in their native conformation. Figure 4.1 gives a schematic representation of how the cross-linked enzyme might be stabilized by reduced conformational entropy (or minimizing unfolded state which the native conformation could unfold into).

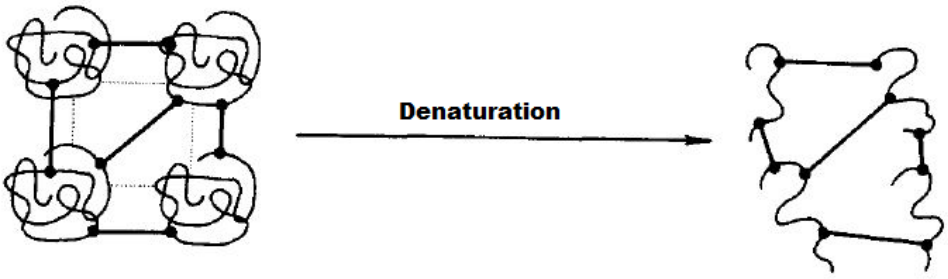

Figure 4.1. *Represents the rigidity imposed to intermolecularly cross-linked protein and thereby reducing the conformational entropy. Adapted from ref. [57].*

4.3 Altered functional properties of the trypsin species

The pH profile of figure 3.23, shows that the TGG and TCCs became increasingly basophilic compared with native trypsin. This is due to higher positive charge, with the consequence being an increase in pI value [99], due to blocking the carboxyl groups via conjugation and cross-linking. The pH profile of an enzyme at particular pH is controlled by ionizable groups present in the active site. Blocking charged residues near active sites, alter the pH profile of an enzyme by changing the pK_a values of the catalytic residues, with the effect decreasing with distance [102]. Hence, the the pK_a value of Asp89 of the active site might be changed in the TGG and in the TCCs, resulting in the aforementioned basophilic behavior.

The proteolytic activity of the trypsin species against azocasein was done in order to assay their activity towards a macromolecular substrate. The activities are given in table 3.10. TCC 1:5 had 43 % and TCC 1:10 had 22 % higher proteolytic activities than native trypsin. TGG had 15 % lesser activity than native trypsin. Since the TCC 1:5 and TCC 1:10 form huge complexes one would think that their catalytic activity would be sterically restricted, however that does not appear to be the case. This enhanced activity phenomena has also been observed for CLEAs compared with their free native enzyme counterpart [50]. It should noted however, that the tryptic concentration of TCCs is both of those trypsin bound in the cross-linked TCC complexes and the unreacted trypsin found in these batches, but this does not explain the increase in higher activity toward azocasein.

Kinetic parameters obtained for native trypsin and TGG, from the non-linear fitting of the data to the Michaelis-Menten equation, are given in table 3.11. Assuming that the enzyme follow Michaelis-Menten kinetics, the turnover number of TGG (k_{cat}) decreases compared with native trypsin by 25 %, resulting in lower turnover of reactant (L-BAPNA) into its products. However, the Michaelis constant (K_m) is decreased by 38 % compared with native trypsin, indicating increasing affinity for the substrate of TGG. This highly reduced Michaelis constant of TGG results in 1.2 times higher catalytic efficiency (k_{cat}/K_m) compared with native trypsin. Michaelis constant, for an enzyme, is usually a fixed value for a given substrate. Erlanger et al., the developers of synthetic substrate L-BAPNA, measured the K_m of L-BAPNA using bovine trypsin to be 0.939 mM incubated in 50 mM

Tris, 20 mM $CaCl_2$ buffer, pH 8.15 at 15 °C. K_m values were obtained using the Lineweaver-Burk transformation of the Michaelis-Menten equation [83]. Simpson and Haard measured the K_m of L-BAPNA using bovine trypsin to be 1.02 mM, incubated in 50 mM Tris, 20 mM $CaCl_2$ buffer, pH 8.2 at 25 °C. K_m values were obtained using non-linear fitting of the Michaelis-Menten equation [103]. TGG, as a D-glucosamine grafted trypsin, can also be considered as a glycated trypsin with several glycoforms. The glycation of the bovine trypsin seems to confer some structural changes that increases the enzyme's affinity for L-BAPNA.
Kato et al. glycated trypsin by dissolving bovine trypsin and glucose in the 1:0.5 w/w proportion, respectively. They subsequently lyophilized the the glucose-trypsin solution and incubated the lyophilized glucose-trypsin powder at 50 °C with 65 % relative humidity for various periods (0-8 days) for glycation via various Maillard reaction to the lysine residues. The batch reacted for 4 days turned out to be the best. Analysis of free amino groups showed that 40% of free amino groups, thus 60 % of lysine residue had been conjugated to glucose. Further analysis was conducted which showed that of those 60 % conjugated lysine groups, 30 % had been converted to fructolysine, 15% were on Schiff base form and 15-20 % had been changed to some Amadori rearrangement products. The glycated trypsin showed altered kinetic parameters. They measured the k_{cat} and K_m of of L-BAPNA using native bovine trypsin to be 0.728 s^{-1} and 0.932 mM, respectively incubated in a Tris (concentration of Tris not specified), 50 mM $CaCl_2$ buffer, pH 8.0. However the they measured the k_{cat} and K_m to be 0.694 s^{-1} and 0.428 mM, respectively, of the glycated trypsin under same conditions. This yielded a 1.7 times higher k_{cat}/K_m value for glycated trypsin versus native trypsin [61]. These findings along with ours suggest that glycation confers some altered spatial conformation arrangement of the secondary structure that yields higher affinity for L-BAPNA.

Since TGG was found to deviate significantly from the kinetical parameters obtained for native trypsin, CD spectropolarimetry was conducted in order to assess the difference in the spatial configuration of the secondary structure of the native trypsin and TGG. As seen from figure 3.26, the CD profiles differentiate significantly at around 208 nm, but negative signals around that wavelenght are attributed to configurations of α helices. Thus, it is likely that spatial configuration of an α helix or helices are changed, in such a way that results in higher affinity of TGG to L-BAPNA compared with native trypsin, resulting in increased overall catalytic efficiency (k_{cat}/K_m).

4.4 Chosen practical aspects of this study – possible applications

In this chapter, chosen example from the study will be discussed with regards to possible application of the binary EDAC/NHSS conjugation method, utilization of glycated (D-glucosamine conjugated) as well as the chitooligosaccharide cross-linked trypsin prepared in this study and the possibility of using the same conjugation procedure to confer stability to other relevant enzymes.

Chemical glycation studies of trypsin (and other enzymes and proteins) has been carried out by few researchers, reporting favorable results [61][62, and references therein]. The focus has been on the use of *in vacuo* glycation. As earlier demonstrated, glycation with

binary mixture of EDAC/NHSS conjugants of D-glucosamine to trypsin was highly efficient. This conjugation procedure could be used to try to conjugate other amino containing sugar to trypsin or other relevant enzymes. Amino sugars that would be interesting to explore include neuraminic acid, daunosamine, D-fructosamine etc.

Conjugation of amino groups of D-glucosamine to carboxyl groups of proteins by solely using EDAC has proven to give poor yields of conjugation [48][67][99].
Ramezani et al. conjugated glucosamine to lysozyme and casein using EDAC. On average two moieties of D-glucosamine were conjugated to each of casein molecule and only 0.11 moieties of D-glucosamine were found to conjugate to each lysozyme molecule, underlining the fact that EDAC is not a very efficient conjugant on it own. Although the degree of conjugation was small, solubility (pH 3 and 6 at 25, 45 and 60 °C), emulsifying activity, foaming capacity and heat stability were all significantly improved upon conjugation for both casein and lysozyme. Furthermore, specific activity of conjugated lysozyme was only marginally reduced [48]. By using the binary mixture of EDAC and NHSS this could yield higher degree of conjugation, thus increasing aforementioned properties even more. Thus, the high degree of D-glucosamine conjugation by using both EDAC and NHSS could be benefical to future research in food science.

D-glucosamine grafted trypsin (TGG) has altered kinetical properties compared with native trypsin against L-BAPNA. Possible altered spatial configuration of α-helix/helices makes TGG to become saturated at much lower concentration of L-BAPNA. Further research on this effect might help to shed light on the effects of glycation on enzymes.

As previously shown in this study, thermal stability improved for the TGG and the TCCs, compared with native trypsin. Furthermore, autolysis was retarded in the case of TGG and totally hindered for the TCCs after 180 minutes incubation without the presence of the stabilizing Ca^{2+} ions. Specific proteolytic activity was sligthly reduced for the TGG but increased for the TCCs compared with native trypsin. This could be of a practical importance since trypsin is the most widely used protease for preparing proteins for mass spectrometrical peptide fingerprints. One of the problems encountered in this preparation is that native protein analytes are not readily digested by the proteolytic enzyme, so they must be denatured to achieve efficient digestion, which obviously denatures the protease as well. Another problem encountered is that trypsin autolysis generates autolytic peptides that complicates the analytical procedures by giving undesirable background[62]. The TGG or the TCCs might prove to be useful for producing peptide digests, since autolysis is not as severe as for native trypsin. Also, the digest solution could be incubated at a higher temperature (instead of 20-40 °C commonly used to digest proteins for mass fingerprint analysis), to speed up the digestion, since the TGG and the TCCs possess an increased thermostability compared with native trypsin. Moreover, since the TCCs have higher specific proteolytic activity than native trypsin, the addition of a denaturant may be unnecessary.

We were unable to find examples of soluble polysaccharide intermolecularly cross-linked trypsin (or on other enzymes) in the literature. In this field the focus has been mainly on intramolecular cross-linking rather than intermolecular cross-linking, which has given mixed results [104].
However, the method of cross-linked enzymes (CLEs) is probably is the most closely

related to our approach. In that approach the cross-linking agent is also the cross-linker, but in our approach the cross-linking agent was the conjugants (EDAC and NHSS) and the cross-linker was the chitooligosaccharides, so our could be considered as a special case of CLEs. Formation of CLEs is one of the first enzyme stabilization procedure introduced. Traditionally, this method has been carried out by adding glutardialehyde into a solution with dissolved enzyme causing cross-links to form between two amino groups on two and more enzyme molecules.
Cao et al. dealt with this topic in a review article published in 2003 [105]. Therein, they stated:

„Enhanced thermostability could be obtained by the cross-linking of dissolved enzyme, but usually required a delicate balance between several factors, such as the amount of cross-linker, temperature, pH and ionic strength. Moreover, intermolecular cross-linking of these highly solvated enzyme molecules often had several drawbacks, such as lower activity retention (usually below 50% of the native activity), poor reproducibility and low mechanical stability. Difficulties were also encountered in handling of the gelatinous CLE and in controlling the geometric parameters of randomly cross-linked enzymes".

They also stated:

„Consequently, in the late 1960's research emphasis switched to carrier-bound enzymes, when a wide range of carriers were specifically developed for enzyme immobilisation and several reactions for binding enzymes to carriers were established".

Low reproducability is a fact of the TCCs synthesized in our lab. However, the trend of increased thermal stability, hindered autolysis, improved storage stability and the shift of the pH optimum to increased alkaline conditions might be useful for industrial application. No gelatinous-like formation was observed and the TCCs were always observed to be dissolved, so the limitation of CLEs does not include the TCCs. The increased thermostability upon cross-linking with chitooligosaccharides has also been demonstrated for horseradish peroxidase [26]. It is thus likely that similar stabilizing effects could be confered to industrially valuble enzymes by using the stabilization techniques presented in this thesis.
The use of mobilized (free) enzymes that have been stabilized in industry is well established. Mobilized enzymes can be used in industrial reactor such as in continuous stirred tank reactors (CSTR) combined with an ultra filtration unit (CSTR/UF). CSTR/UF allows continuous processing with mobilized enzymes. In combined CSTR/UF the enzyme-catalyzed product (as well as unreacted substrate if present) and the enzyme solution is passed through an ultra filtration unit, which is permeable to product/substrate but impermeable to the enzyme. Thus, the enzyme is continously removed and recycled back into the reactor [106]. Stabilizing industrially valuble enzymes by conjugation with D-glucosamine or by cross-linking with chitooligosaccharides for the utilization in mobilized-compatible reactor systems is worth further research.

It is well known that glucosamine/chitosan are natural non-toxic substances and it is likely that they lack antigenicity. Thus conjugation of these substances on therapeutic proteins might give favourable results. In this study we have showned that EDAC/NHSS binary conjugant mixture is highly efficient in accomplishing this.

5 Conclusions

In summary, the overall findings of this study are twofold:

1. EDAC/NHSS conjugation of D-glucosamine and cross-linking chitooligosaccharides to/with, respectively, was successful. The binary conjugant mixture of EDAC/NHSS proved to be a good method to achieve the conjugation and the crosslinking. The cross-linked enzyme, TCC, were shown to form very heterogenous and polydisperse complexes, and the D-glucosamine grafted enzyme, TGG, was showned to form several glycoforms of a narrow range, with an average of 12 D-glucosamine moieties reacting to each trypsin molecule. The higher ratio, of preparation of chitooligosaccharide cross-linked with trypsin, TCC 1:10, seemed not form bigger complexes than TCC 1:5. On the contrary, the lower ratio, TCC 1:5, of preparation of chitooligosaccharide cross-linked with trypsin formed bigger complexes than TCC 1:10.

2. Stability and functional properties of these trypsin species (i.e. TGG and the TCCs) were increased and altered, respectively, compared with native trypsin. Thermal stability improved, stability towards thermal inactivation (in case of TGG) increased, autolysis was retarded, storage stability improved, pH profile shifted toward more alkaline conditions, proteolytic activity improved (in case of the TCCs) and catalytic efficiency (k_{cat}/K_m) improved (in case of the TGG). However, no stabilizing effect against urea was observed for either TGG and the TCCs. Furthermore, since catalytic efficiency was increased upon D-glucosamine conjugation, scanning for alteration in the microenvironment of TGG was conducted, which showed a slight alteration. This slight but significant alteration of the spatial configuration, probably of a α helix/helices, seems to increase the affinity of the glycated trypsin for the syntethic substrate L-BAPNA.

References

[1] Zhang, Z., He, Z., and Guan, G. (1999). *Thermal stability and thermodynamic analysis of native and methoxypolyethylene glycol modified trypsin.* Biotechnol. Tech. **13**: 781-786.

[2] García, A., Hernández, K., Chico, B., García, D., Villalonga, M.L., and Villalonga, R. (2009). *Preparation of thermostable trypsin-polysaccharide neoglycoenzymes through Ugi multicomponent reaction*. J. Mol. Catal. B-Enzym. **59**: 126-130.

[3] Ó'Fagáin, C. (2003). *Enzyme stabilization – recent experimental progress.* Enzyme. Microb. Tech. **33**: 137-149.

[4] Wong, Y.H., and Tayyab, S. (2012). *Protein stabilizing potential of simulated honey sugar cocktail under various denaturation conditions.* Process Biochem. **47**: 1933-1943.

[5] Davis, B.G., and Díaz-Rodríguez, A. (2011). *Chemical modification in the creation of novel biocatalysts.* Curr. Opin. Chem. Biol. **15**: 211-219.

[6] Freeman, A. (1984). *Understanding enzyme stabilization*. Trends. Biotechnol **2**: 147-148

[7] Iyer, P.V., and Ananthanarayan, L. (2008). *Enzyme stability and stabilization – aqueous and non-aqueous environment*. Process. Biochem. **43**: 1019-1032.

[8] Szilágyi, A., Kardos, J., Osváth, S., Barna, L. and Závodszky, P.(2007). *Protein folding*. In A. Lajtha (Ed.), Handbook of neurochemistry and molecular Neurobiology. Neural protein metabolism and function (Chapter 10). New York: Springer Science.

[9] Marshall, J.J. (1978). *Manipulation of the properties of enzymes by covalent attachment of carbohydrate.* Trends. Biochem. Sci. **3**: 79-83.

[10] Schmid, R. (1979). Stabilized soluble enzymes. *Adv. Biochem. Eng.* **12**: 41-118.

[11] P00760 (TRY1_BOVIN) Reviewed, UniProtKB/Swiss-Prot (2013). Retrieved 21st of December 2013 from *http://www.uniprot.org/uniprot/P00760*.

[12] Walsh, K. A. (1970). *Trypsinogens and trypsins of various species*. Methods Enzymol. **19**: 41-63.

[13] Apweiler R., Bairoch A., and Wu C.H. (2004). *Protein sequence databases.* Curr. Opin. Chem. Biol. **8**:76-80.

[14] Protparam Tool - Swiss Institute of Bioinformatics (2013). Retrieved (and calculated) 21st of December 2013 *from http://web.expasy.org/protparam/* using the bovine β-trypsin Uniprot sequence of ref. [11].

[15] Rawlings, N.D., Barrett, A.J. and Bateman, A. (2012). *MEROPS: the database of proteolytic enzymes, their substrates and inhibitors*. Nucleic Acids Res. **40**: 343-350.

[16] MEROPS-Summary for family S1. (2013) Retrieved 21st of December 2013 from: *http://merops.sanger.ac.uk/cgi-bin/famsum?family=S1*.

[17] Merkel, J.R. and Sipos, T. (1970). *An effect of calcium ions on the activity, heat stability and structure of trypsin*. Biochemistry **9**: 2766-2775.

[18] Abita, J. P., Delaage, M., Lazdunski, M., and Savrda, J. (1969). *The mechanism of activation of trypsinogen*. Eur. J. Biochem. **8**: 314-324.

[19] Bier, M., and Nord, F. F. (1951). *The effect of certain ions and of radiation on crystalline trypsin*. Arch. Biochem. Biophys. **31**: 335-336.

[20] Duke, J.A., Bier, M., and Nord, F.F. (1952). *On the mechanism of enzyme action. LIII. The amphoteric properties of trypsin*. Arch. Biochem. Biophys. **40**: 424-436.

[21] Bulaj, G., and Otlewski, J. (1995). *Ligand-induced changes in the conformational stability of bovine trypsinogen and their implications for the protein function.* J. Mol. Biol. **247**: 701-716.

[22] Lazdunski, M., and M. Delaage. (1967). *Structural studies on trypsinogen and trypsin. State diagrams.* Biochim. Biophys. Acta. **140**:417-434.

[23] Harris, J.I. (1956). *Effect of urea on trypsin and alpha-chymotrypsinogen*. Nature **177**: 471-473.

[24] Amiza, M.A. and Owusu Apenten, R.K. (1996*). Urea and heat unfolding of cold-adapted atlantic cod (Gadus Morhua) trypsin and bovine trypsin*. J Sci Food Agric. **70**: 1-10.

[25] Jakubowski, H. (25. Nov 2013).: Mechanism of enzyme catalysis. *Serine protease mechanism.* Retrieved 21st of January 2014 from *http://employees.csbsju.edu/hjakubowski/classes/ch331/catalysis/olcatenzmech.html*

[26] Stefán Bragi Gunnarsson. (2011). *Effect of chitosan on thermal stability of horseradish peroxidase*. M.Sc. Thesis. University of Iceland: Iceland.

[27] Arbia, W., Arbia, L., Adour, L., and Amrane, A. (2013). *Chitin extraction from crustacean shells using biological methods – A review*. Food Technol. Biotechnol. **51**: 12-25.

[28] Rinaudo, M. (2006). *Chitin and chitosan: Properties and applications.* Prog. Polym. Sci. **31**: 603-632.

[29] Fannar Jónsson (2005). *Áhrif kítósans á stöðugleika nautatrypsíns* [In Icelandic]. M.Sc. Thesis. University of Iceland: Iceland.

[30] Wang, Q. Z., Chen, X.G., Liu, N., Wang, S.X., Liu, C.S., Meng, X.H., and Liu, C.G. (2006). *Protonation constants of chitosan with different molecular weight and degree of deacetylation.* Carbohyd. Polym. **65**: 194-201.

[31] Pillai, C.K.S., Paul, W., and Sharma, C.P.(2009). *Chitin and chitosan polymers: Chemistry, solubility and fiber formation.* Prog. Polym. Sci. **34**: 641-678.

[32] DeSantis, G., and Jones, J.B. (1999). *Chemical modification of enzymes for enhanced functionality.* Curr. Opin. Biotech. **10**: 324-330.

[33] Klibanov, A.M. (1983). *Stabilization of enzymes against thermal inactivation.* Adv. Appl. Microb. **29**: 1-28.

[34] Venkatesh, R., and Sundaram, P.V. (1998). *Modulation of stability of bovine trypsin after in vitro structural changes with a variety of chemical modifiers.* Protein Eng. **11**: 691-698.

[35] Nelson, D.L., and Cox, M.M. (2005). *Lehninger Principles of biochemistry (4th. ed.).* New York: W.H. Freeman and Company.

[36] Him, H.J., Steif, C., Vogl, T., Meyer, R., Renner, M., and Ledermüller, R. (1993). *Fundamentals of protein stability.* Pure Appl. Chem. **65**: 947-952.

[37] Ahern, T., and Manning, M.C.(Eds.) (1992). *Stability of protein pharmaceuticals part A: Chemical and physical pathways of protein degradation.* New York: Plenum Press.

[38] Branden, C., and Tooze, J. (1999). *Introduction to protein structure (2nd ed.).*New York: Garland Science.

[39] Thornton, J.M.(1982). *Conformation of terminal regions in proteins*. Nature **295**: 13-14.

[40] T.E. Creighton (Ed.). (1989). *Protein function – a practical approach.*Oxford: IRL Press.

[41] Pace, C.N. (1990). *Measuring and increasing protein stability.* Trends Biotechnol. **8**: 93-98.

[42] Jaenicke, R.(1990). *Protein Structure and function at low temperatures*. Philos. Trans. R. Soc. Lond.B.**326**: 535-553.

[43] Becktel, W.J., and Schellman, J.A. (1987). *Protein stability curves*. Biopolymers **26**: 1859-1877.

[44] Brock, T.D.(1985). *Life at high temperatures*. Science. **230**: 132-138.

[45] Tanford, C. (1968). *Protein denaturation*. Adv. Protein. Chem. **23**: 121-282.

[46] Kristjánsson, M.M, and Magnússon, Ó. Th. (2001). *Effect of lyotropic salts on the stability of a subtilisin-like proteinase from a psychrotrophic Vibrio-species, Proteinase K and Aqualysin I.* Protein Pept. Lett. **8**: 249-255.

[47] Ahern, T., and Manning, M.C.(Eds.) (1992). *Stability of protein pharmaceuticals part B: In vivo pathways of degradation and strategies for protein stabilization.* New York: Plenum Press.

[48] Ramezani, R., Esmailpour, M., and Aminlari, M. (2008). *Effect of conjugation with glucosamine on the functional properties of lysozyme and casein.* J. Sci. Food Agric. **88**: 2730-2737.

[49] Davis, B.G. (2003). *Chemical modification of biocatalysts.* Curr. Opin. Biotechnol. **14**: 379-386.

[50] Sheldon, R.A.(2007). *Cross-linked enzyme aggregates (CLEA®s): Stable and recyclable biocatalysts.* Biochem. Soc. T. **35**: 1583-1587.

[51] Janeček, S. (1993). *Strategies for obtaining stable enzymes*. Process Biochem. **28**: 435-445.

[52] Marshall, J.J., and Rabinowitz, M. (1976). *Preparation and characterization of dextrin-trypsin conjugate.* J. Biol. Chem. **251**: 1081-1087.

[53] Häring, D. and Schreier, P. (1998). *Novel biocatalysts by chemical modification* of known enzymes: Cross-linked microcrystals of the semisynthetic peroxidase seleno-subtilisin. Angew. Chem. Int. Ed. **37**: 2471-2473.

[54] Govardhan, C.P.(1999). *Crosslinking of enzymes for improved stability and performance*. Curr. Opin. Biotech. **10**: 331-335.

[55] Tananchai, P. (2011). *Stabilization of enzymes by chemical modifications*. Ph.D. Thesis. Massey University: New Zealand.

[56] Gauthier, M. A., and Klok, H-A. (2010). *Polymer-protein conjugates: an enzymatic activity perspective*. Polym. Chem. **1**, 1352-1373.

[57] Martinek, K., and Torchilin, V.P. (1988). *Stabilization of enzymes by intramolecular cross-linking using bifunctional reagents*. Method. Enzymol. **137**: 615-626.

[58] Darias, R., and Villalonga, R. (2001*). Functional stabilization of cellulase by covalent modification with chitosan*. J. Chem. Technol. Biot. **76**: 489-493.

[59] Vazquez-Duhalt, R., Tinoco, R., D'Antonio, P., Topoleski, L. D.T., and Payne, G.F. (2001). *Enzyme conjugation to the polysaccharide chitosan: Smart biocatalysts and biocatalytic hydrogels*. Bioconjugate Chem. **12**: 301-306.

[60] Brinkley, M. (1992). *A brief survey of methods for preparing protein conjugates with dyes, haptens and crosslinking reagents*. Bioconjugate Chem. **3**: 2-13.

[61] Kato, Y., Matsuda, T., and Nakamura, R. (1993). *Improvement of physicochemical and enzymatic properties of bovine trypsin by non-enzymatic glycation*. Biosci. Biotech. Biochem. **57**: 1-5.

[62] Pham, V.T., Ewing, E., Kaplan, H., Choma, C., and Hefford, M.A. (2008). *Glycation improves the thermostability of trypsin and chymotrypsin*. Biotechnol. Bioeng. **101**: 452-459.

[63] Khalifah, R. G., Todd, P., Booth, A.A., Yang, S.X., Mott, J.D., Hudson, B.G. (1996). *Kinetics of nonenzymatic glycation of ribonuclease A leading to advanced glycation end products. Paradoxical inhibition by ribose leads to facile isolation of protein intermediate for rapid post –Amadori studies*. Biochemistry **35**: 4645-4654.

[64] Sasvári, Z,. and Asbóth, B. (1999). *Crosslinking of glucoamylases via carbohydrates hardly affects catalysis but impairs stability*. Biotechnol. Bioeng. **63**: 459 – 463.

[65] Hermanson, G.T. (2008). *Bioconjugate techniques (2nd ed)*. NewYork: Elsevier.

[66] Hoare, D.G., and Koshland Jr, D.E. (1967). *A Method for the Quantitative Modification and Estimation of Carboxylic Acid Groups in Protein.* J. Biol. Chem. **242**: 2447-2453.

[67] Wriston, J.C. (1973). *Modification of chymotrypsinogen with 1-aminoglucose*. FEBS Lett.**33**: 93-96.

[68] Grabarek, Z., and Gergely, J. (1989). *Zero-length crosslinking procedure with the use of active esters.* Anal. Biochem. **185**: 131-135.

[69] Carraway, K.L, and Koshland Jr, D.E. (1968). *Reaction of tyrosine residues in proteins with carbodiimide reagents.* Biochim. Biophys. Acta**. 160**: 272-274.

[70] Carraway, K.L, and Triplett, R.B. (1970). *Reaction of carbodiimides with protein sulfhydryl groups*. Biochim. Biophys. Acta. **200**: 564-566.

[71] Kislinger, T., Humeny, A., Peich, C.C., Becker, C-M., and Pischetsrieder, M. (2005). *Analysis of protein glycation products by MALDI-TOF/MS*. Ann. N.Y. Acad. Sci. **1043**: 249–259.

[72] Glish, G.L., and Vachet, R.W. (2003). *The basics of mass spectrometry in the twenty-first century*. Nat. Rev. Drug. Discov. **2**: 140-150.

[73] R.A. Meyers (Ed.). *Encyclopedia of analytical chemistry*. Chichester: John Wiley & Sons Ltd.

[74] Chang, R. (2000). *Physical chemistry for the chemical and biological sciences (3rd ed.)*. Sausalito: University Science Books.

[75] Greenfield, N.J. (20. Sept 2004). *Circular dichroism* [pdf]. Retrieved 11 March 2014 from *http://www.niu.edu/analyticallab/cd/handout.pdf*

[76] Kelly, S.M., Jess, T.J., and Price, N.C. (2005). *How to study proteins by circular dichroism.* Biochim. Biophys. Acta. **1751**: 119-139.

[77] Gore, M.G. (Ed.). (2000). *Spectrophotometry & Spectrofluorimetry. Practical approach.* New York: Oxford University Press.

[78] Carr, R., and Wright. (2013). *Nanoparticle tracking analysis – A review of applications and usage 2010-2012* [Brochure]. NanoSight Ltd.

[79] Filipe, V., Hawe, A., and Jiskoot, W.(2010). *Critical Evaluation of Nanoparticle Tracking Analysis (NTA) by NanoSight for the Measurement of Nanoparticles and Protein Aggregates*. Pharm. Res. **27**: 796-810.

[80] PD-10 Desalting columns [Pdf].(n.d.). Retrieved 11th of March 2014 from *https://www.gelifesciences.com/gehcls_images/GELS/Related%20Content/Files/1314723116657/litdoc52130800BB_20110830191706.pdf*.

[81] Thannhauser, T.W., Konishi, Y., and Scheraga, H.A. (1984). *Sensitive quantitative analysis of disulfide bonds in polypeptides and proteins*. Anal. Biochem. **138**: 181-188.

[82] Labouesse J. and Gervais. M. (1967). *Preparation of Chemically Defined E N-Acetylated Trypsin*. European. J. Biochem. **2**: 215-223.

[83] Erlanger, B.F., Kokowsky, N., and Cohen, W. (1961). *The preparation and properties of two new chromogenic substrates of trypsin.* Arch. Biochem. Biophys. **95**: 271-278.

[84] Department of Biochemistry, Science Institute- University of Iceland. *Mæliaðferðir fyrir ThermoMax Plate Reader – Prótein og Ensím* [In Icelandic]. R.H. Íslands: Reykjavik, Iceland.

[85] *Britton, H. T. K., and Robinson, R.A. (1931). Universal buffer solutions and the dissociation constant of veronal.* J. Chem. Soc.: 1456–1462.

[86] Bell, R., Stevens, W.K., Jia, Z., Samis, J., Côté, H.C.F., MacGillivrayi, R.T.A., and Nesheim, M.E. (2000). *Fluorescence properties and functional roles of tryptophan residues 60d, 96, 148, 207, and 215 of thrombin*. J. Biol. Chem. **275**: 29513-29520.

[87] Bisswanger, H. (2004). *Practical enzymology*.Weinheim: WILEY Verlag GmbH & Co. KgaA.

[88] SIGMA ALDRICH®. *Azocasein protease substrate.* Retrieved 23rd of January 2014 from *http://www.sigmaaldrich.com/catalog/product/sigma/a2765?lang=en&region=IS.*

[89] Myers, J.K., Pace, N., and Scholtz, J.M.(1997). *Helix propensities are identical in proteins and peptides*. Biochemistry **36**: 10923-10929.

[90] Invitrogen. (2007). Xcell Sure Lock™ Mini-Cell Version I [Manual].

[91] Novex. BenchMark™ Unstained Protein Ladder [Pamphlet]. (2013). Retrieved 12th of March 2014 from *http://tools.lifetechnologies.com/content/sfs/manuals/ BenchMarkUnstained/ProteinLadder_man.pdf.*

[92] Bjarni Ásgeirsson. *Verklegar æfingar í lífefnafræði fyrir námskeiðið: Lífefnafræði 3* [In Icelandic]. Reykjavík: Háskólaprent.

[93] The PyMOL Molecular Graphics System, Version 1.5.0.4 Schrödinger, LLC.

[94] Villanueva, G. B., and Herskovitz, T. T. (1971). *Exposure of the tyrosyl and tryptophyl residues in trypsin and trypsinogen*. Biochemistry **10**: 3358-3365.

[95] Al-Obeidi, A.M. and Light, A. (1988). *Size-exclusion High Performance Liquid Chromatography of Native Trypsinogen, the Denatured Protein, and Partially Refolded Molecules*. J. Biol. Chem. **263**: 8642-8645.

[96] Aymard, C., and Belarbi, A. (2000). *Kinetics of thermal deactivation of enzymes: A simle three parameters phenomenological model can describe the decay of enzyme activity, irrespectively of the mechanism.* Enzyme Microb. Tech. **27**: 612-618.

[97] Fischer, J., Ulbrich, R., Ziemann, R., Flatau, S., Wolna, P., Schleiff, M., Pluschke, V., and Schellenberger, A. (1980). *Thermal inactivation of immobilized enzymes: A kinetic study.* J. Solid-Ph. Biochem. **5**: 79-95.

[98] Robert, C., and Cadet, F. (1996). *Thermal denaturation of an enzyme – a choice of model.* Biochem. Educ. **24**: 154-157.

[99] Baek, W.O., and Vijayalakshmi, M.A. (1997). *Effect of chemical glycosylation of RNase A on the protein stability and surface histidines accessibility in immobilized metal ion affinity electrophoresis (IMAGE) system*. Biochim. Biophys. Acta. **1336**: 394-402.

[100] Lim, W.K., Rösgen, J., and Englander, S.W. (2009). *Urea, but not guanidinium, destabilizes proteins by forming hydrogen bonds to the peptide group.* P. Natl. Acad. Sci. Usa. **106**: 2595-2600.

[101] O'Brien E.P., Dima, R.I., Brooks, B., and Thirumalai, D. (2007). *Interactions between hydrophobic and ionic solutes in aqueous guanidinium chloride and urea solutions: lessons for protein denaturation mechanism.* J. Am. Chem. Soc. **129**: 7346-7353.

[102] Vidya, J., Ushasree, M.V., and Pandey, A. (2014). *Effect of surface charge alteration on stability of l-asparaginase II from Escherichia sp.* Enzyme Microb. Tech. **56**: 15-19.

[103] Simpson, B.K., and Haard, N.F. (1984). *Purification and characterization of trypsin from the Greenland cod (Gadus ogac) .1. Kinetic and thermodynamic characteristics.* Can. J. Biochem. Cell Biol. **62**: 894-900.

[104] Rajput, Y.S., and Gupta, M.N.(1986). *Reaction of trypsin with some crosslinking reagents*. Enzyme Microb. Technol. **9**: 161-163.

[105] Cao, L., van Langen, L., and Sheldon, R.A. (2003). *Immobilised enzymes: carrier-bound or carrier-free?.* Curr. Opin. Biotech. **14**: 387-394.

[106] Conroy, P.J. (1997). Combined CSTR/UF Reactor. Retrieved 4th of April 2014 from: *http://www.rpi.edu/dept/chem-eng/Biotech-Environ/IMMOB/combo.htm*